Particle Detectors for Colliders

Semiconductor Tracking Detectors

Robert S. Orr
University of Toronto

Generic Detector

A detector cross-section, showing particle paths

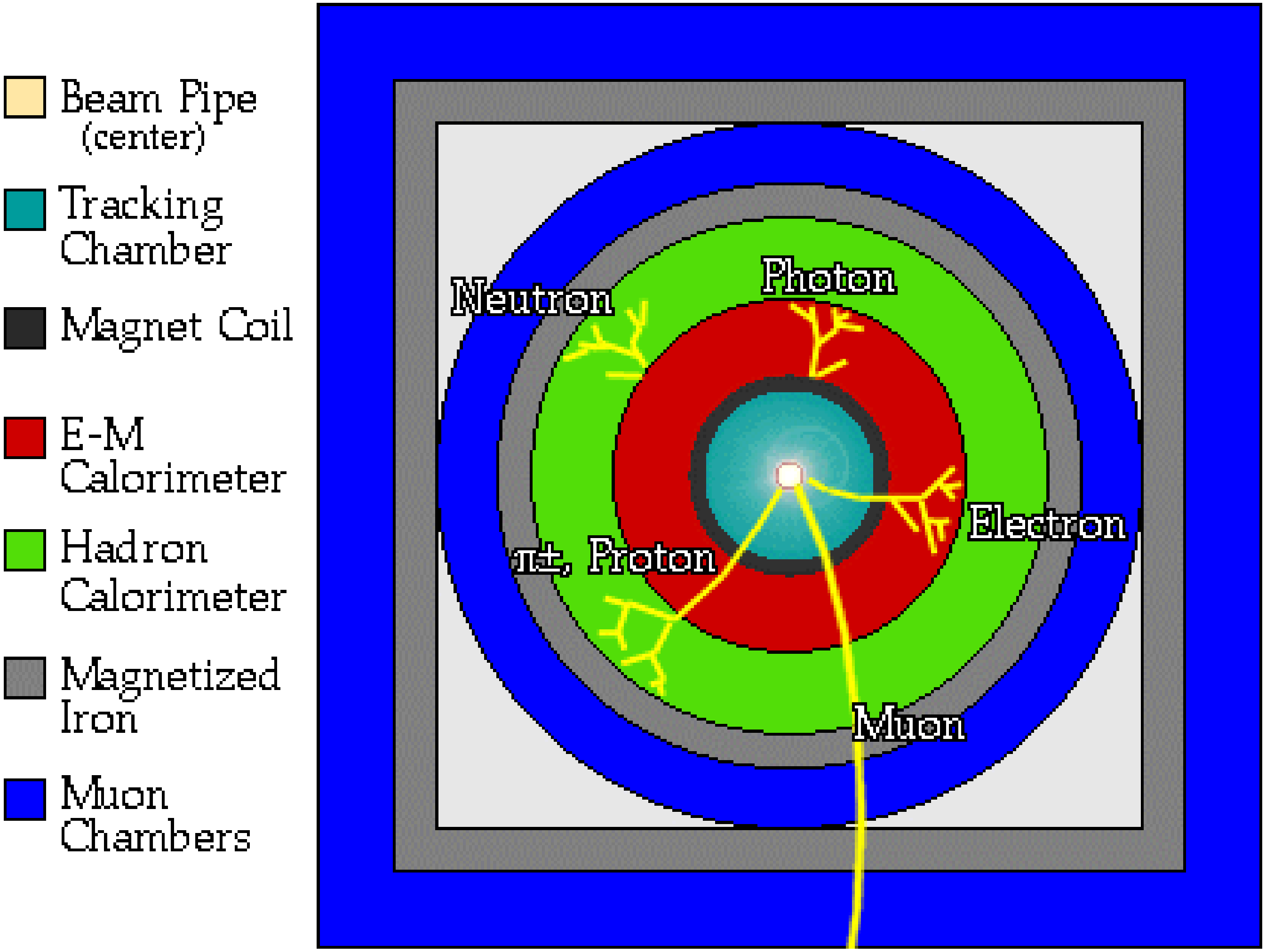

- Layers of Detector Systems around Collision Point

Solid State Detectors

- Specifically
  - microstrip & pixel trackers
- Have become trackers of choice (if affordable)
  - high spatial resolution
  - radiation hard
    - rely on development of micro-electronics fabrication techniques
- Central to heavy flavour tagging, lifetimes
  - vertex detection
    - B flavour
    - Top
    - Higgs

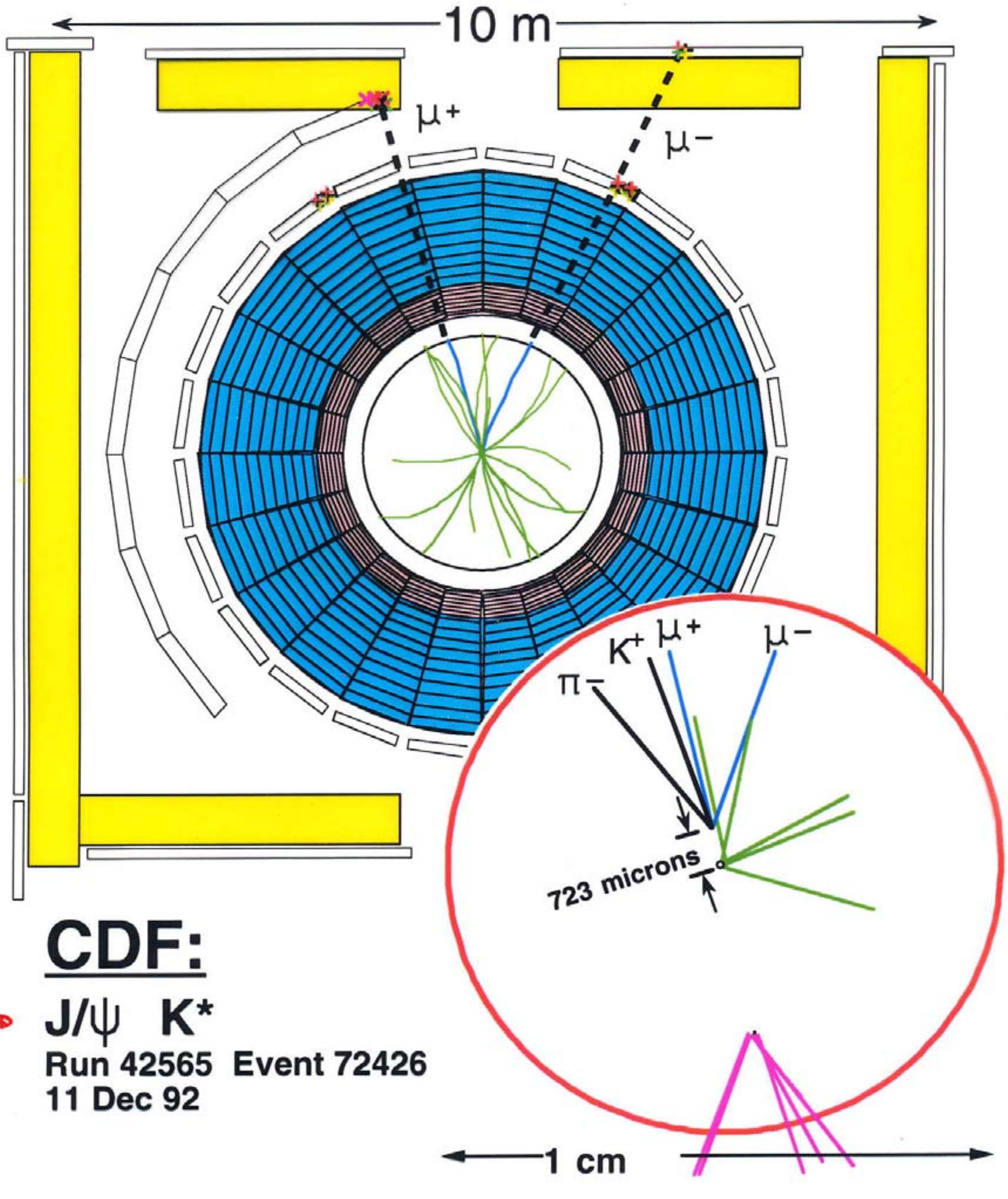

CDF:

$B^0 \rightarrow$ J/ψ K^*

Run 42565 Event 72426
11 Dec 92

Top Quark Discovery at CDF

e + 4 jet event

40758_44414

24-September, 1992

TWO jets tagged by SVX

fit top mass is 170 +- 10 GeV

e^+, Missing E_t, jet #4 from top

jets 1,2,3 from top (2&3 from W)

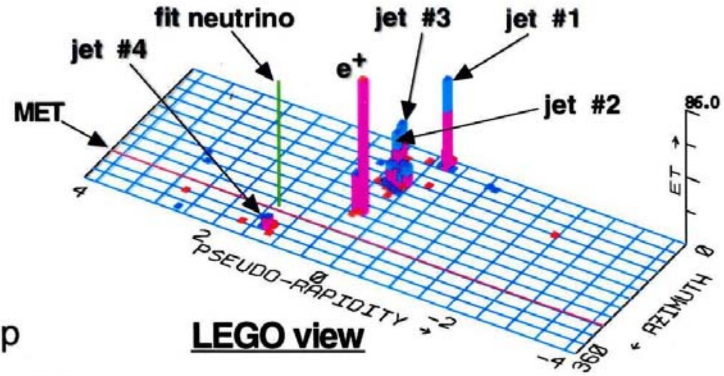

LEGO view

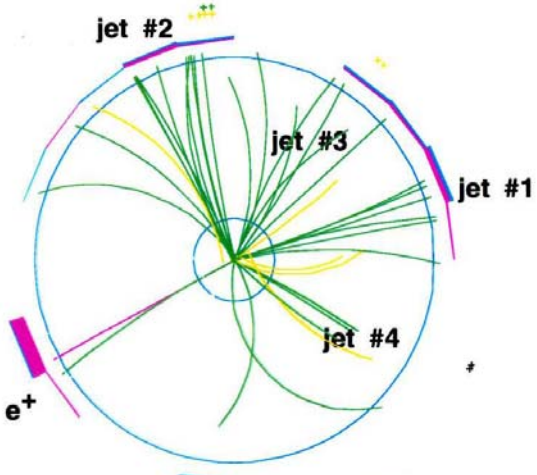

Tracking View

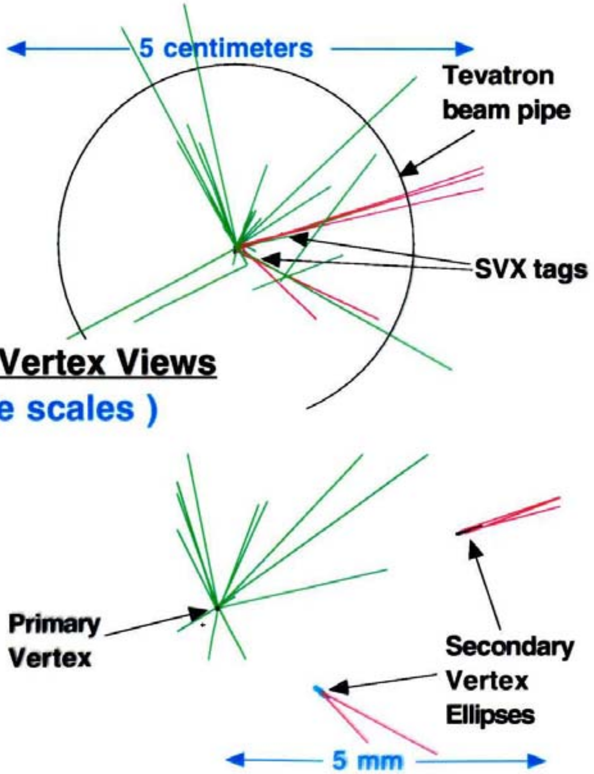

Two Vertex Views

(note scales)

Utility of Si Tracker

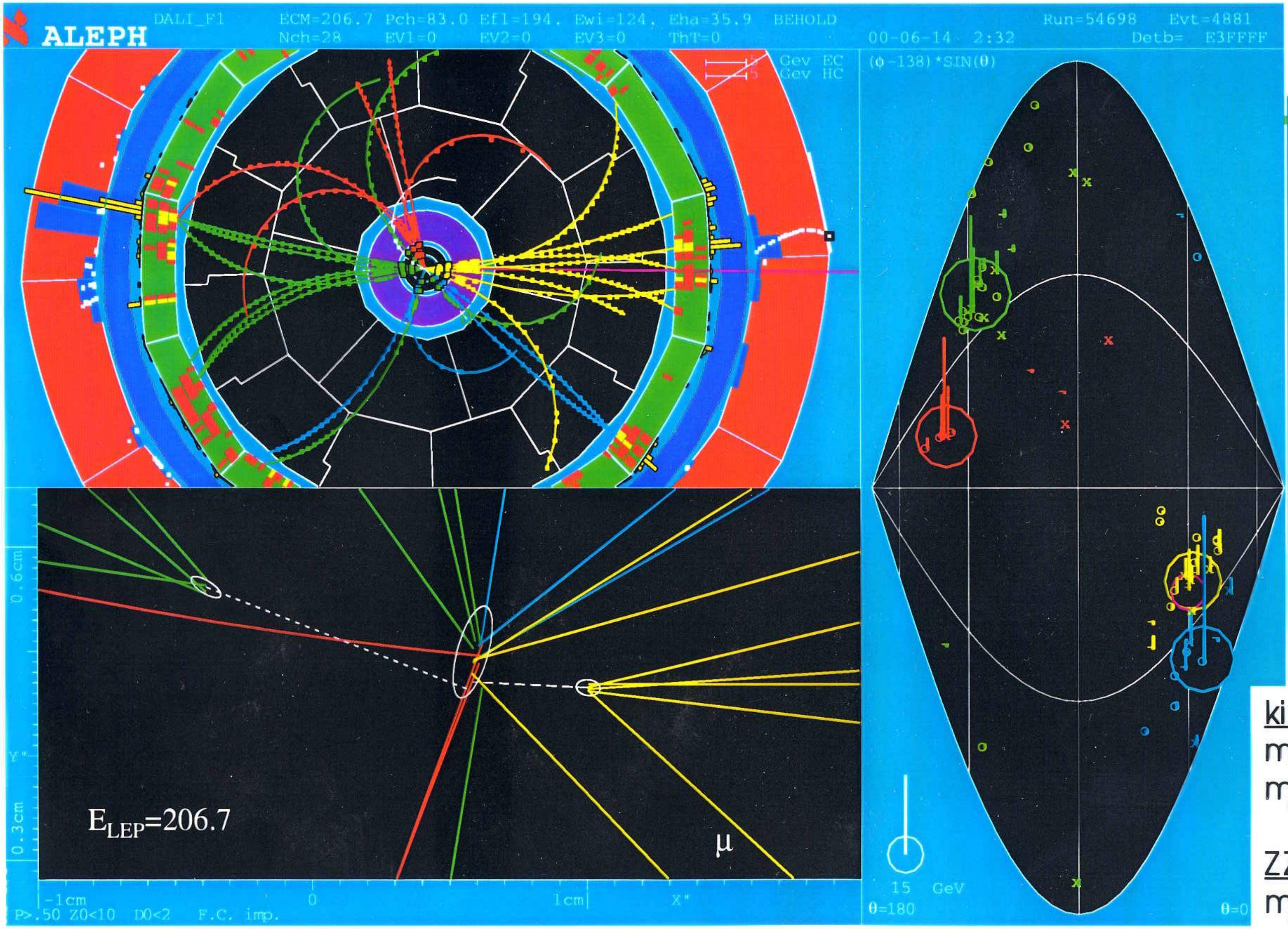

2 b cand.

HZ hyp.

m_H=114 GeV ±3 GeV

NN = 0.996

jet	b-tag:
Z	
1	0.14
2	0.01
H	
3	0.99

kin. mass fit

m_H=112.4GeV

m_Z=93.3GeV

ZZ hyp.

m_Z=102 GeV

m_Z=91.7GeV

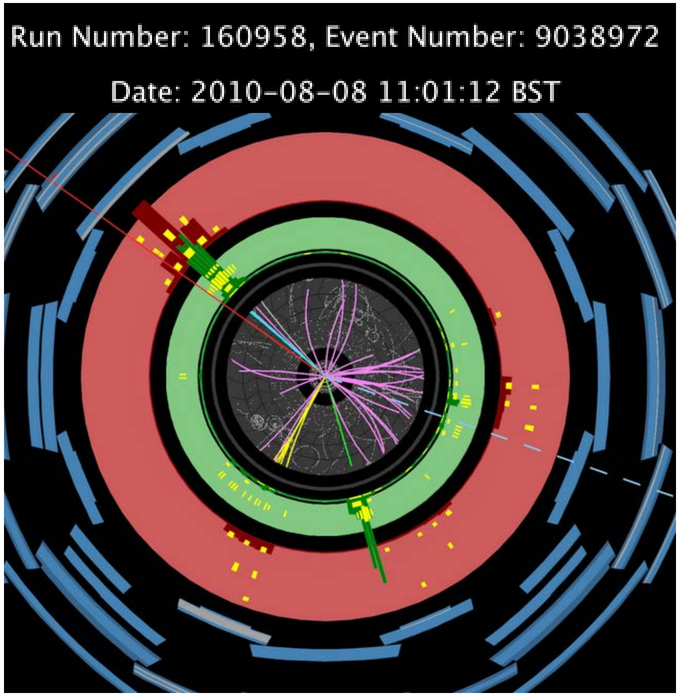

TOP PAIR
eμ DILEPTON

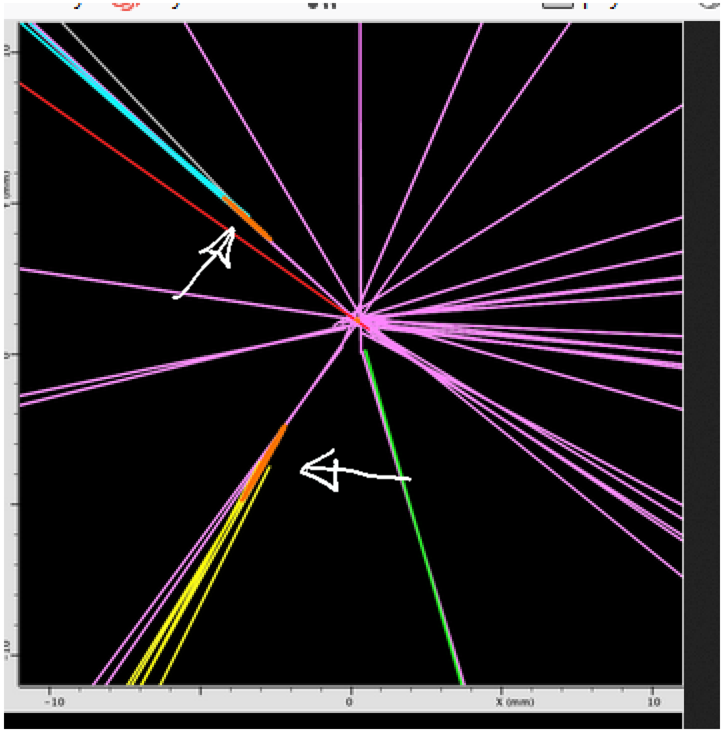

TWO TAGGED
B-JETS

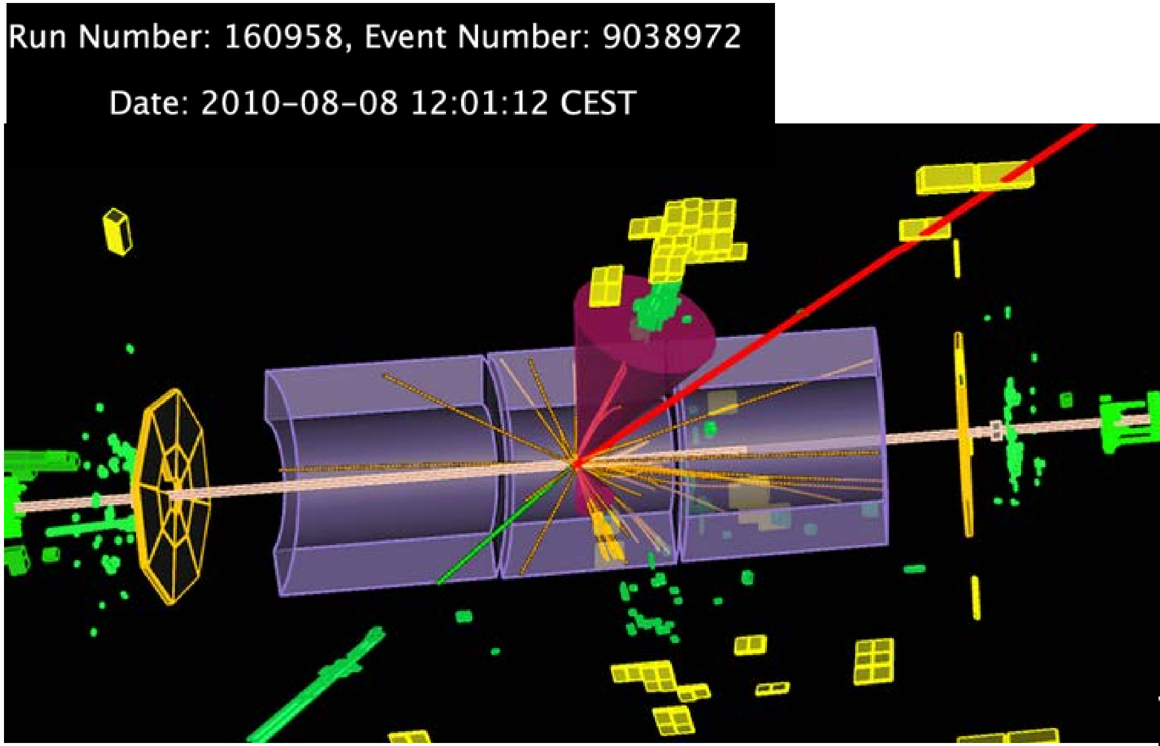

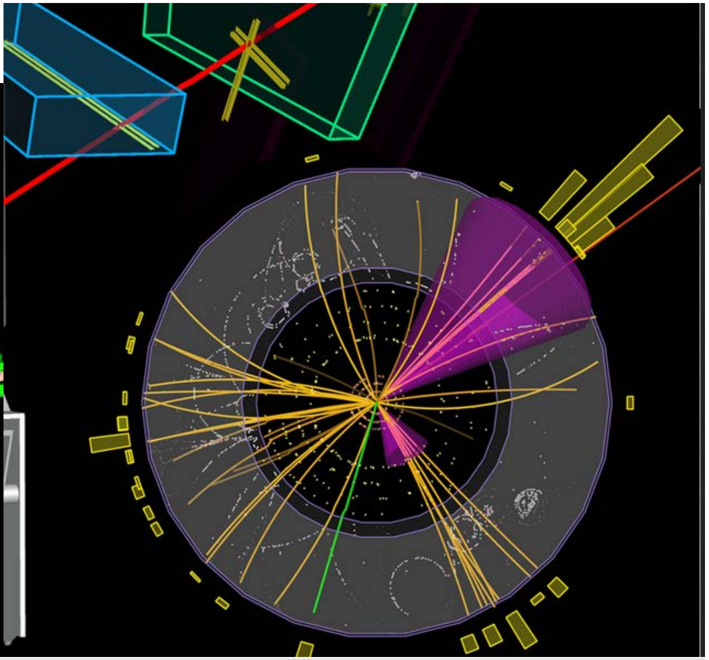

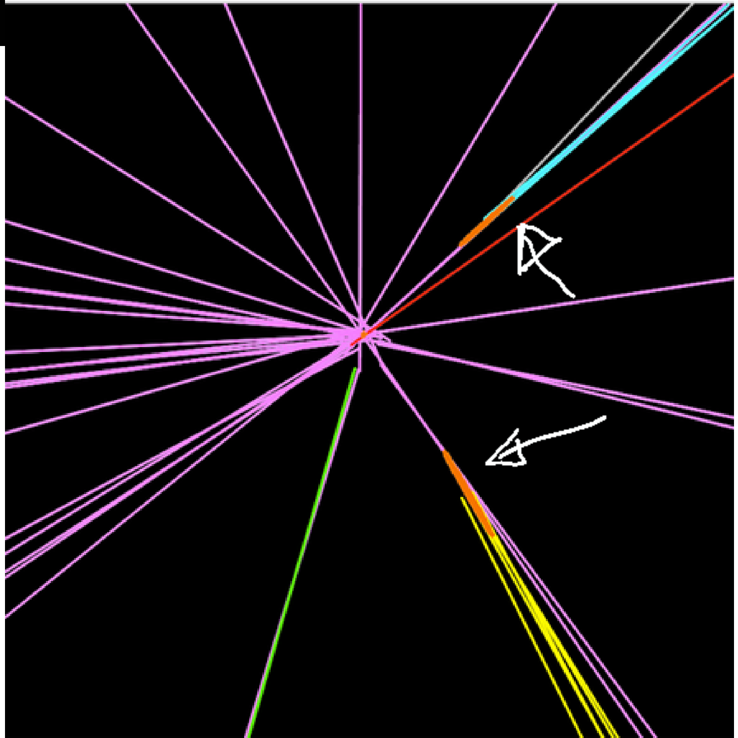

TOP PAIR eμ DILEPTON

TWO TAGGED B-JETS

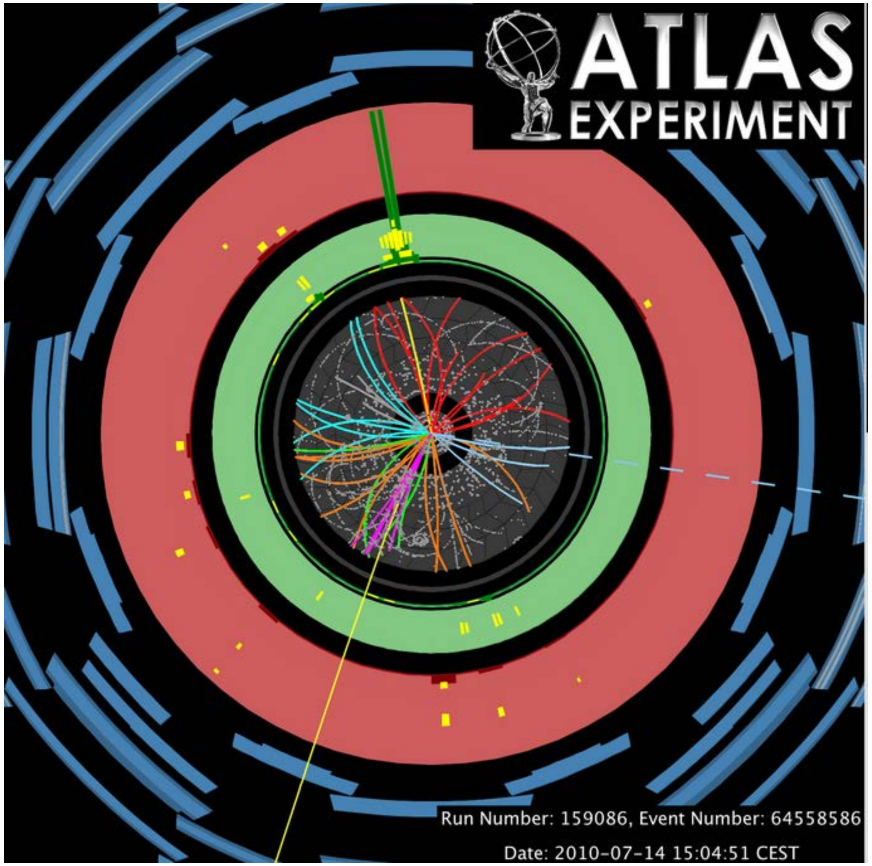

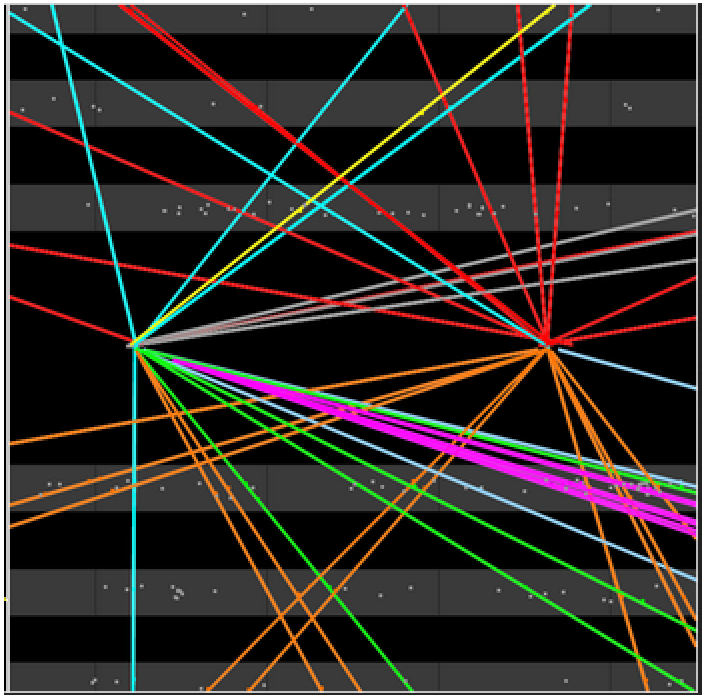

- IDENTIFY CORRECT PRIMARY VERTEX

- TAG B-JET

SECONDARY VERTEX

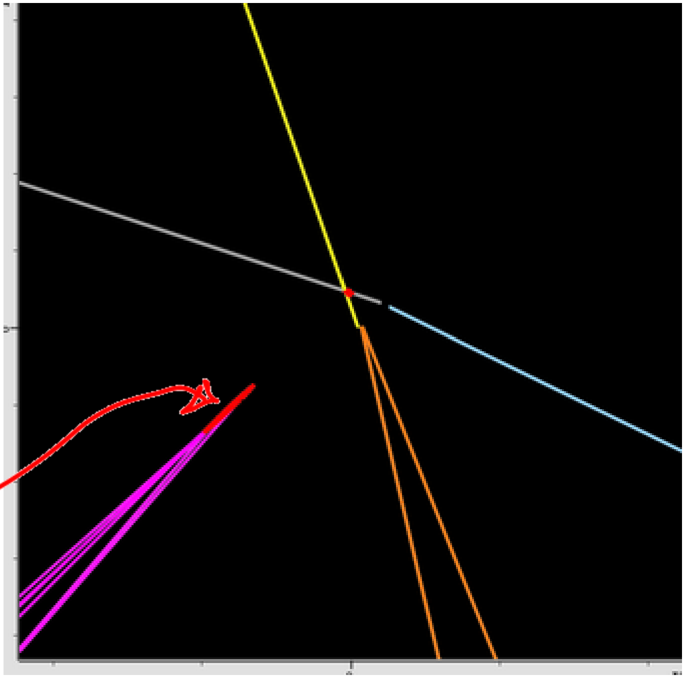

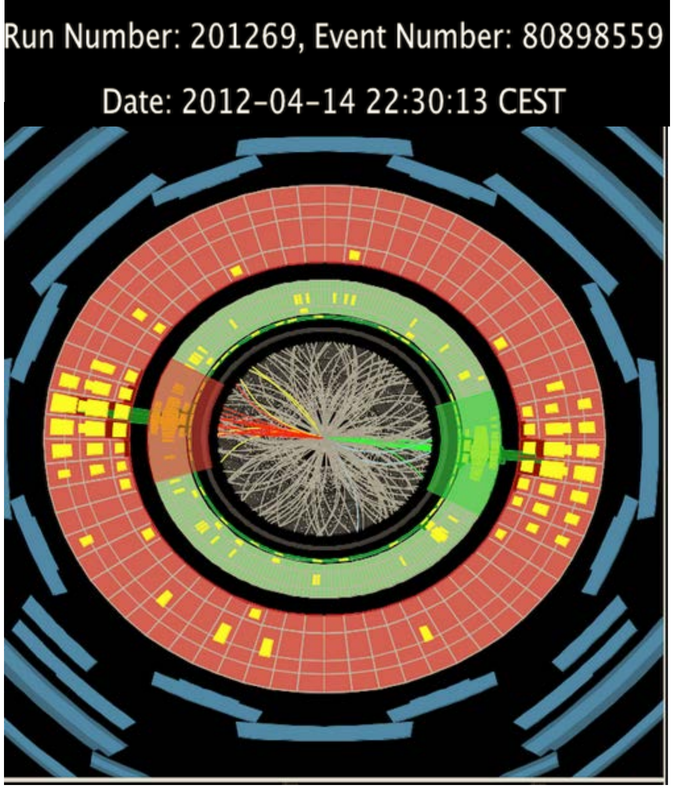

HIGH MASS DIJET

$M_{JJ} = 4.23$ TeV

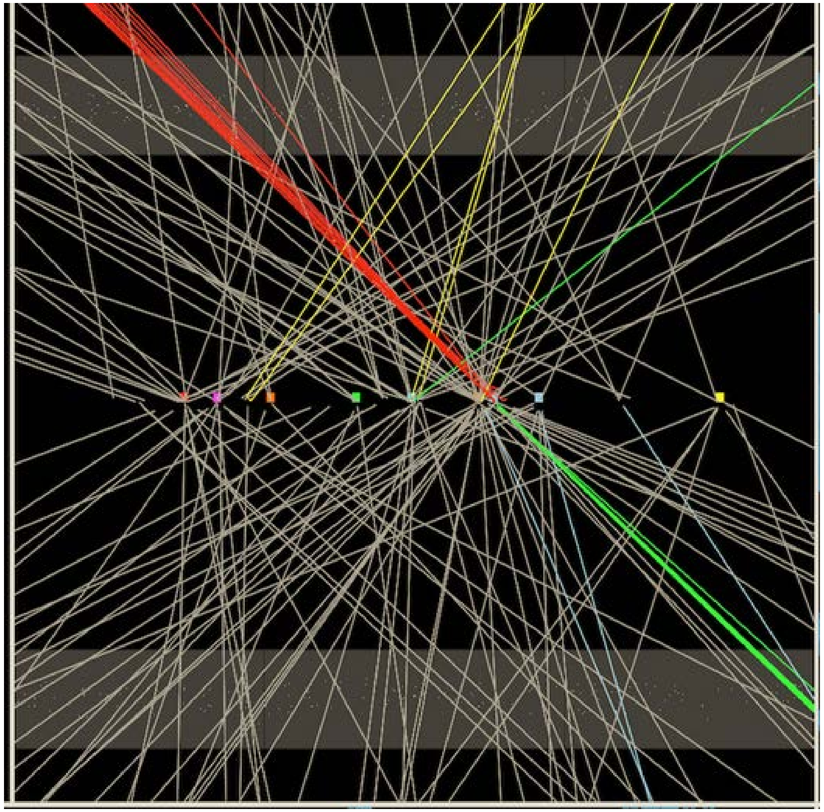

HIGH MULTIPLICITY

IDENTIFY CORRECT PRIMARY VERTEX OUT OF 9.

Semiconductors

- Have a large energy gap

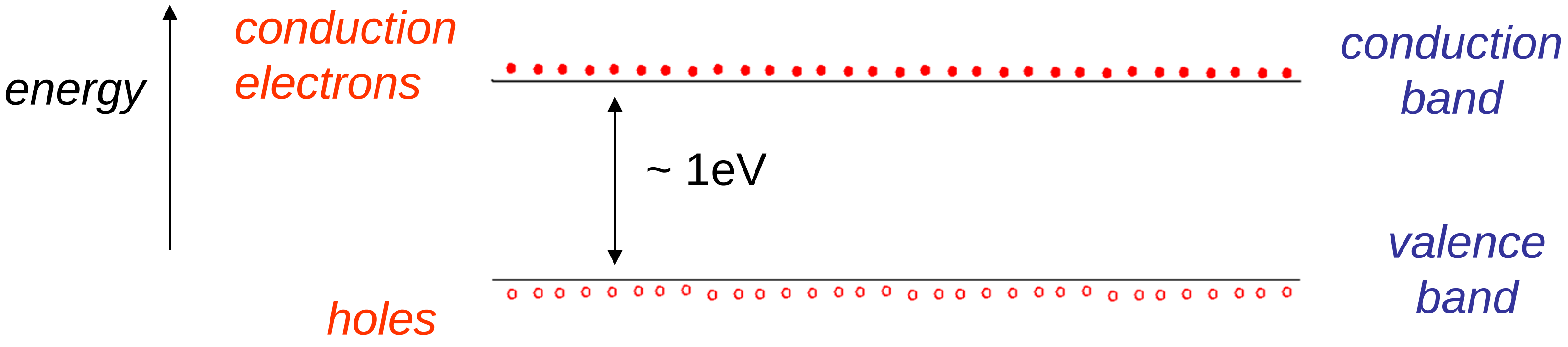

energy

conduction electrons

conduction band

~ 1eV

valence band

holes

- Small number of charge carriers in conduction band
  - electrons thermally excited across the band gap

$$n_i = AT^{3/2}\exp\left(\frac{-E_g}{2kT}\right)$$

$n_i = 1.5\times10^{10}\,cm^{-3}$ in pure silicon at room temp

increases with temperature

Doped Semiconductors

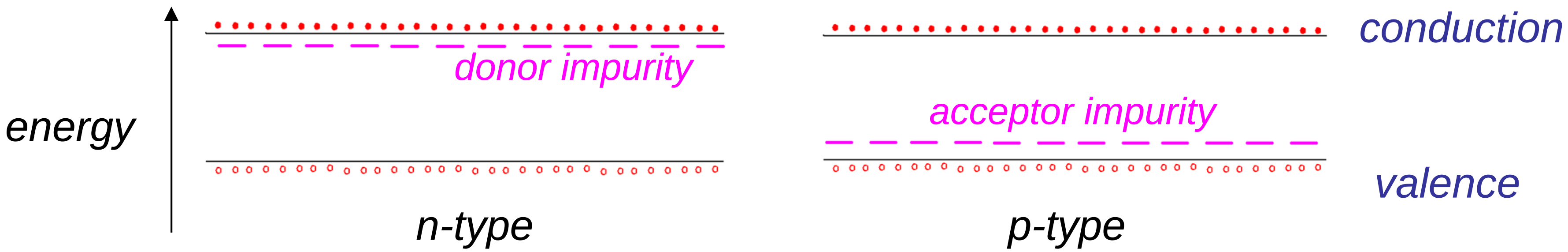

- In n-type , extra conduction electrons easily excited into conduction band

-increase conductivity

- In p-type, valence electrons excited into impurity band – holes in valence band conduct

  - n-type - electrons – majority carriers
  - p-type - holes – majority carriers

p-n Junction

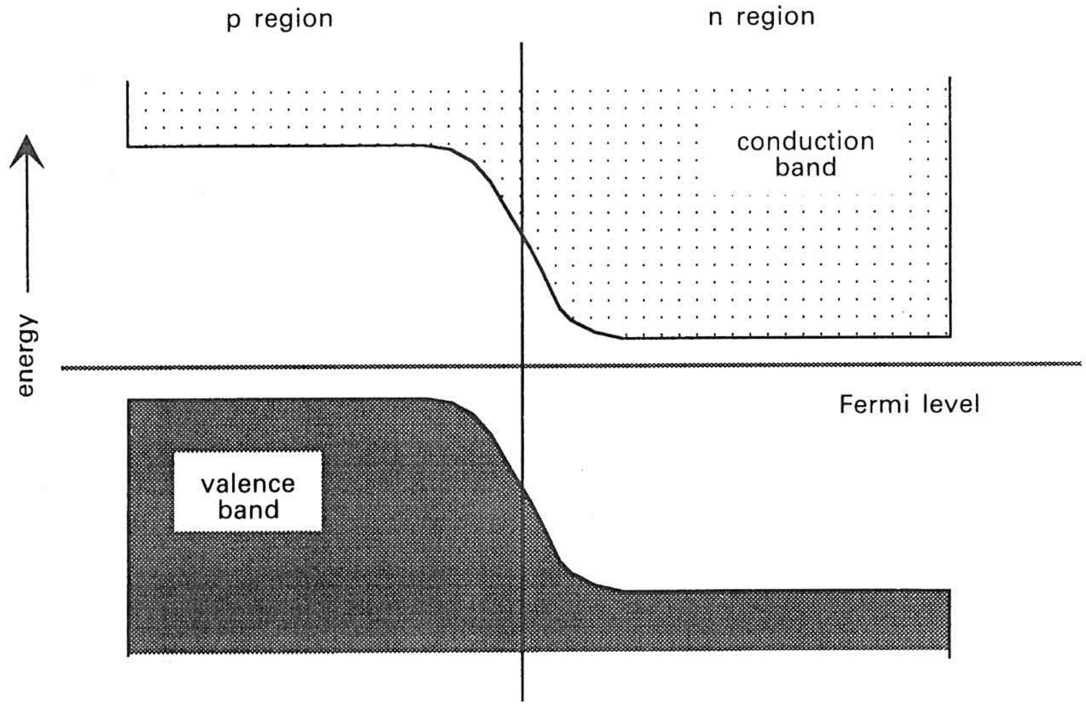

p-type

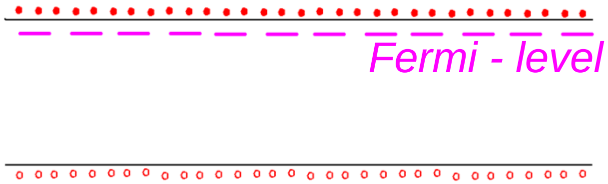

n-type

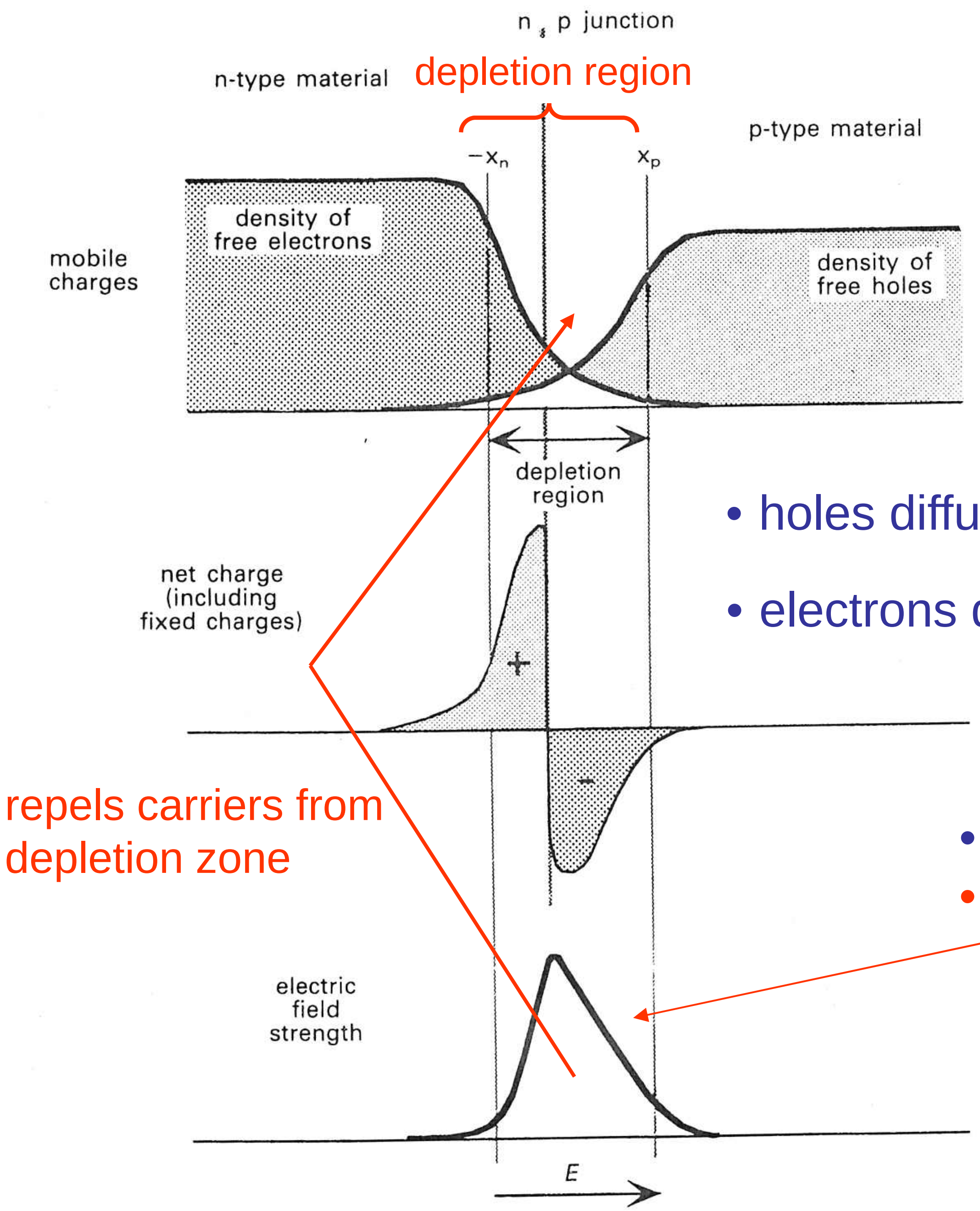

depletion region

repels carriers from depletion zone

- Both n & p are initially electrically neutral

- holes diffuse into n-region - “fill” electrons

- electrons diffuse into p-region - “fill” holes

⇓

- charge buildup
- electric field

depletion zone grows with bias

reverse bias – no current

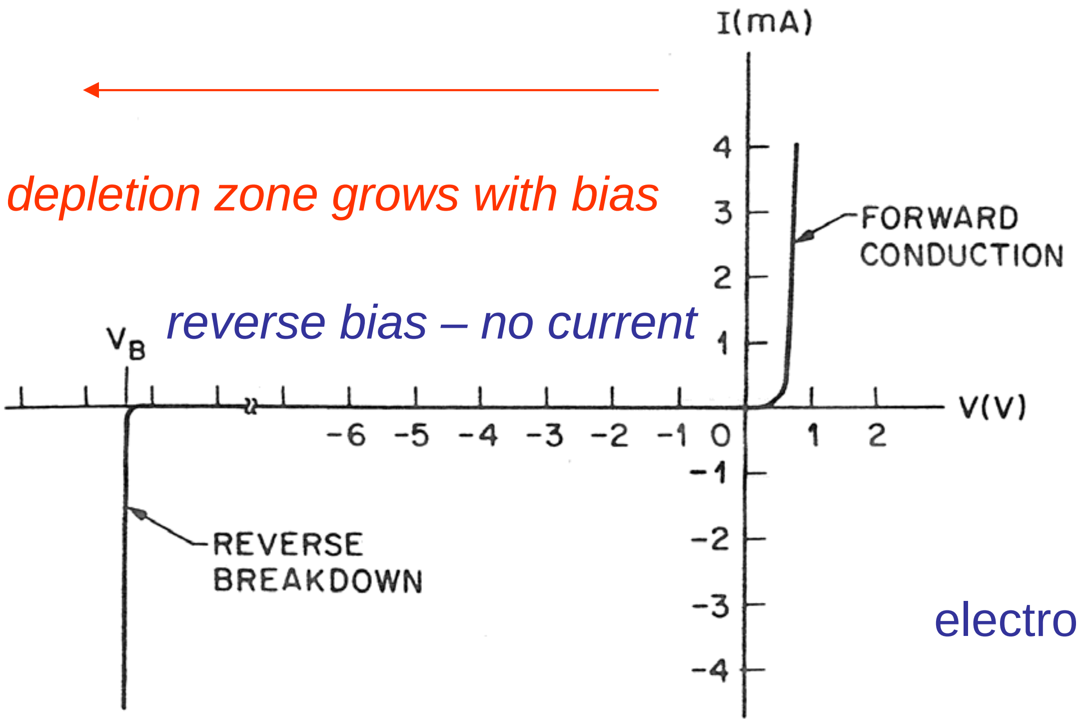

majority carrier current

electrons and holes have different mobility

$$\mu_H = \tfrac{1}{3}\mu_e$$

no bias

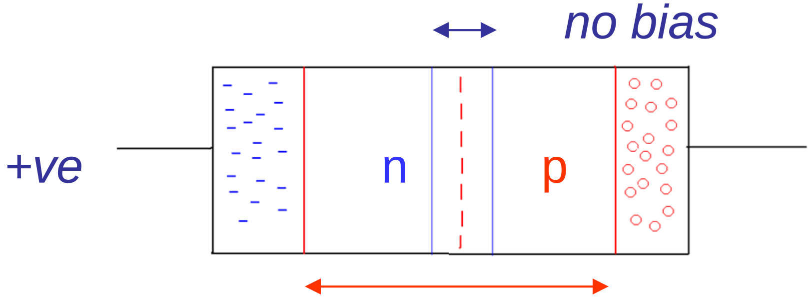

depletion zone
with reverse bias

for $V_0 = 300V$ $d = 5\,mm$ cf $75\,\mu$

need high resistivity Si for large bias voltage
- high purity or compensated

Depletion Zone as a Detector

- Reverse biased p-n junction – no majority carriers – no current
- Ionizing particle passing through depletion zone
- Liberates electron-hole pairs – current flows

- Intrinsic field not high enough to efficiently collect carriers – small signal
- Small depletion layer – large capacitance – large noise into electronics

- Depth of Depletion Zone

resistivity

dielectric constant

$$1.054\times10^{-12}\,\frac{F}{cm}$$

$$d=\left[2\varepsilon\mu_e\rho\left(V_0+V_B\right)\right]^{\frac{1}{2}}$$

electron mobility

contact

bias

$$V_0\approx 1V$$

Principle of micro-strip Detector

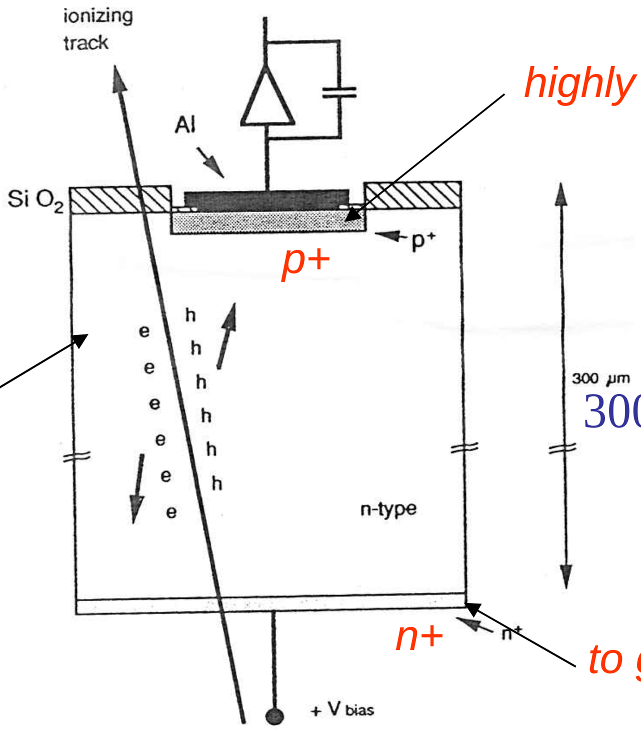

highly doped to exclude depletion zone

insulator

p+

fully depleted n-type detector zone

300μ *for 60V*

n+

to get ohmic connection

- 1 e-h pair / 3.6 eV - 10^2 e-h per micron - dense
- unlike gas – no multiplication of primary ionization 3×10^4 for 300μ
- noise reduced by full depletion – reduce capacitance

Fabrication

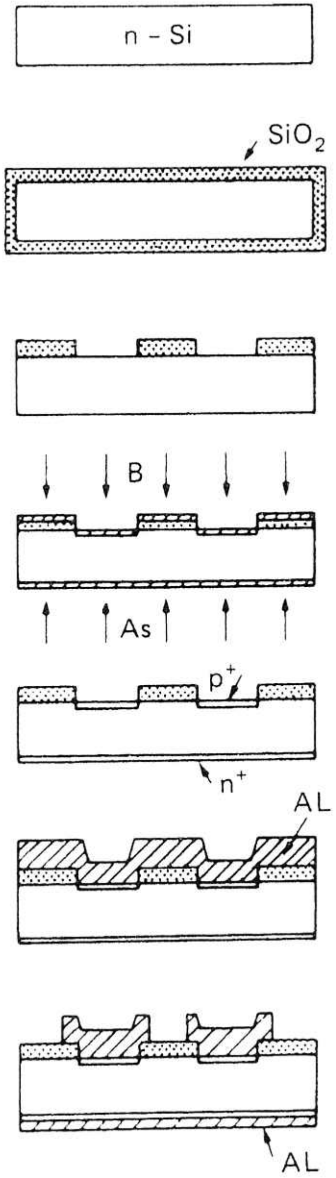

n - Si WAFER

OXIDE PASSIVATION

OPENING OF WINDOWS

DOPING BY ION IMPLANTATION
B : 15 keV 5×10^{14} cm^{-2}
As : 30 keV 5×10^{15} cm^{-2}

ANNEALING AT 600°C, 30 MIN

AL METALLIZATION

AL PATTERNING AT THE FRONT

AL - REAR CONTACT

- micro strip structure

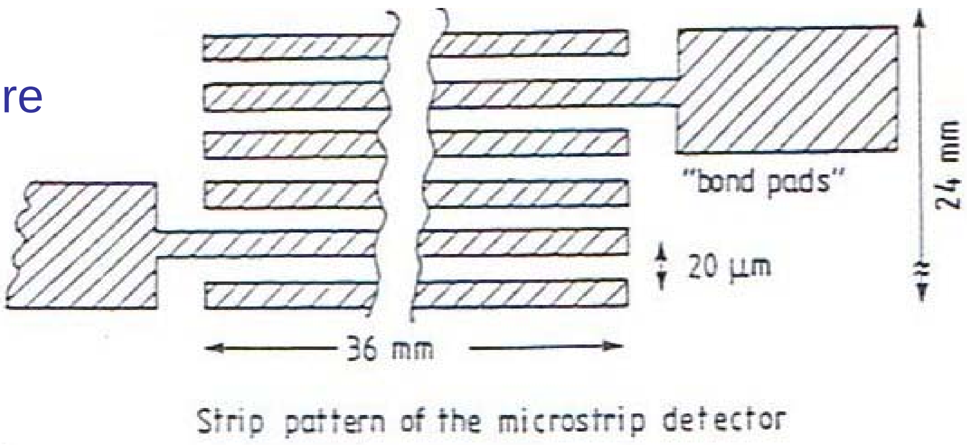

Strip pattern of the microstrip detector

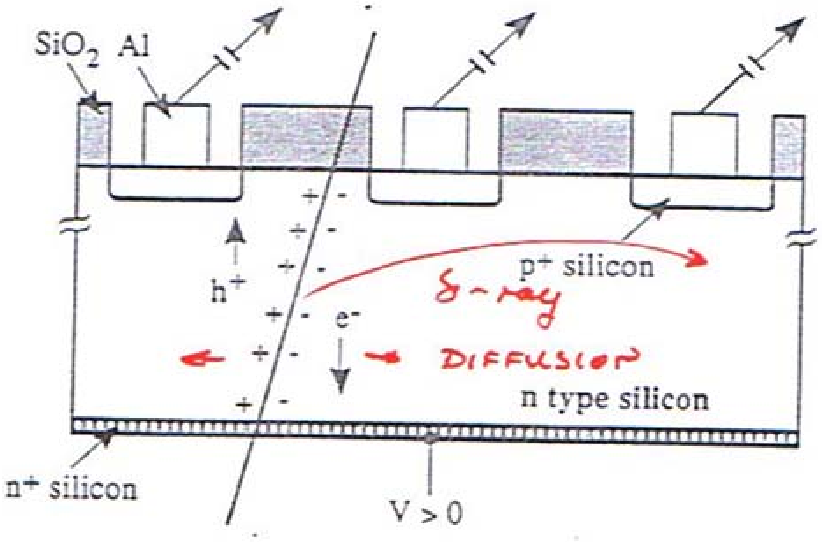

- position resolution < 10 microns
- limited by diffusion and delta-rays

Capacitive Charge - Division

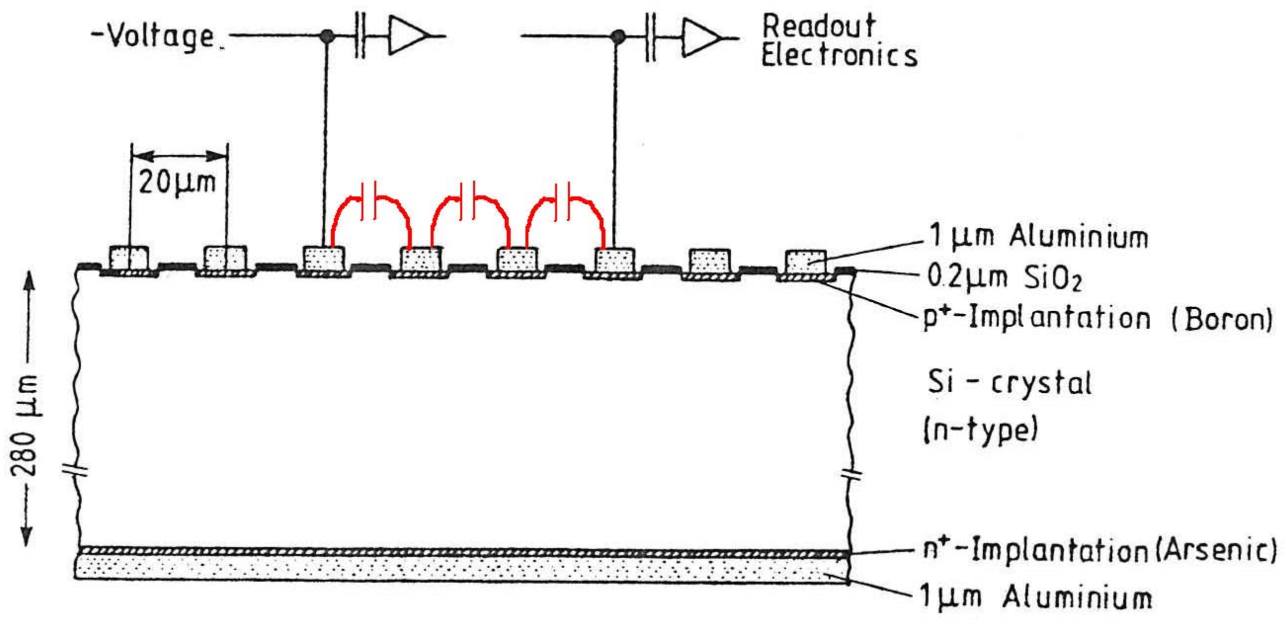

Cross-section of the microstrip detector with capacitative charge division

$$\sigma = \frac{pitch}{\sqrt{12}}$$

- many strips resulting from 20μ pitch
  - ⇨ many electronics channels – many $$
- stray capacitive coupling of strips – read out every n^{th} strip

⇨ read out every 6^{th} strip – effective 120μ pitch -- $\sigma \sim 8\mu$

Time Development of Signal

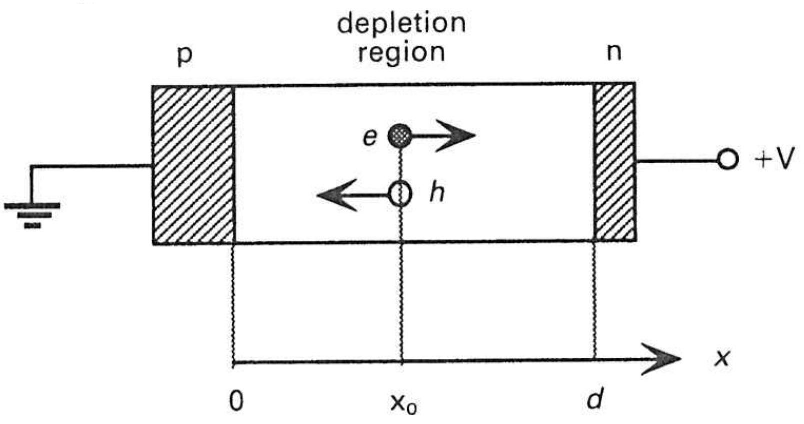

resistivity ρ

dielectric constant ε_s

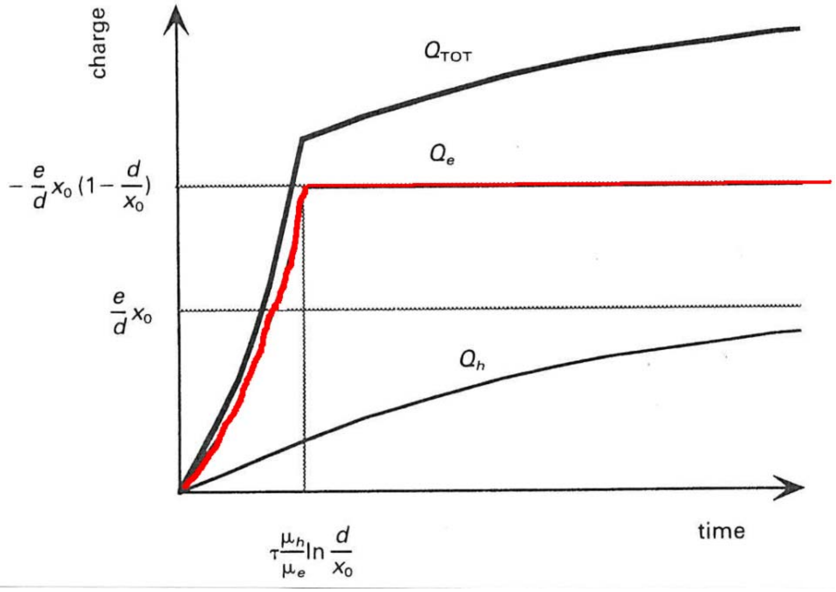

electrons dominate rise time

$$Q_e = \frac{e}{d}x_0\left(1-\exp\frac{\mu_e t}{\mu_h \tau}\right)$$

$$\tau = \varepsilon_s \rho$$

$$Q_h = \frac{e}{d}x_0\left(1-\exp\frac{\cancel{\mu_h} t}{\cancel{\mu_h} \tau}\right)$$

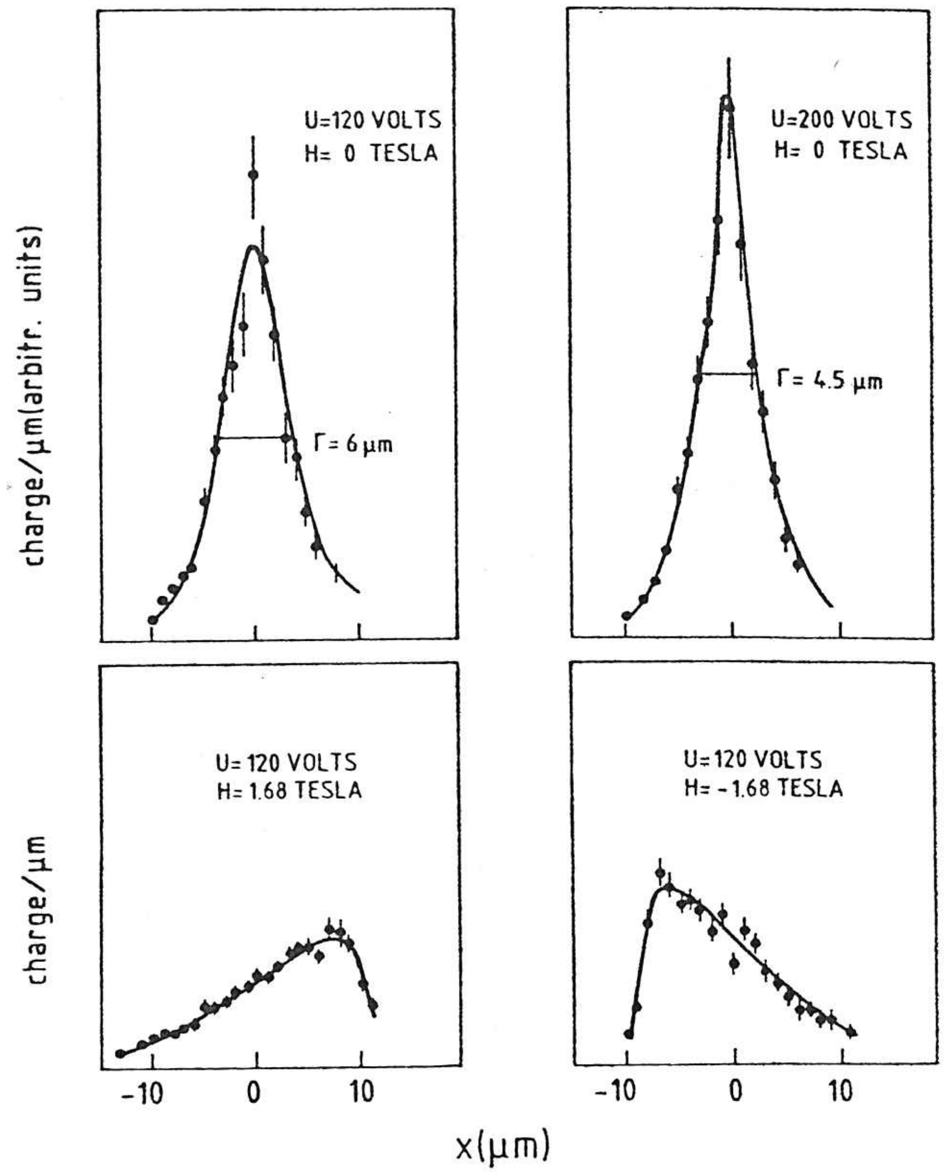

field off

- Effect of magnetic field on space resolution

field on

LORENTZ ANGLE IN B-FIELD

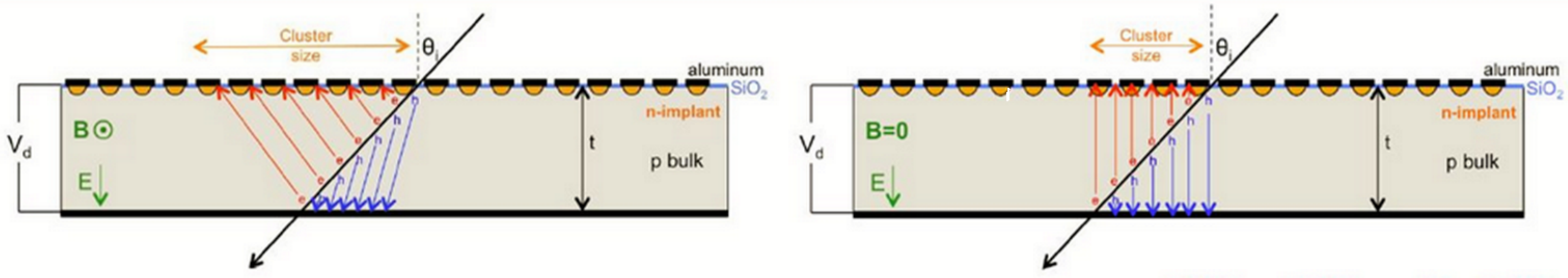

With Magnetic field

Without Magnetic field

$$\text{Cluster Size} \approx t \cdot \tan\theta_i$$

└ LORENTZ ANGLE

$$\tan(\theta_L) = \mu_H B = r_H \mu_d B$$

HALL MOBILITY

HALL FACTOR

DRIFT MOBILITY

$$\mu_d = \frac{v_s / E_c}{\left[1 + \left(\frac{E}{E_c}\right)^{\beta}\right]^{1/\beta}}$$

E_c, β – PARAMETERS – SEE ATLAS-INDET-2001-004

CALCULATING THE DEPLETION DEPTH

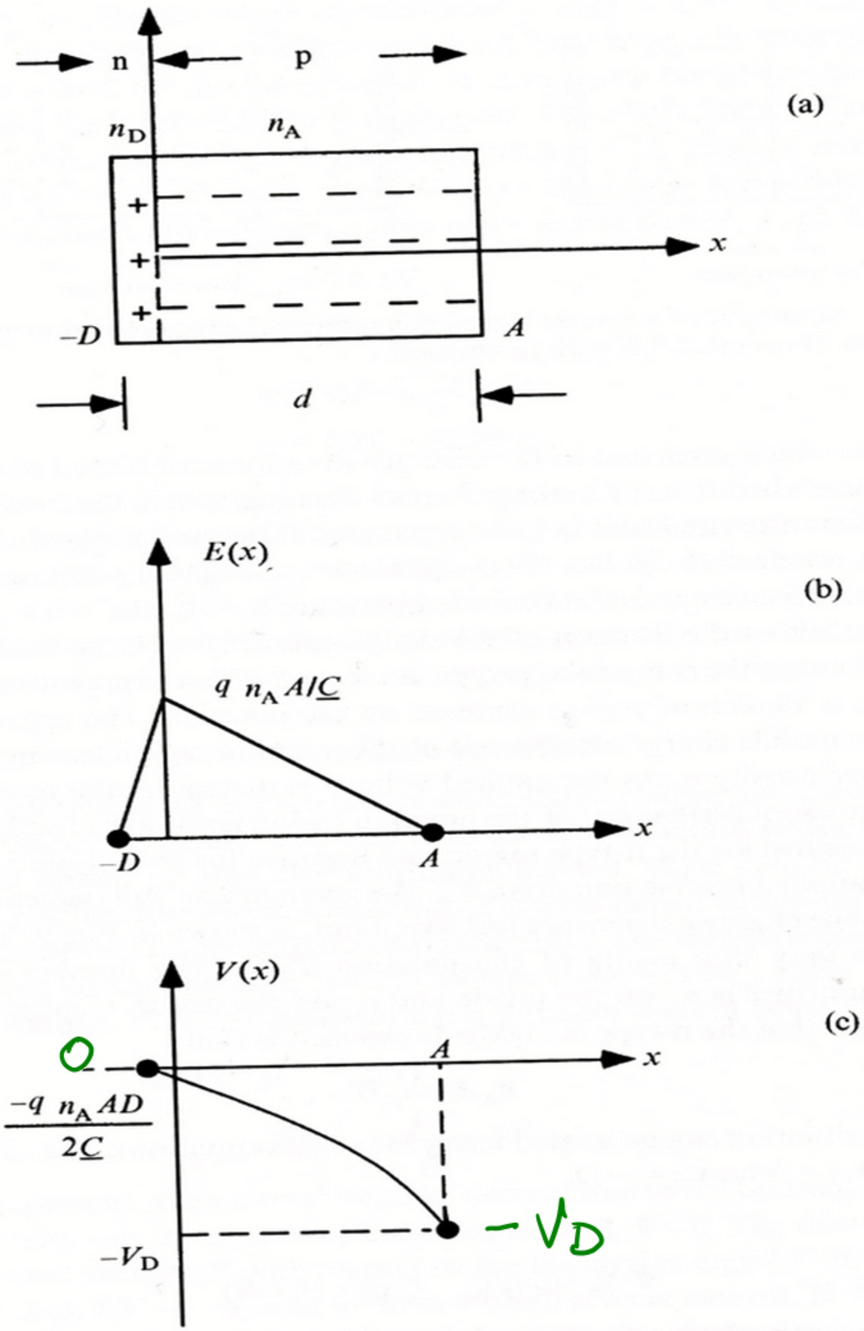

Fig. 9.4. (a) Geometry of a p-n junction. The static charge number density is n_D

FULLY DEPLETED JUNCTION

N_D = NUMBER DENSITY OF DONOR IMPURITIES

N_A = NUMBER DENSITY OF ACCEPTOR IMP.

BEHAVIOUR OF ELECTRIC FIELD.

VOLTAGE

USE $\bar{\nabla} \cdot \bar{E} = \frac{qn}{\varepsilon}$

CHARGE ON ELECTRON

NUMBER DENSITY

ACTUALLY $\varepsilon_r \varepsilon_0$

TO GET THE ELECTRIC FIELD

$$\int_{x_1}^{x_2} \bar{\nabla} \cdot \bar{E} \, dx = \left[\frac{qn}{\varepsilon} \cdot x \right]$$

$$E(x>0) \; [0 \to A] = \left[\frac{qn}{\varepsilon} \right]_x^A = \frac{-qn_A [x-A]}{\varepsilon}$$

$$E(x<0) \; [-D \to x] = \left[\frac{qn}{\varepsilon} \right]_{-D}^{x} = \frac{qn_D [x+D]}{\varepsilon}$$

THE JUNCTION HAS TO REMAIN ELECTRICALLY NEUTRAL

$$n_A \cdot A = n_D \cdot D$$

$$E(x<0) = q \left\{ \frac{n_A \cdot A}{D} \right\} \left\{ \frac{x+D}{\varepsilon} \right\}$$

NOW WE WANT TO GET THE VOLTAGE DISTRIBUTION

$$\bar{E} = -\bar{\nabla} V \rightarrow \int \bar{E} = -V$$

$\int \bar{E}_s$ ON LAST PAGE

$V(x=A) = -V_D$

$V(x=-D) = 0$

↑ WE CAN CHOOSE THIS

$$V(x>0) = \int q n_A \cdot \frac{x}{\varepsilon} dx - \int \frac{q n_A \cdot A}{\varepsilon}$$

$$= q n_A \frac{x^2}{2\varepsilon} - q n_A \frac{x \cdot A}{\varepsilon} + K \qquad \textcircled{1}$$

WHEN $x = A$, $V = -V_D$

$$-V_D = \frac{q n_A}{\varepsilon}\left(\frac{A^2}{2} - A^2\right) + K$$

$$-V_D = -\frac{q n_A}{\varepsilon}\left(\frac{A^2}{2}\right) + K$$

$$K = \frac{q n_A}{\varepsilon}\frac{A^2}{2} - V_D$$

$$K = q\frac{m_A}{\varepsilon}\frac{A^2}{2} - V_D$$

NOTICE THAT $\frac{(x-A)^2}{2} = \frac{x^2}{2} - Ax + \frac{A^2}{2}$

FROM ① ABOVE → PUTTING IN VALUE OF K

$$V(x>0) = \frac{qn_A}{\varepsilon}\left\{x^2 - Ax + \frac{A^2}{2}\right\} - V_D$$

$$V(x>0) + V_D = \frac{qn_A}{\varepsilon}\frac{(x-A)^2}{2} \quad — ②$$

NOW DO SAME THING FOR $x < 0$

$$V(x<0) = -\int q\frac{n_A \cdot A}{D}\left(\frac{x+D}{\varepsilon}\right)dx$$

$$= -q\frac{m_A \cdot A}{D}\frac{x^2}{2\varepsilon} - qn_A \cdot \frac{AD}{D\varepsilon} \cdot x + K$$

$$V(x) = -q\frac{n_A \cdot A}{D}\,\frac{x^2}{2\varepsilon} - q\,n_A \cdot \frac{A\,D}{D\varepsilon}\cdot x + K$$

AT $x = -D$, $V = 0$ BY DEFINITIONS

$$0 = -q\frac{n_A \cdot A}{D}\cdot\frac{D^2}{2\varepsilon} + q\frac{n_A \cdot A \cdot D^2}{D\varepsilon} + K$$

$$K = q\,n_A \cdot \frac{A\,D^2}{D\,2\varepsilon} - \frac{q\,n_A}{\varepsilon}\cdot D \cdot A$$

$$= q\,n_A\,\frac{A \cdot D}{2\varepsilon} - q\frac{n_A\,A \cdot D}{\varepsilon}$$

$$K = -q\,n_A\frac{DA}{2\varepsilon}$$

$$V(x<0) = -q\frac{n_A\,A}{D\,\varepsilon}\left(-\frac{x^2}{2} - x - \frac{D}{2}\right) = -\frac{q\,n_A}{D\varepsilon}\,\frac{(x+D)^2}{2}$$ ③

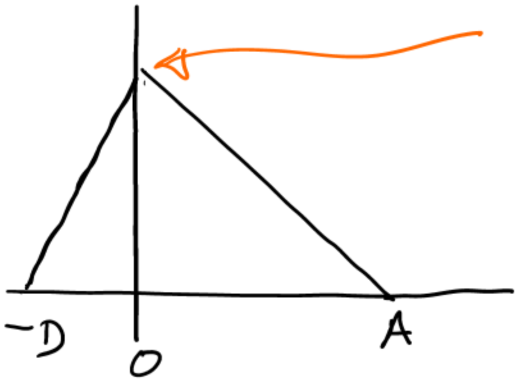

VOLTAGE HAS TO BE CONTINUOUS AT THE JUNCTION

$$V(x<0) = V(x>0) \quad \text{AT } x=0$$

$$-\frac{q n_A \cdot A (x+D)^2}{2D\varepsilon} = \frac{q n_A}{2\varepsilon}(x-A)^2 - V_D$$

$$V_D = \frac{q n_A \cdot A (x+D)^2}{2D\varepsilon} + \frac{q n_A}{2\varepsilon}(x-A)^2$$

$$= q n_A \left[\left\{ \frac{x^2}{D} + D + 2\frac{Dx}{D} \right\} + x^2 - 2Ax + A^2 \right]$$

$x=0$

$$= \frac{q n_A}{2\varepsilon} \left\{ AD^2 + A^2 \right\}$$

$$V_D = \frac{q n_A}{2\varepsilon} A (A+D)$$

WHAT WE WANTED

$$V_D = \frac{q n_A}{2\varepsilon} A (A+D)$$

USUALLY DETECTORS HAVE ASYMMETRIC DOPING

FOR EXAMPLE IF $n_D \gg n_A$, $A \gg D$

$$d = A + D \longrightarrow A$$

$$V_D = \frac{q n_A d^2}{2\varepsilon}$$

DO NOT CONFUSE WITH ρ

n LAYER IS VERY THIN , PUT $n_A = p$

$$E(x>0) = -q n_A (x-A)/\varepsilon \longrightarrow -qp(x-d)/\varepsilon$$

$$V(x>0) = \frac{q n_A (x-A)^2}{2\varepsilon} - V_D \longrightarrow qp(x-d)^2/2\varepsilon - V_D$$

PUTTING $V(x=0) \sim 0$

$$\text{BIAS VOLTAGE} \longrightarrow V_D = \frac{[qp]\, d^2}{2\varepsilon} \longleftarrow$$

DEPTH OF DEPLETION ZONE

$$V_D = \frac{[qp]\, d^2}{2\varepsilon}$$

$$d = \left(\frac{2\varepsilon V_D}{qp}\right)^{\frac{1}{2}}$$

RESISTIVITY

$$\rho = \frac{1}{q\mu n_A} = \frac{1}{q\mu p}$$

$$\frac{1}{qp} = \mu\rho$$

$$d = \sqrt{2\varepsilon\rho\mu V_D}$$

CAN PUT IN THE CONTACT POTENTIAL $V_0 \approx 1\,V$

$$d = \sqrt{2\varepsilon\rho\mu(V_D + V_0)}$$

V_D = BIAS VOLTAGE – 300V IN MODERN DETECTOR

TIME DEVELOPMENT OF SIGNAL PULSE

WE HAVE CHARGES MOVING IN AN ELECTRIC FIELD

$$E(x) = -q\rho\,(x-d)/\varepsilon \,, \quad \text{BUT } q\frac{\rho}{\varepsilon} = \frac{2V_D}{d^2}$$

$$E(x) = -\frac{2V_D}{d^2}(x-d)$$

TAKE SIMPLE CASE OF POINT IONIZATION @ $x=0$, $t=0$

FOR THE MOVING CHARGE

$$dx = \mu E\, dt = -\mu\frac{2V_D}{d^2}(x-d)\,dt$$

$$\int_{x_i}^{x_f}\frac{dx}{x-d} = -\mu\frac{2V_D}{d^2}\int_0^t dt$$

$$\ln(x_f-d) - \ln(x_i-d) = -\frac{2\mu V_D}{d^2}\cdot t$$

$$\ln\left\{\frac{x_f-d}{x_i-d}\right\} = -\boxed{\frac{2\mu V_D}{d^2}}\cdot t$$

$$\boxed{\frac{2\mu V_D}{d^2}} \rightarrow \frac{1}{\tau_D}$$

τ_D IS TIME FOR A CHARGE TO MOVE THRU DISTANCE d IN FIELD $E(0)$

$$x_f - d = (x_i - d)\,e^{-t/\tau_D}$$

$$x \rightarrow 0$$

$$x_f = d\left(1 - e^{-t/\tau_D}\right)$$

USING $\left\{\begin{matrix}\text{POTENTIAL ENERGY}\\ \text{CHANGE}\end{matrix}\right\}$ = WORK DONE FOR CHARGE MOVING IN $E(x)$

$$I(t) = \frac{dQ}{dt} = \mu\, q_s \frac{E^2}{V_D}$$

CURRENT

TOTAL SIGNAL CHARGE

NEED THIS

$$E(x) = \frac{-2V_D}{d^2}(x-d)$$

$$E^2(x) = \frac{4V_D^2}{d^4}\left[d(1-e^{-t/\tau_D}) - d\right]^2$$

$$E^2(x) = \frac{4V_D^2}{d^4}\cdot d^2 e^{-2t/\tau_D}$$

so $I(t) = \frac{\mu q_s}{V_D}\cdot \frac{4V_D^2}{d^2} e^{-2t/\tau_D}$

$$= \mu q_s \frac{4V_D}{d^2} e^{-2t/\tau_D} \qquad \mu = \frac{d^2}{2\tau_D V_D}$$

$$I(t) = 4 q_s \frac{d^2}{2\tau_D}\cdot\frac{1}{d^2} e^{-2t/\tau_D}$$

$$I(t) = \frac{2q_s}{\tau_D}\cdot e^{-2t/\tau_D}$$

Signal from Si Detector

SAME TREATMENT
AS SIGNAL IN GAS TUBE

$$I(t) = \frac{dQ}{dt} = \frac{\mu q_s E^2}{V_B}$$

$$= \frac{4\mu q_s V_B}{d^2} \exp\left(-\frac{2t}{\tau_D}\right)$$

$$= \frac{2q_s}{\tau_D} \exp\left(-\frac{2t}{\tau_D}\right)$$

$$I(0) = \frac{2q_s}{\tau_D}$$

$$I(\infty) = 0$$

$$\tau_D = \frac{d^2}{2\mu V_D} = \frac{d}{\mu E(0)}$$

- for a source charge q_s ~ 5*fC*

- peak electron (hole) currrent *710 nA* (240 nA)

- How does this compare to the noise level?

electron mobility $\mu_e \sim 1400\, cm^2 V^{-1} s^{-1}$

drift velocity $\sim 42\, \mu\, ns^{-1}$

for 300μ $\tau_D \sim 7\, ns$

DEPLETION LAYER PROPERTIES

FOR A PARALLEL PLATE CAPACITOR

$$C = \frac{\varepsilon A}{d} \leftarrow \text{AREA}$$

CAPACITANCE PER UNIT AREA

$$\frac{C}{A} = \frac{\varepsilon}{d} = \sqrt{\frac{1}{2\mu\rho(V_0+V_D)}}$$

INCREASING V_D → $\frac{C}{A} \propto \frac{1}{\sqrt{V_D}}$

IN $d = \sqrt{2\varepsilon\mu\rho(V_0+V_D)}$ PUT $\rho = \frac{1}{q\mu n_A}$

$$d = \sqrt{\frac{2\varepsilon(V_0+V_D)}{q\, n_A}} \leftarrow \text{DOPING CONCENTRATION}$$

$$d \propto \left(\frac{1}{M_A}\right)^{1/2}$$

$$d \propto \left(\frac{1}{n_A}\right)^{1/2}$$

- ONLY CHARGES RELEASED IN THE DEPLETION ZONE ARE COLLECTED & GIVE A SIGNAL
- HIGH DOPING → SMALL d
- FOR SMALL DOPING → NEED INTRINSIC CARRIER CONCENTRATION SMALL.

RESISTIVITY $\rightarrow \rho = \dfrac{1}{q\, n_i\, \mu}$ n_i → INTRINSIC

NEED HIGH RESISTIVITY (PURITY) SILICON

20 000 Ω cm ALLOWS $n_A \sim 2.3 \times 10^{11} / \mathrm{cm}^3$

$$d_{MAX} = \frac{\varepsilon\, E_{BREAKDOWN}}{q\, n_A}$$

20 000 Ω cm → 16,000 V/mm → 10 mm DEPLETION

10 cm IN Ge

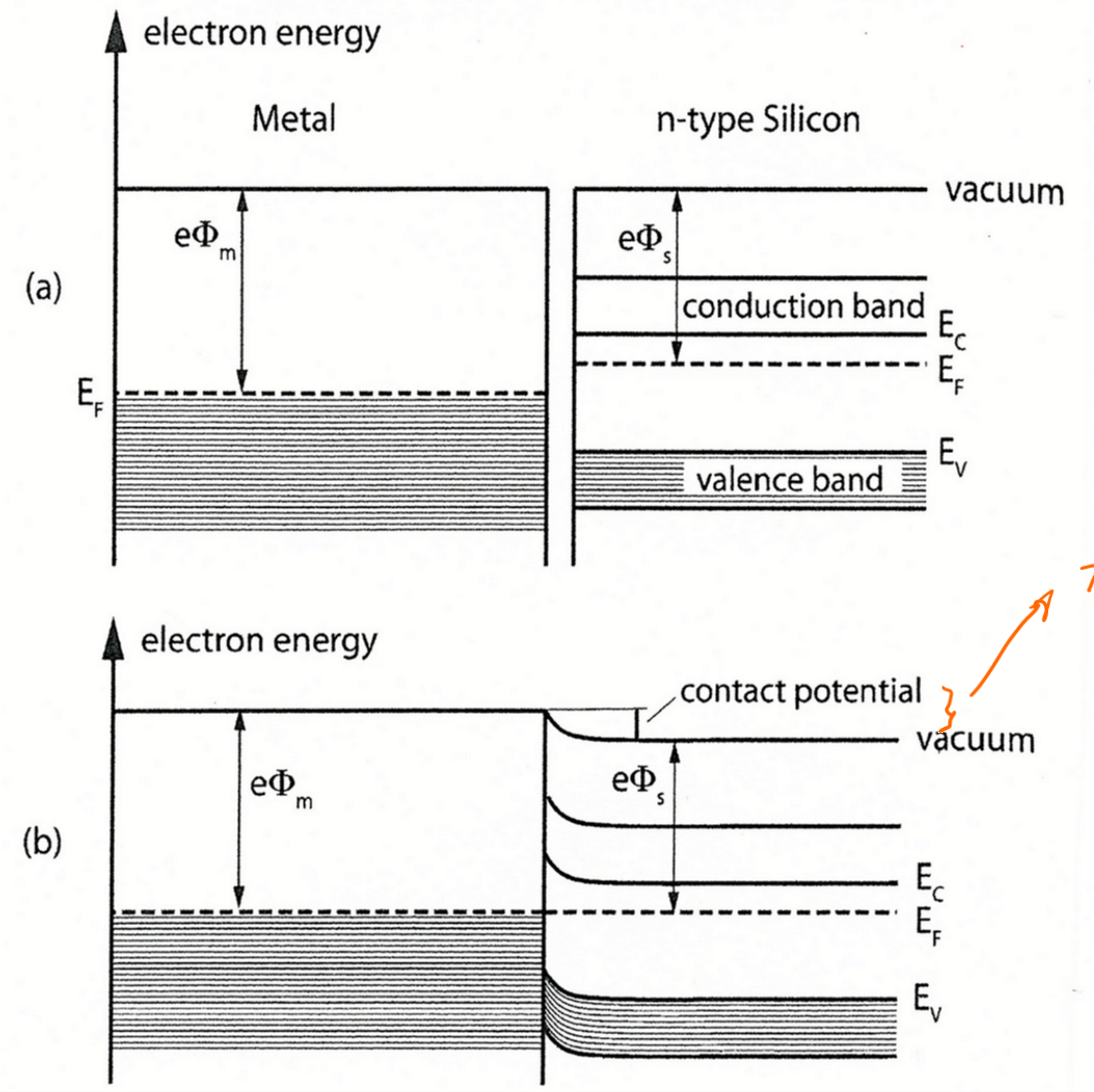

NO CONTACT

TO GET FROM Si INTO METAL ELECTRONS MUST OVERCOME THIS POTENTIAL

CONTACT

ON PREVIOUS PAGE, WORK FUNCTION IS ENERGY NEEDED TO MOVE ELECTRON FROM FERMI LEVEL IN SILICON TO POINT OUTSIDE

ON CONTACT

SPACE CHARGE IN METAL, DEPLETION ZONE IN SILICON

→ HOW TO GET ELECTRON (HOLES) OUT?

→ VERY HIGH DONOR CONCENTRATION AT INTERFACE

→ d VERY SMALL, CARRIERS TUNNEL THRU

"OHMIC" CONTACT n^+ or p^+ ALLOWS CARRIERS TO PASS WITH LOW RESISTANCE FROM SILICON INTO METAL CONTACT → ELECTRONICS.

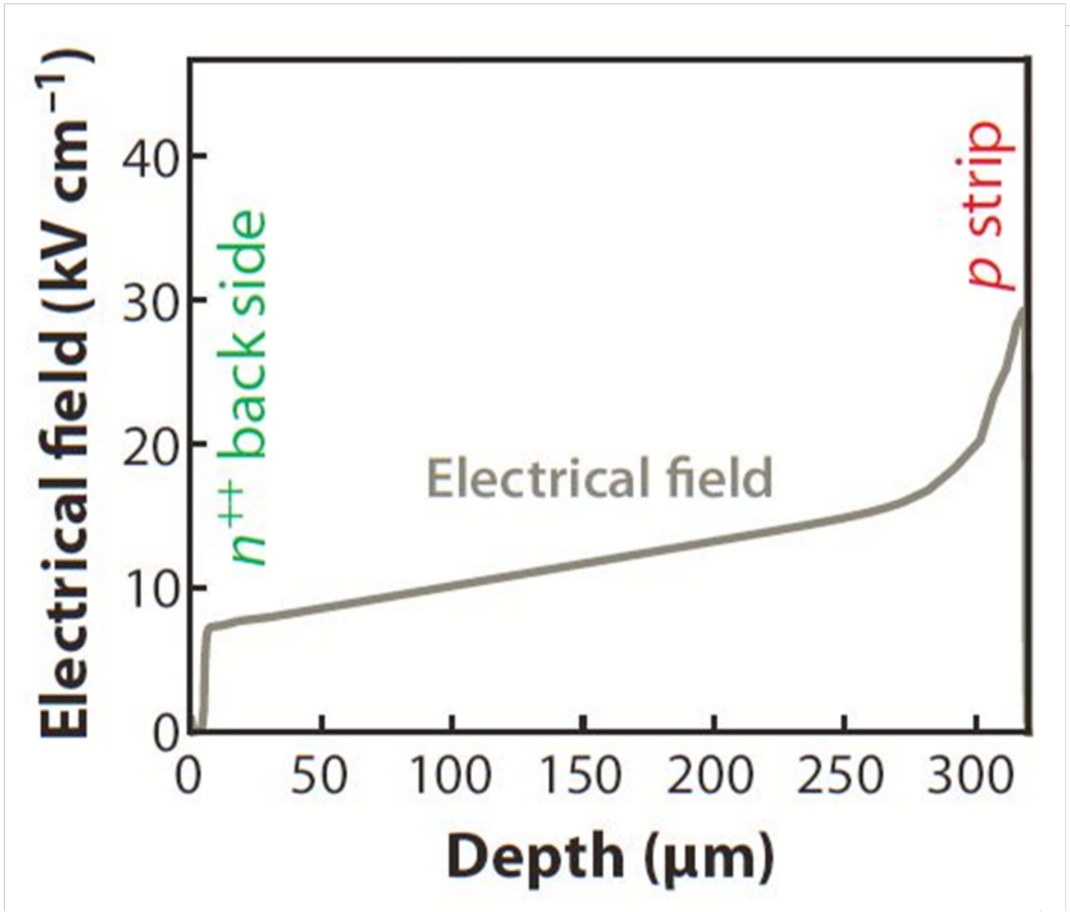

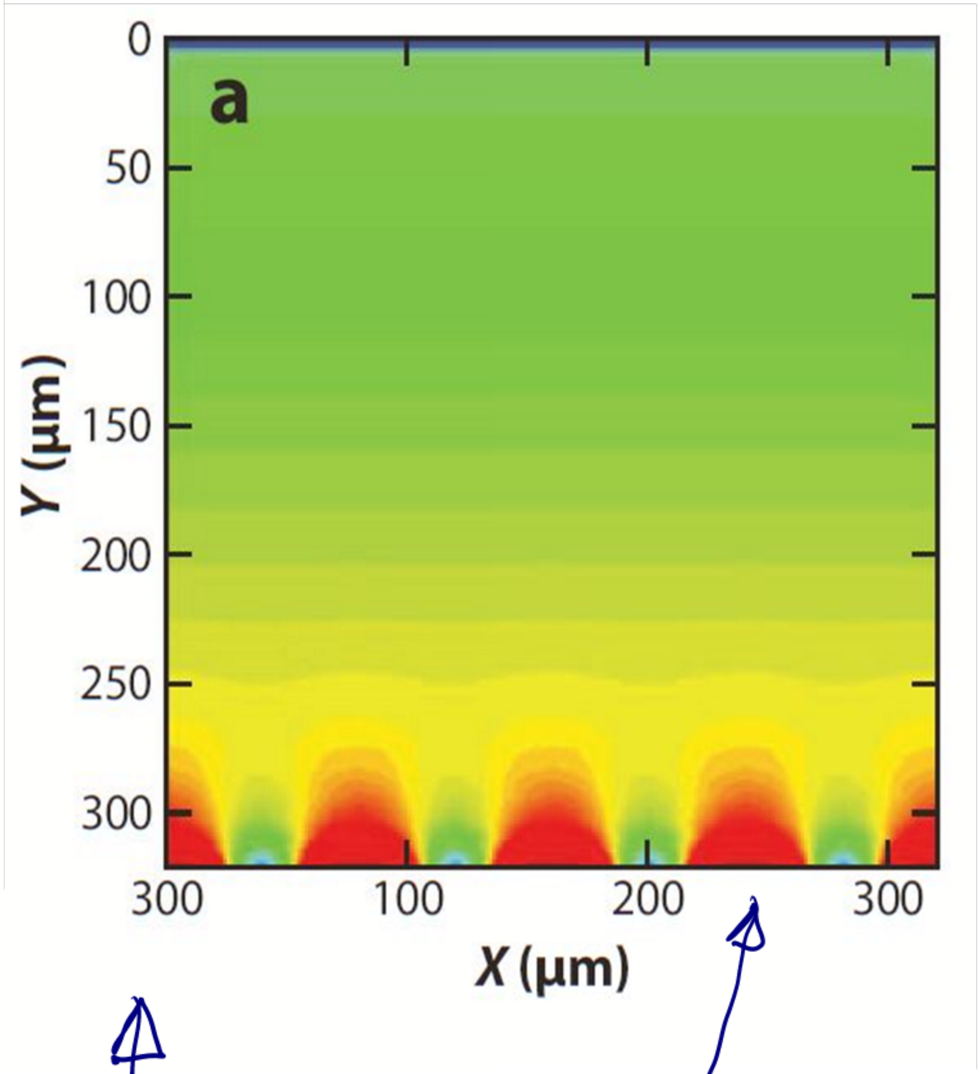

SIMULATION

DEPTH

STRIPS

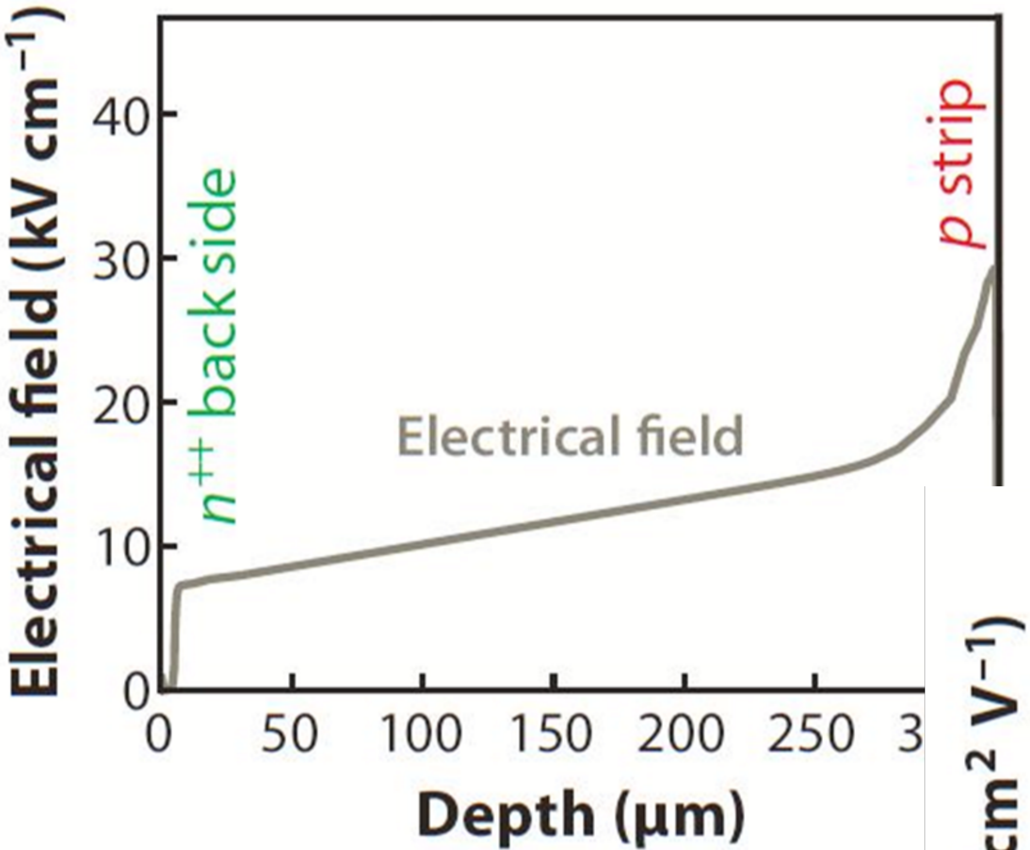

MOBILITY IS FIELD DEPENDENT

→ POSITION DEPENDENT

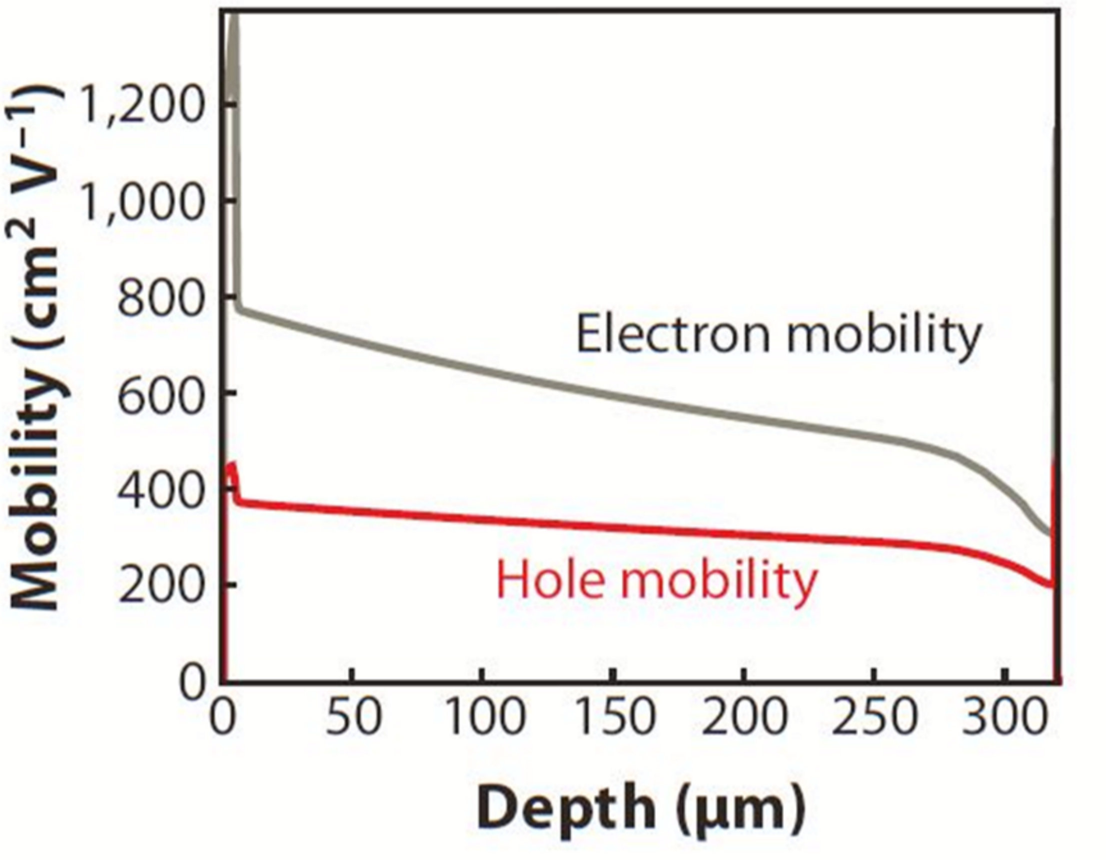

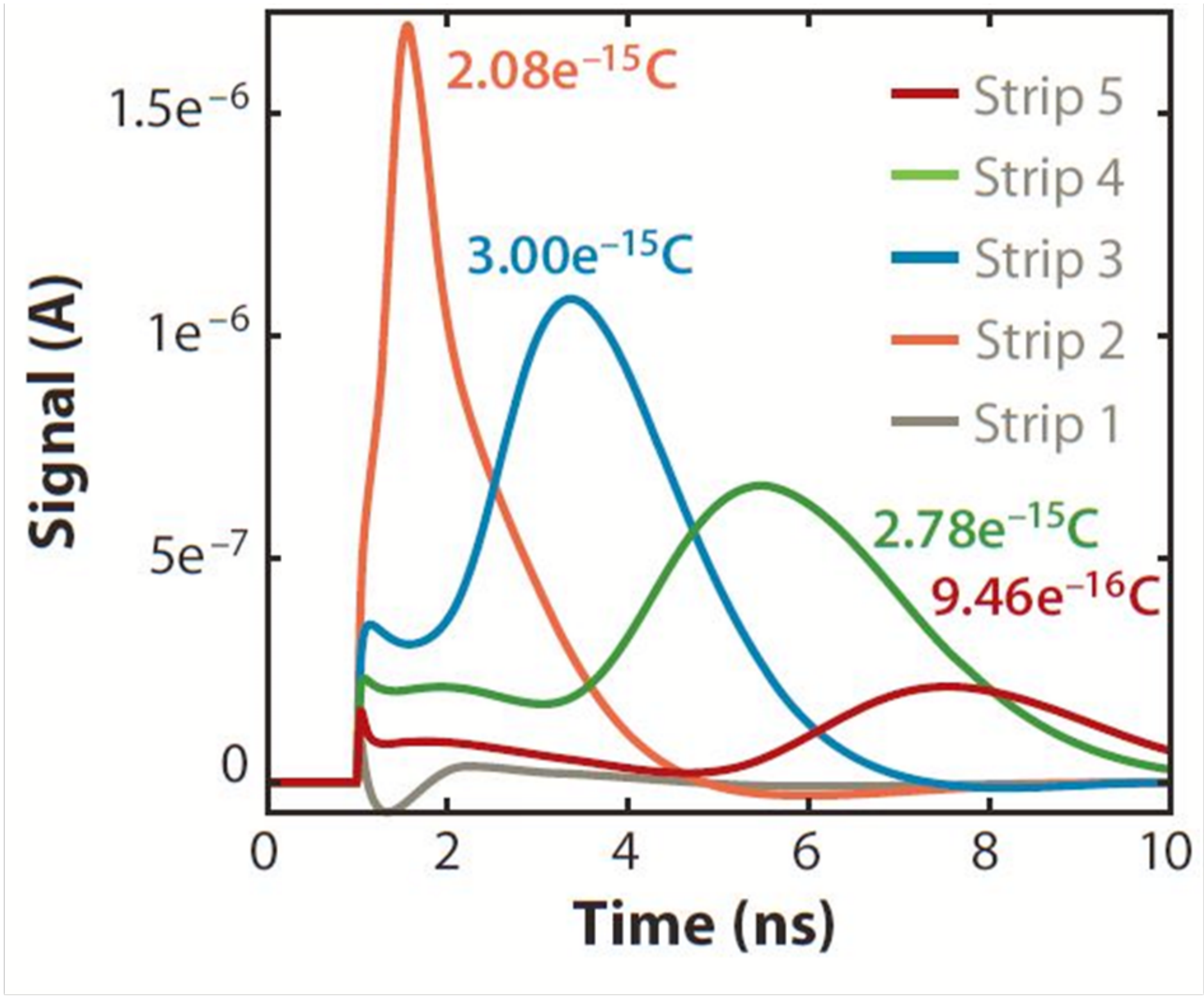

SIMULATION OF A TRACK PASSING THRU SENSOR AT 45°

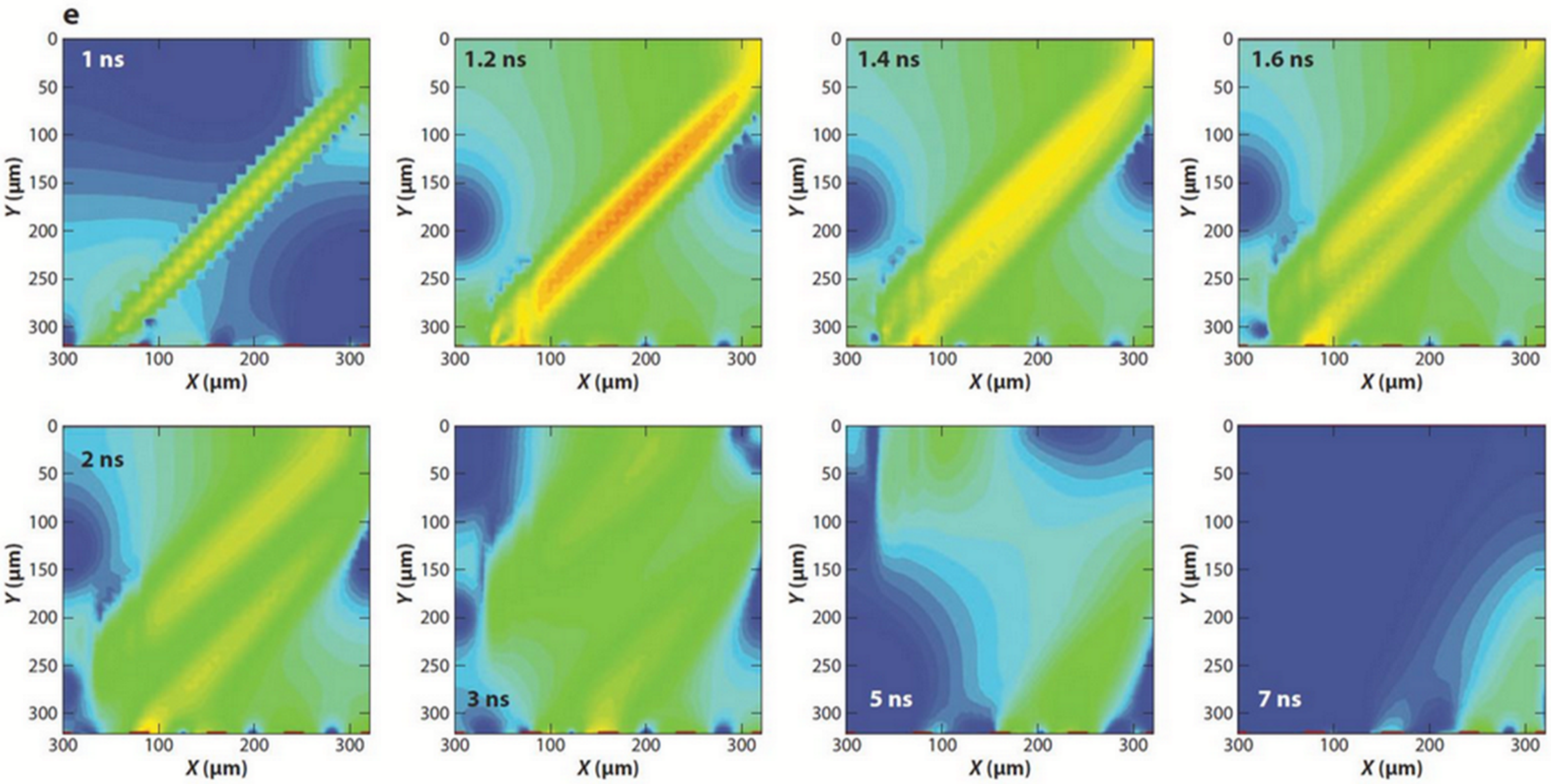
e
1 ns
1.2 ns
1.4 ns
1.6 ns
2 ns
3 ns
5 ns
7 ns
Y (μm)
0
50
100
150
200
250
300
X (μm)
300
100
200
300

$$I(t) = \frac{2q_s}{\tau_D} \cdot e^{-2t/\tau_D} \quad \text{———} \; \circledast$$

$\boxed{\text{Appendix}}$ → RECAP OF CHARGE MOVING IN ELECTRIC FIELD

energy in field $U = \frac{CV^2}{2} \rightarrow dU = CV\,dV$ ①

But $Q = CV \rightarrow dQ = C\,dV$

change in energy of field = work done by field on DRIFTING CHARGE

change in field energy

$$dU = \underbrace{CV}_{Q}\,\underbrace{dV}_{\frac{dQ}{C}}$$

$$\underline{dU} = Q\frac{dQ}{C} = F\,dx = q(t)E\,\langle v_d\rangle\,dt$$

charge induced on electrodes → $dQ(t) = q(t)\langle v_d\rangle\,dt\,\frac{E}{V}$ use $\frac{EC}{Q} = \frac{E}{V}$

$$\frac{dQ(t)}{dt} = I(t) = q\,v_d\,\frac{E}{v} \qquad v = \mu E$$

$$= q\mu\frac{E^2}{V}$$

detector is current source
+
capacitor

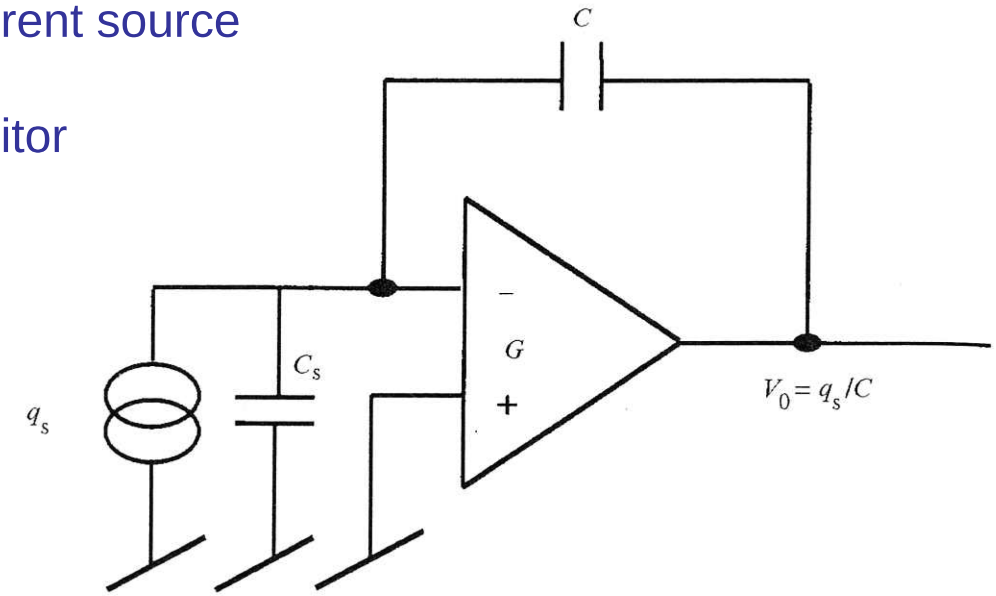

Fig. 9.10. Charge sensitive preamplifier.

$$Q = CV$$

$$I = \frac{dQ}{dt} = C\frac{dV}{dt}$$

$$V_{OUT} \propto q_S$$

- Using $Q = CV$, $I = C\frac{dV}{dt}$.

output voltage of OP amp $V_o \propto q_s$

if $G >> \frac{C_s}{C}$ then $(G \to \infty)$ $V_o = \frac{q_s}{C}$

- dissipative elements such as resistors are a source of intrinsic "thermal noise"

the size of the thermal currents is set by the thermal energy kT of the resistor

- Noise spectrum is uniform over all frequencies

kT per f

$\frac{\omega}{2\pi} = f$

$f = 2\pi\omega$

1 hz = 2π rad.

$f = \frac{\omega}{2\pi}$

$\frac{4kT}{2\pi}$

from Spieler

$$i_{nd}^2 = 2eI$$

$$i_{nb}^2 = 4kT/R_B$$

$$e_{ns}^2 = 4kTR_S$$

these come from diagrams over page

cf

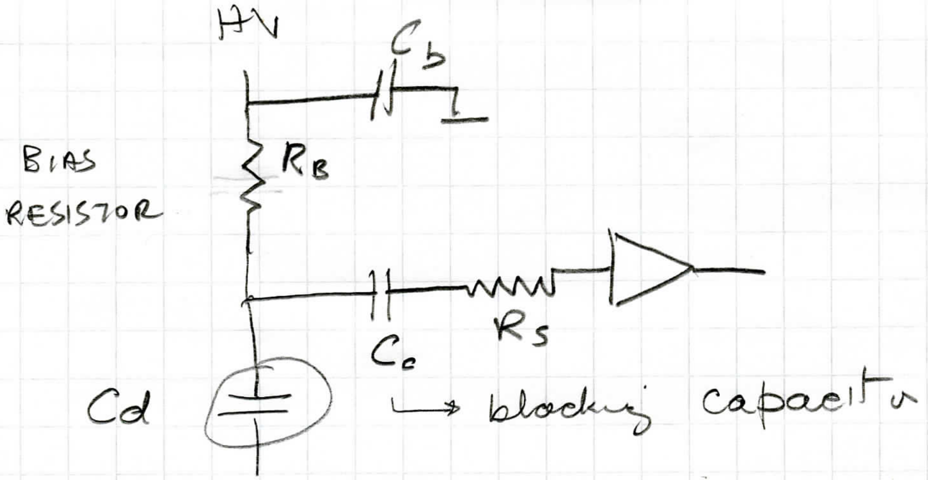

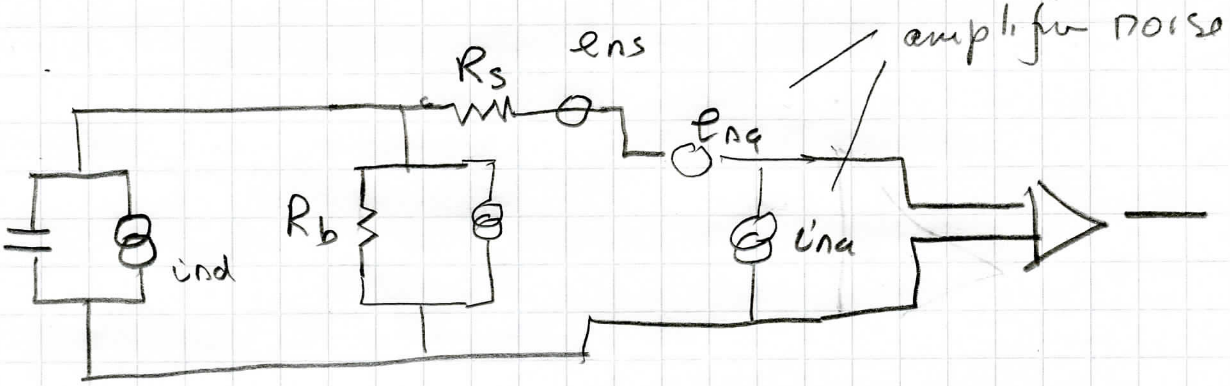

- leakage current i_{nd} shot noise

- Resistors SHUNTING INPUT — noise CURRENT Sour.

- Resistors in SERIES — noise voltage

origin of series / ∥el noise

$$i_{nd}^2 = 2eI_d \longleftarrow \text{bias current}$$

$$i_{nb}^2 = 4kT/R_B$$

$$e_{ns}^2 = 4kT R_s$$

GREEN

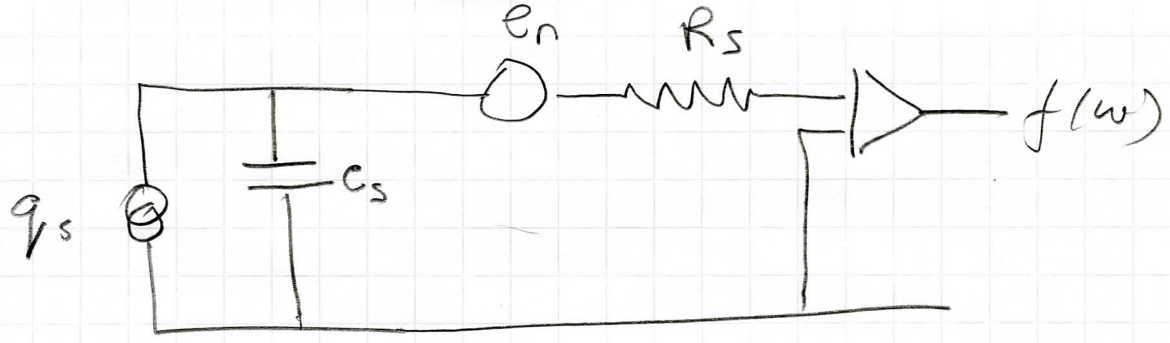

$$P = I^2 R$$

$$I^2 = \frac{P\,df}{R} = \frac{4KT}{R}\,df$$

$$= \frac{2KT}{R}\frac{d\omega}{\pi}$$

noise due to standing current is

$$dI_s = 2q\,df = q\,\frac{d\omega}{\pi}$$

$$dI^2 = q\,I\,\frac{d\omega}{\pi}$$

for an input transistor which is a forward biased

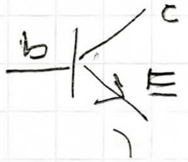

$$R_B = \frac{KT}{q\underset{\uparrow}{I_E}} = \frac{1}{g_m}$$

standing emitter current

3 sources of noise

1) thermal noise in Source resistor R_S

2) Shot noise due to standing current in front end emitter I_E

3) thermal noise in base resistor R_B

these currents flow into the source capacitance since we assume that $R_S \gg \frac{1}{\omega C_S}$ $\Leftarrow$ Reactance

Note that $I = C\frac{dV}{dt} = Ci\omega V$

$X_L = 2\pi f L$

means that capacitace reactance is

$X_C = \frac{1}{\underbrace{2\pi f}_{\omega} C}$

$V = IR \quad R = V/I = \frac{1}{i\omega C}$

so for the noise voltage we have

$$dV^2 = \underset{\substack{\uparrow \\ \text{thermal noise} \\ \text{in Source} \\ \text{Resistor}}}{dI_T^2 Z_{C_S}^2} + \underset{\substack{\uparrow \\ \text{Shot noise} \\ \text{in emitter}}}{dI_S^2 Z_{C_S^2}^2} + \underset{\substack{\uparrow \\ \text{BASE} \\ \text{RESISTOR} \\ \text{thermal noise}}}{dI_T^2 R_B^2}$$

$g_m = \frac{i_{out}}{V_{in}}$

$\frac{1}{R} = \frac{i}{V}$

$V = Vi$

$$\frac{2kT}{R_S(\omega C_S)^2} + \frac{q I_B}{(\omega C_S)^2} + \frac{2kT R_B^2}{R_B}$$

$$= \left[\frac{2kT}{R_S}\frac{1}{(\omega C_S)^2} + \frac{q I_B}{(\omega C_S)^2} + \frac{2kT}{g_m}\right]\frac{d\omega}{\pi}$$

$$\langle V^2\rangle = \int_0^\infty |f(\omega)|^2 \, \frac{dV^2}{d\omega} \cdot d\omega$$

now $\int_0^\infty |f(\omega)|^2 = \frac{\pi}{4}$

so $$\langle V^2\rangle = G^2 \Big[\underbrace{\left(\frac{kT}{2R_s} + q\frac{I}{4}\right)\frac{\tau}{C_s^2}}_{\text{SHUNT =PARALLEL}} + \underbrace{\frac{kT}{2g_m\tau}}_{\text{SERIES}} \Big) \Big]$$

noise going into C_s diverges at low frequency

series thermal noise diverges at high frequency

hence shaper 

Optimum filter is when frequency distribution of source = frequency pass of filter $= \frac{1}{\tau}$

$V = \frac{Q}{C}$ input $q_s \xrightarrow[\text{amp}]{} \frac{q_s G}{C_s} \cdot \frac{1}{e} = V$

frequency distribution of signal

$$V = \frac{q_s}{C_s} e^{-t/\tau} \cdot G$$

at $t = \tau$

$$V = \frac{q_s}{C_s} \frac{G}{e}$$

$$\langle V^2 \rangle = \left(\frac{q_s}{C_s} \cdot \frac{G}{e} \right)^2$$

write in terms of equivalent noise q
(i.e ... equivalent to so many electrons)

$$\langle V^2 \rangle = \left(\frac{ENC}{C_s} \frac{G}{e} \right)^2$$

$$ENC = \frac{C_s \cdot e}{G} \sqrt{\langle V^2 \rangle}$$

$$ENCP = \frac{\cancel{C_s}\, e}{\cancel{G}} \sqrt{\cancel{G^2} \left(kT/2R_s + q \frac{I_B}{4} \right)} \frac{\sqrt{\tau}}{\cancel{C_s}}$$

$$ENCP = e \sqrt{\left(\frac{kT}{2R_s} + q \frac{I_B}{4} \right) \tau}$$

$$ENCS = e C_s \sqrt{\frac{kT}{2 g_m}} \frac{1}{\tau}$$

For low noise T small

R_s large

I_B small } minimise $\parallel^{l}$

C_s small

R_B small } minimize serial

high speed means τ small, but series noise goes as $\frac{1}{\sqrt{\tau}}$

plot of noise $\parallel^{l}$ part is independent of C_s

series part – increases with C_s

---

so far have neglected transistor as source of noise

ⓔn in equivalent circuit

$$ENCS = \frac{e_n C_s}{\sqrt{\tau}}$$

Equivalent Circuit of Detector + Amplifier

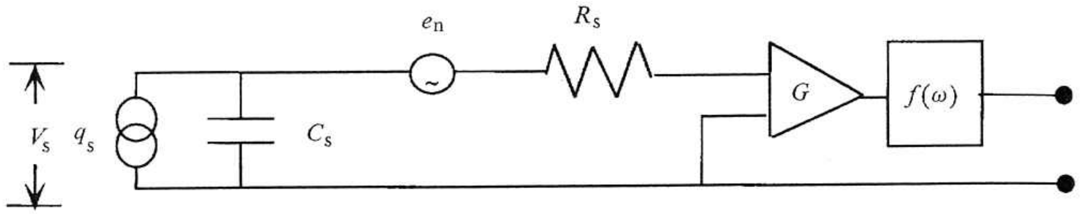

Fig. 9.11. Amplifier and bandwidth limiting filter, $f(\omega)$ with source capacitance, C_s, source resistance, R_s, source charge, q_s, and input noise voltage, e_n.

- resistors – source of thermal noise – thermal energy kT
  - noise is spread uniformly over all frequencies

$$I_T \rightarrow P = VI_T = I_T^2 R$$

$$dI_T^2 = \frac{2kT}{R}\left(\frac{d\omega}{\pi}\right)$$

thermal noise

- current made of – discrete carriers

$$dI_S^2 = qI\left(\frac{d\omega}{\pi}\right)$$

shot noise

- need to limit bandwidth or infinite noise

9.5 Noise sources – thermal and shot noise 193

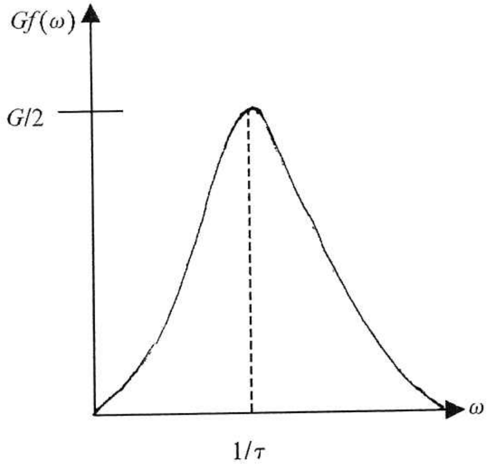

Plot of the transfer function $Gf(\omega)$ which $\to 0$ as $\omega \to 0$ and as $\omega \to \infty$ and $= 1/\tau$.

- frequency filter

$$f(\omega) = G\left[\frac{\omega\tau}{1+(\omega\tau)^2}\right]$$

$$\int_0^\infty f^2(\omega)\cdot d\omega = \frac{\pi}{4}$$

$$dI_s^2 = qI\,\frac{d\omega}{\pi}$$

$$\sqrt{qI} = 0.4\,nA\sqrt{I\ Hz}$$

$$\sqrt{\frac{2kT}{R}} = 0.9\,nA\sqrt{\frac{Hz}{R}}$$

- for a frequency range of 100 MHz and 1mA
- 126 nA – pretty close to signal

$$dI_T^2 = \frac{2kT}{R}\,\frac{d\omega}{\pi}$$

Three sources of noise

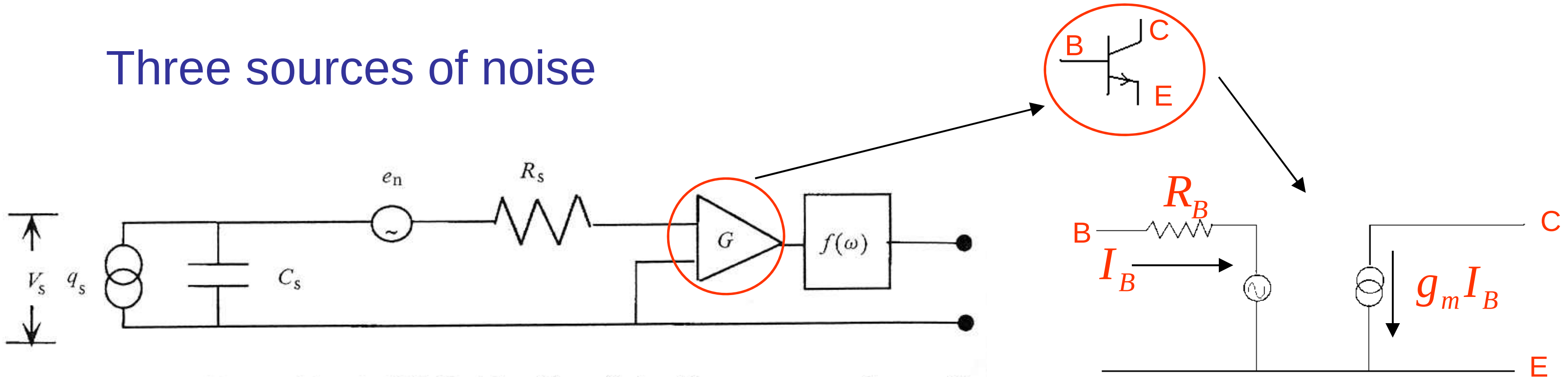

Fig. 9.11. Amplifier and bandwidth limiting filter, $f(\omega)$ with source capacitance, C_s, source resistance, R_s, source charge, q_s, and input noise voltage, e_n.

- Thermal – R_S
- Shot - I_E
- Thermal - R_B

SEE NEXT SLIDE

$$d\overline{V}^2 = d\overline{I}_T^2 Z_{C_S}^2 + d\overline{I}_S^2 Z_{C_S}^2 + d\overline{I}_T^2 R_B^2$$

$$= \left[\frac{2kT}{R_S(\omega C_S)^2} + \frac{qI_B}{(\omega C_S)^2} + \frac{2kT}{g_m} \right] \left(\frac{d\omega}{\pi} \right)$$

$\frac{1}{\omega^2}$ constant

After shaping (filter)
Equivalent Noise Charge

$$ENCP = 2.72\sqrt{\tau\left(\frac{kT}{2R_S} + q\frac{I_B}{4}\right)}$$

$$ENCS = 2.72 C_S \sqrt{\frac{kT}{2g_m \tau}}$$

- Low temp
- R_S large
- I_B small
- C_S small
- R_B small

parallel noise

series noise

THREE SOURCES OF NOISE

- THERMAL NOISE IN SOURCE RESISTOR R_S
- SHOT NOISE DUE TO STADING EMITTER CURRENT IN AMPLIFIER TRANISTOR
- THERMAL NOISE IN BASE RESISTOR

THE NOISE CURRENTS DEVELOP A VOLTAGE ACROSS THE SOURCE CAPACITANCE.

SO THEY LOOK JUST LIKE THE SIGNAL ACROSS THE SOURCE CAPACITANCE

FOR A CAPACITOR $Z_C = 1/i\omega C$

FOR A RESISTOR $Z_R = R$

SO YOU MIGHT EXPECT VOLTAGE ACROSS R & C TO BE OUT OF PHASE. BUT THEY ARE STATISTICALLY INDEPENDET → ADD IN QUADRATURE

$$d\bar{v}^2 = \overset{\text{THERMAL NOISE IN CAP}}{\underset{\frac{2kT}{R_s}}{d\bar{I}_T^2}\,\underset{\frac{1}{(\omega C_s)^2}}{Z_{C_s}^2}} + \overset{\text{SHOT NOISE IN CAP}}{\underset{qI_B}{d\bar{I}_s^2}\,Z_{C_s}^2} + \overset{\text{THERMAL NOISE IN BASE RESISTOR}}{\underset{\frac{2kT}{R_B}}{d\bar{I}_T^2}\,\underset{\frac{1}{g_m}}{R_B^2}}$$

$$d\bar{v}^2 = \left[\frac{2kT}{R_s(\omega C_s)^2} + \frac{qI_B}{(\omega C_s)^2} + \frac{2kT}{g_m}\right]\frac{d\omega}{\pi}$$

RMS VOLTAGE

$$\langle v^2\rangle = \int_0^\infty |f(\omega)|^2\,\frac{d\bar{v}^2}{d\omega}\,d\omega$$

$$= G^2\left[\left(\frac{kT}{2R_s} + \frac{qI_B}{4}\right)\frac{\tau}{C_s^2} + \frac{kT}{2g_m\tau}\right]$$

$$\langle V^2 \rangle = G^2 \left[\underbrace{\left(\frac{kT}{2R_s} + q\frac{I}{4} \right) \frac{\tau}{C_s^2}}_{\text{"SHUNT = ||el"}} + \underbrace{\frac{kT}{2 g_m \tau}}_{\text{"SERIES"}} \right]$$

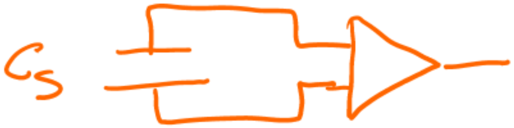

$\tau \sim \frac{1}{\omega}$

DIVERGES AS $\omega \to 0$

DIVERGES AT LARGE ω

THIS IS WHY WE NEED FILTER

FREQUENCY RESPONSE = FREQUENCY OF SIGNAL

$$V = q_s / C$$

FREQUENCY DISTRIBUTION OF SIGNAL $q_s e^{-t/\overset{\text{FILTER}}{\tau}} \cdot G$

IF PEAK SIGNAL = PEAK FILTER

$\tau \sim t$

$$V = \frac{q_s}{C_s} e^{-t/\tau} \cdot G$$

$$V = \frac{q_s}{C_s} \cdot \frac{G}{e}$$

NOT ELECTRIC CHARGE

$$\langle V^2 \rangle = \left(\frac{q_s}{C_s} \cdot \frac{G}{e} \right)^2$$

WRITE IN TERMS OF EQUIVALENT NOISE CHARGE

$$\langle V^2 \rangle = \left(\frac{ENC}{C_s} \cdot \frac{G}{e} \right)^2 \Rightarrow ENC = \frac{C_s \cdot e}{G} \cdot \sqrt{\langle V^2 \rangle}$$

FOR A SIGNAL CHARGE q_s, IF THE FILTER MATCHES THE FREQUENCY DISTRIBUTION OF THE SOURCE

2.72....

$$q_s \rightarrow \frac{q_s G}{C_s} / e = V$$

CHARGE ENC $\rightarrow \left(ENC \cdot \frac{G}{C_s e} \right)^2 \equiv \langle V^2 \rangle$

NOISE CHARGE
FROM ALL SOURCES

$$ENC\,P = (G_s e/G) \sqrt{\langle V^2 \rangle_P} \equiv e \sqrt{\tau \left(\frac{kT}{2R_s} + q \frac{I_B}{4} \right.}$$

$$ENC\,S = (C_s e/G) \sqrt{\langle V_2 \rangle_S} \equiv e\, C_s \sqrt{\frac{kT}{2g_m} \frac{1}{\tau}}$$

$P \Rightarrow \|^{el}$ RESISTOR ; $S \Rightarrow$ SERIES RESISTOR

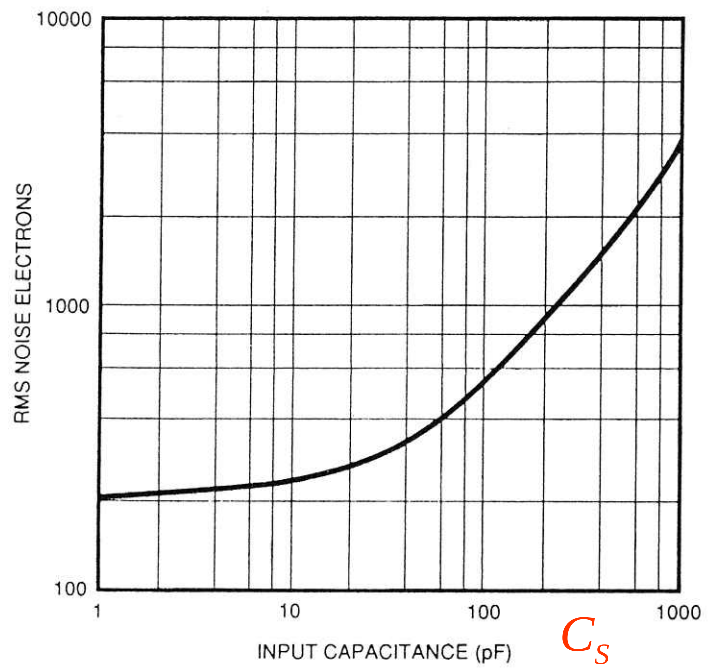

C_S

- minimize detector cap – minimize noise
- long strips? – cheap – too noisy

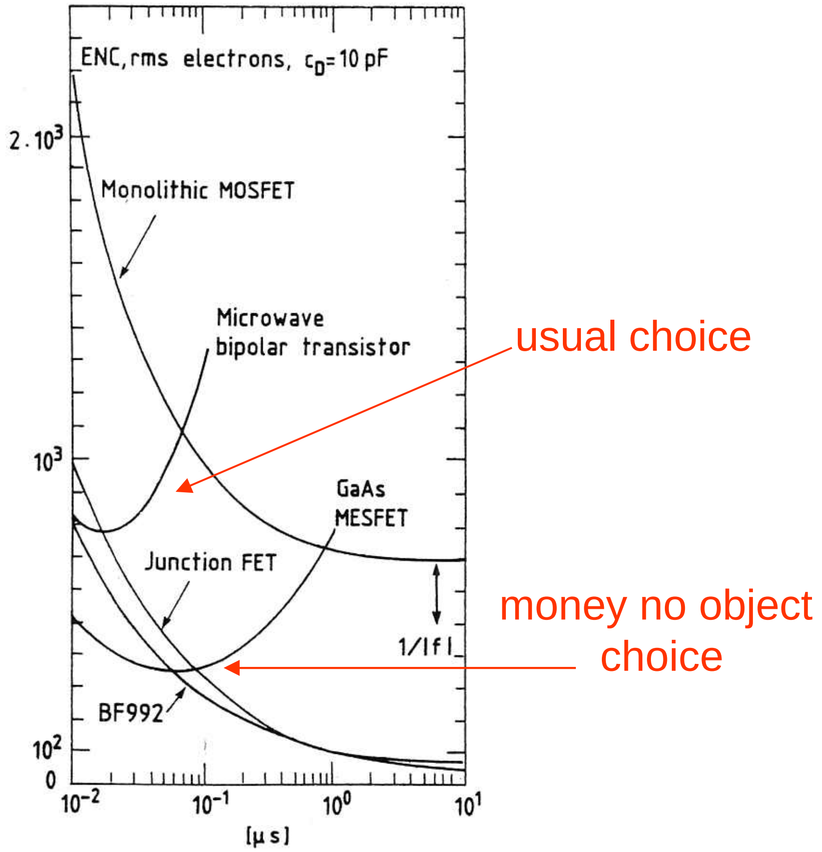

usual choice

money no object choice

- transistor noise

$$\left.\begin{array}{l} C_S = 25\ pF \\ \tau = 25\,ns \end{array}\right\} \sim 1000 \text{ electrons}$$

cf signal ~ 31000 electrons

Total Noise

(a)

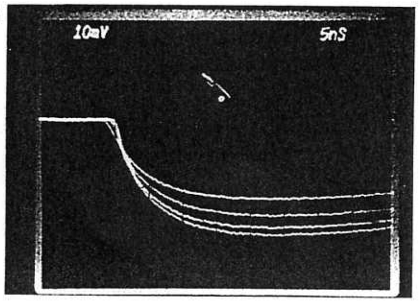

raw

(b)

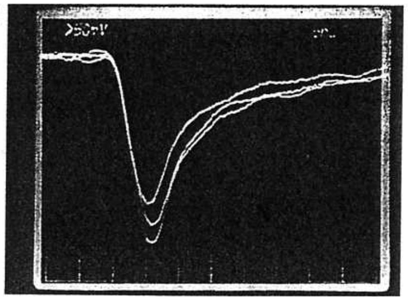

cancel tail

(c)

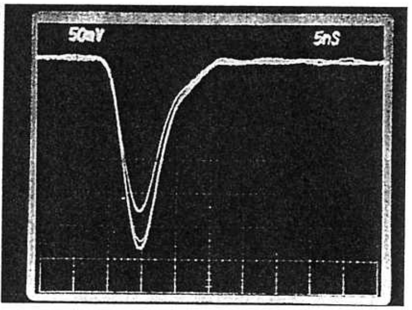

pole-zero shaping

(d)

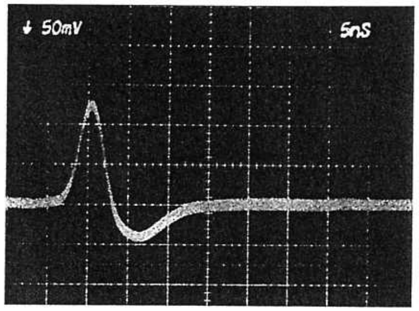

impulse response
- noise

series noise

$q_s \sim 51\ fC$

$g_m \sim \cancel{25\Omega^{-1}}$ → 4×10^{-2}

$C_S \sim 30\ pF$

$\tau \sim 10\,ns$

~~1125~~ electrons
1152

parallel noise

$R_S \sim 1M\Omega$

$I_B \sim 1mA$

825 electrons

add in quadrature

$$\frac{\text{Signal}}{\text{Noise}} \sim 23$$

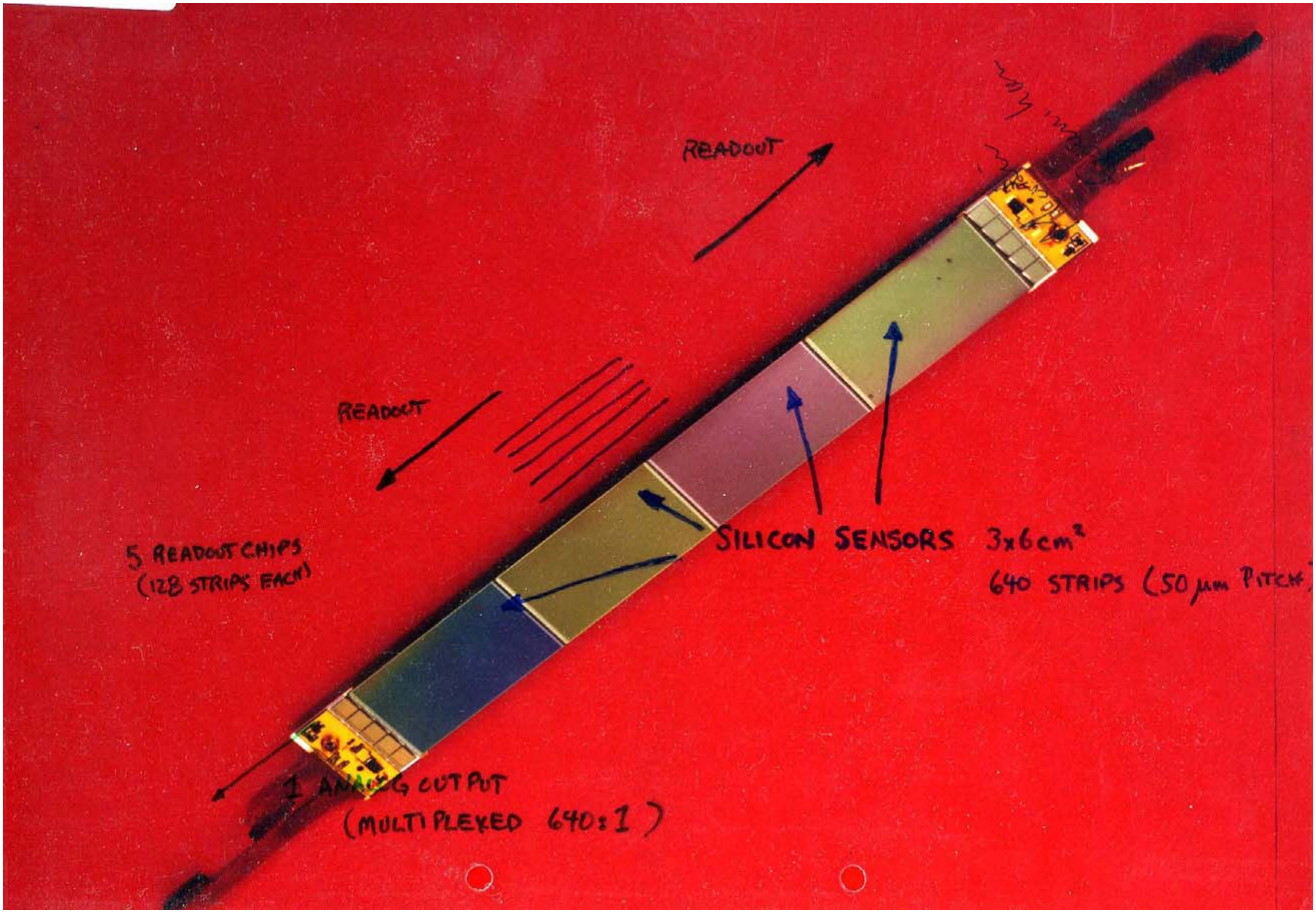
READOUT
READOUT
5 READOUT CHIPS
(128 STRIPS EACH)
SILICON SENSORS 3x6cm²
640 STRIPS (50 μm PITCH)
1 ANALOG OUTPUT
(MULTIPLEXED 640:1)

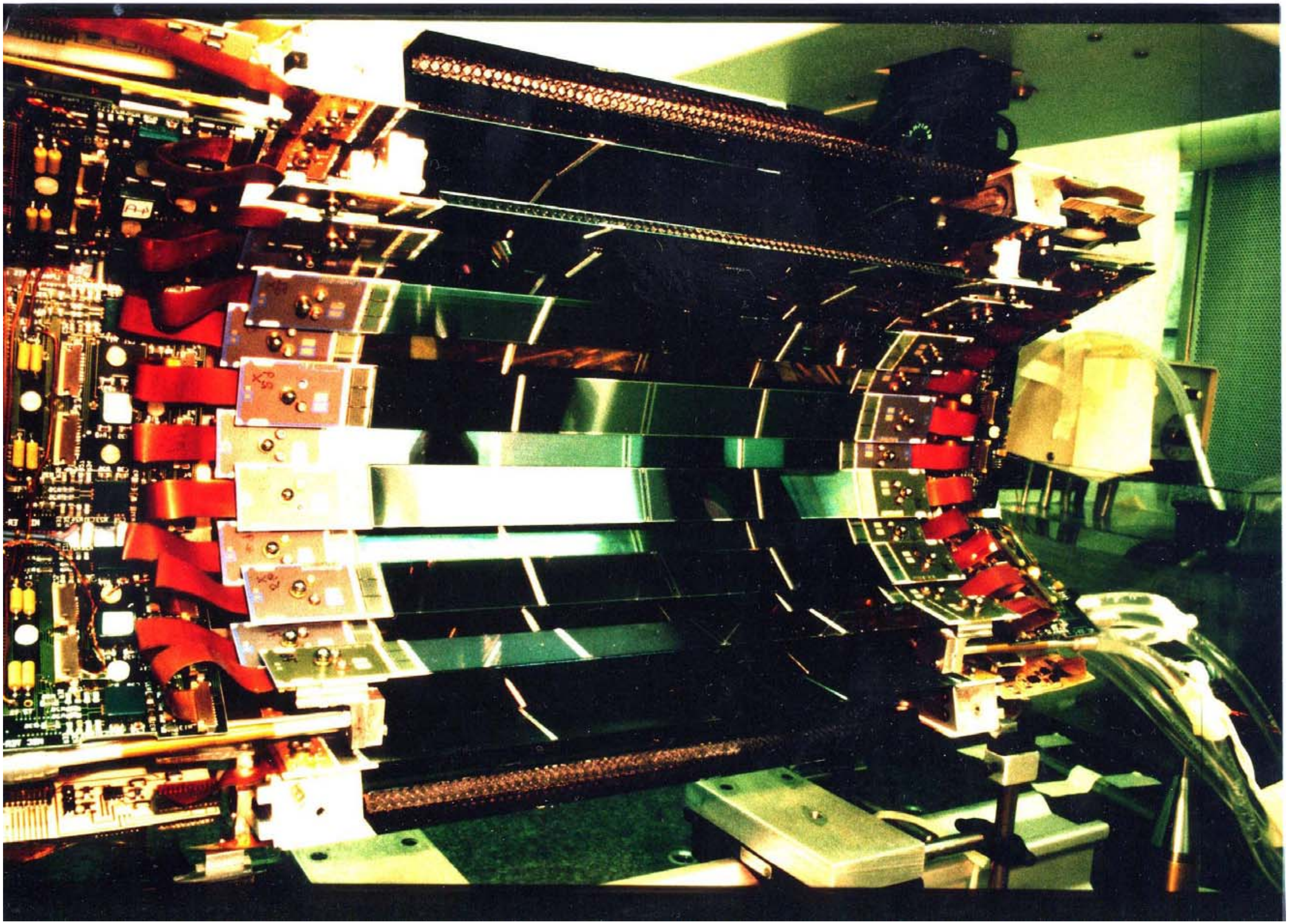

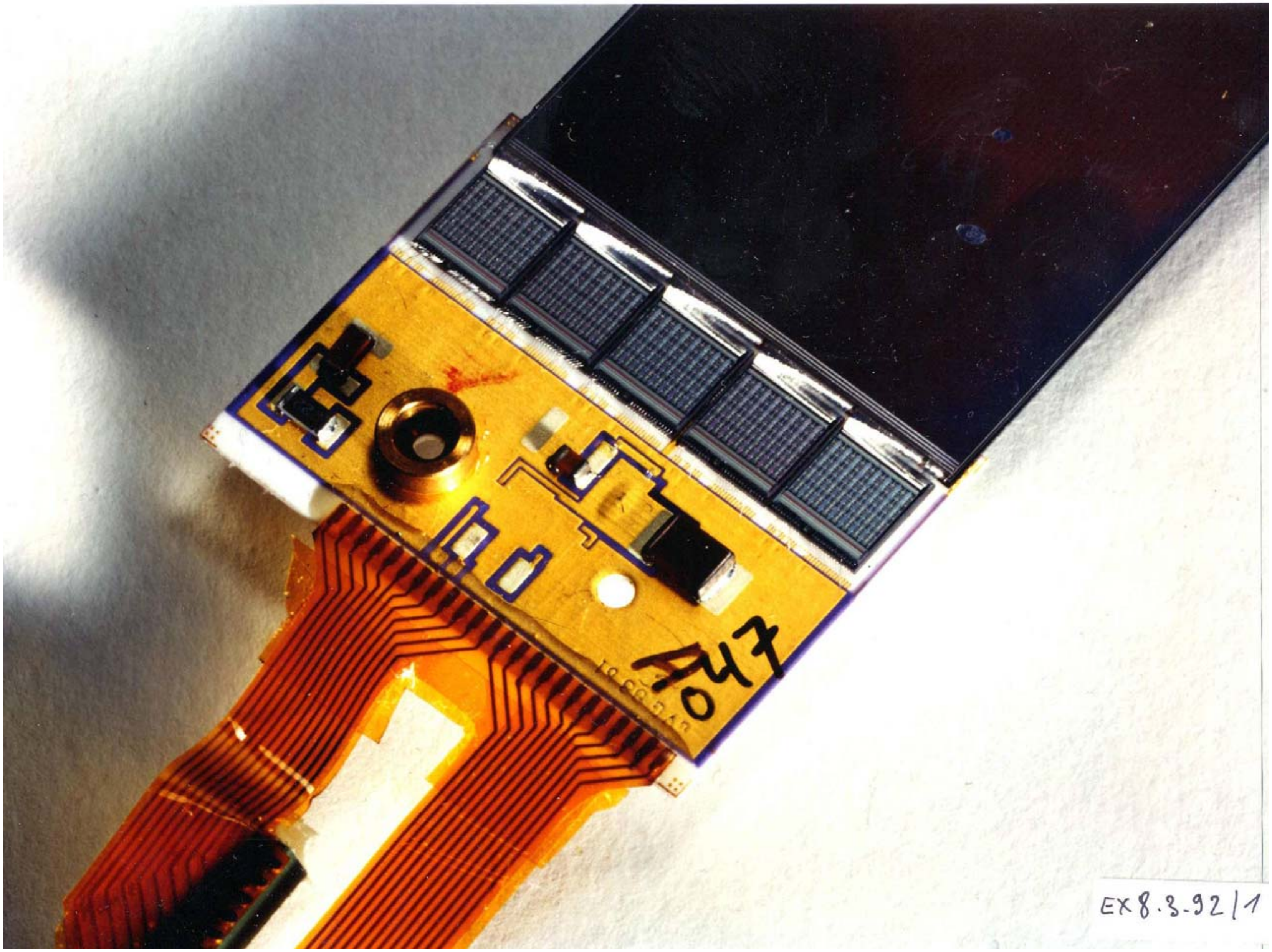
047
EX 8.3-92/1

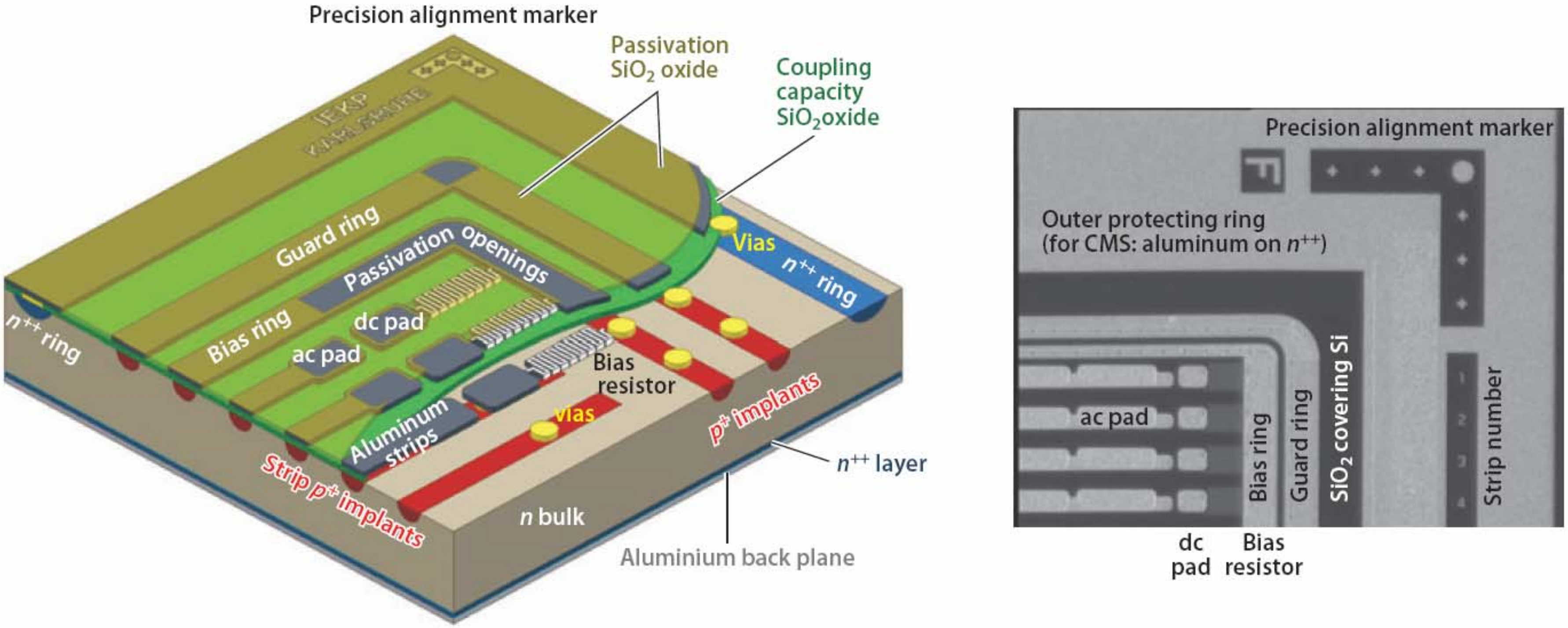

Figure 2

(*a*) Three-dimensional schematic of a single-sided, ac-coupled, polysilicon resistor–biased sensor showing the baseline of the CMS sensor at the LHC. During operation, the bias ring is connected to the GND (ground) potential, which is then distributed via the polysilicon bias resistors to the p^+ implant strips. The aluminum back plane is set to positive high voltage, depleting the full n-bulk volume of free-charge carriers by forming a pn-junction p^+ strip to n bulk. The long strips and thin decoupling oxide allow high coupling capacitances to be implanted directly into the sensor. The guard ring shapes the field at the borders. The n^{++} ring defines the active volume and prevents high field in the edge regions. (*b*) View of an actual sensor surface with a strip pitch of 80 μm.

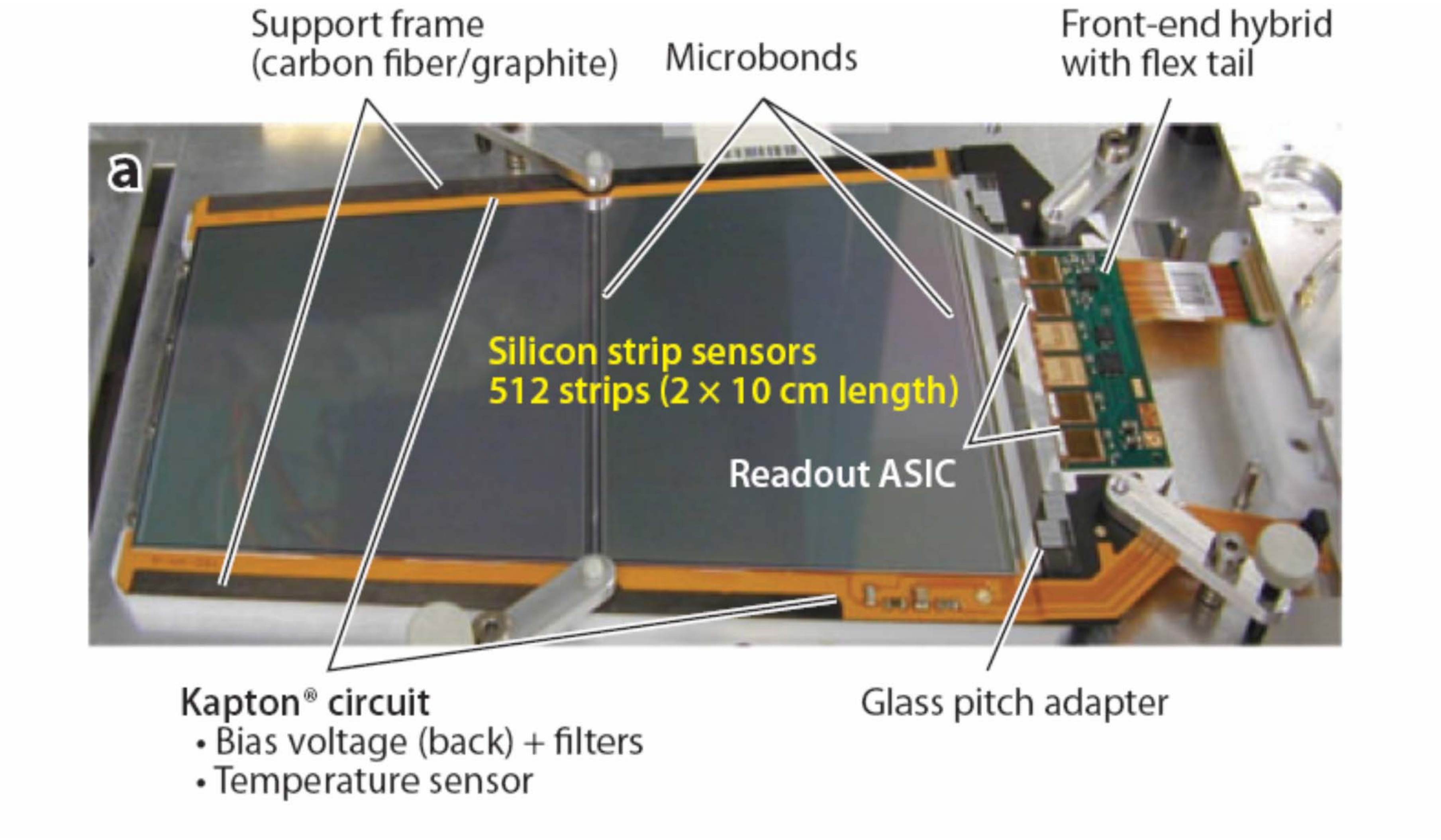
Support frame
(carbon fiber/graphite)
Microbonds
Front-end hybrid
with flex tail
a
Silicon strip sensors
512 strips (2 × 10 cm length)
Readout ASIC
Kapton® circuit
• Bias voltage (back) + filters
• Temperature sensor
Glass pitch adapter

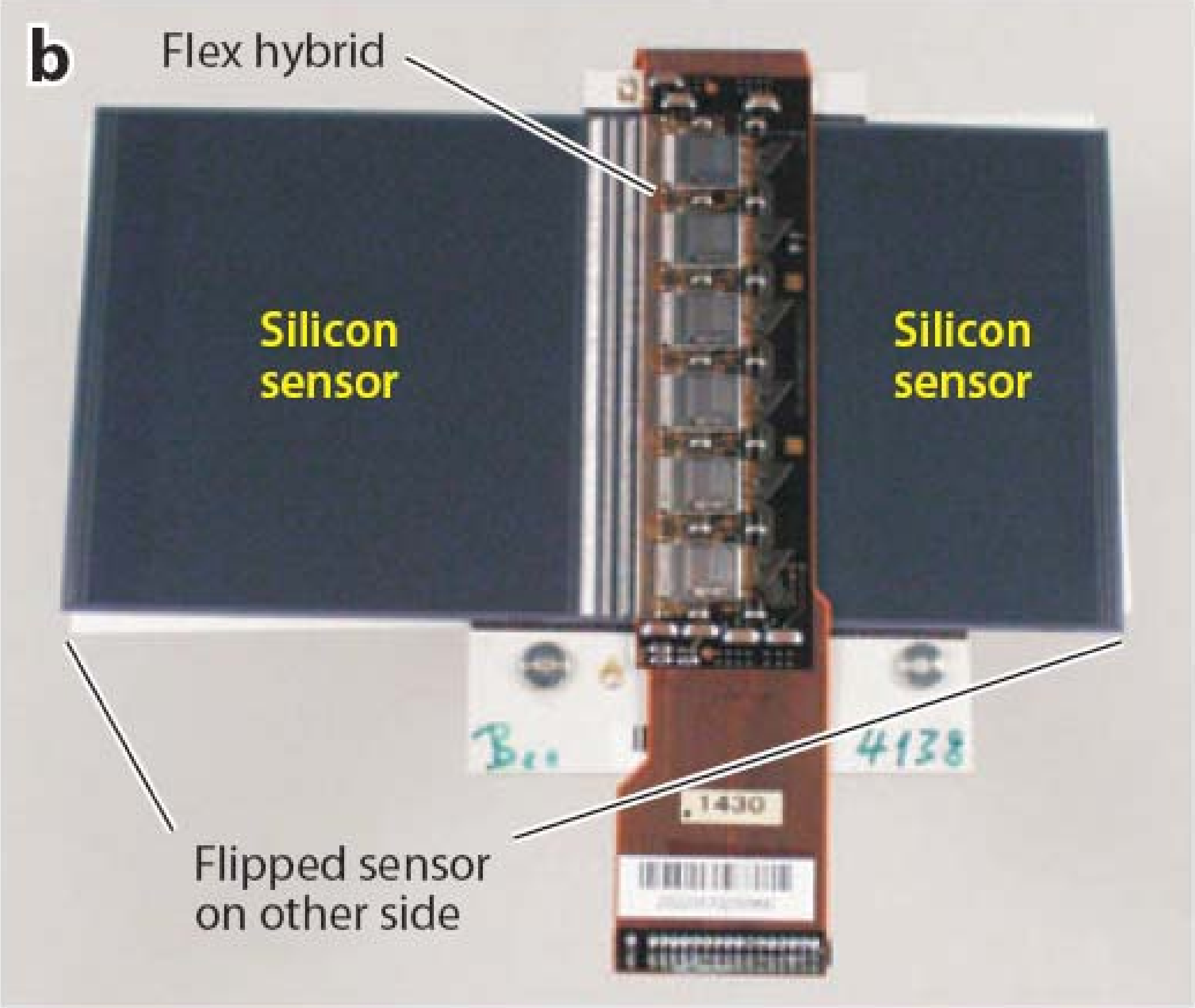
b
Flex hybrid
Silicon sensor
Silicon sensor
B..
4138
.1430
Flipped sensor on other side

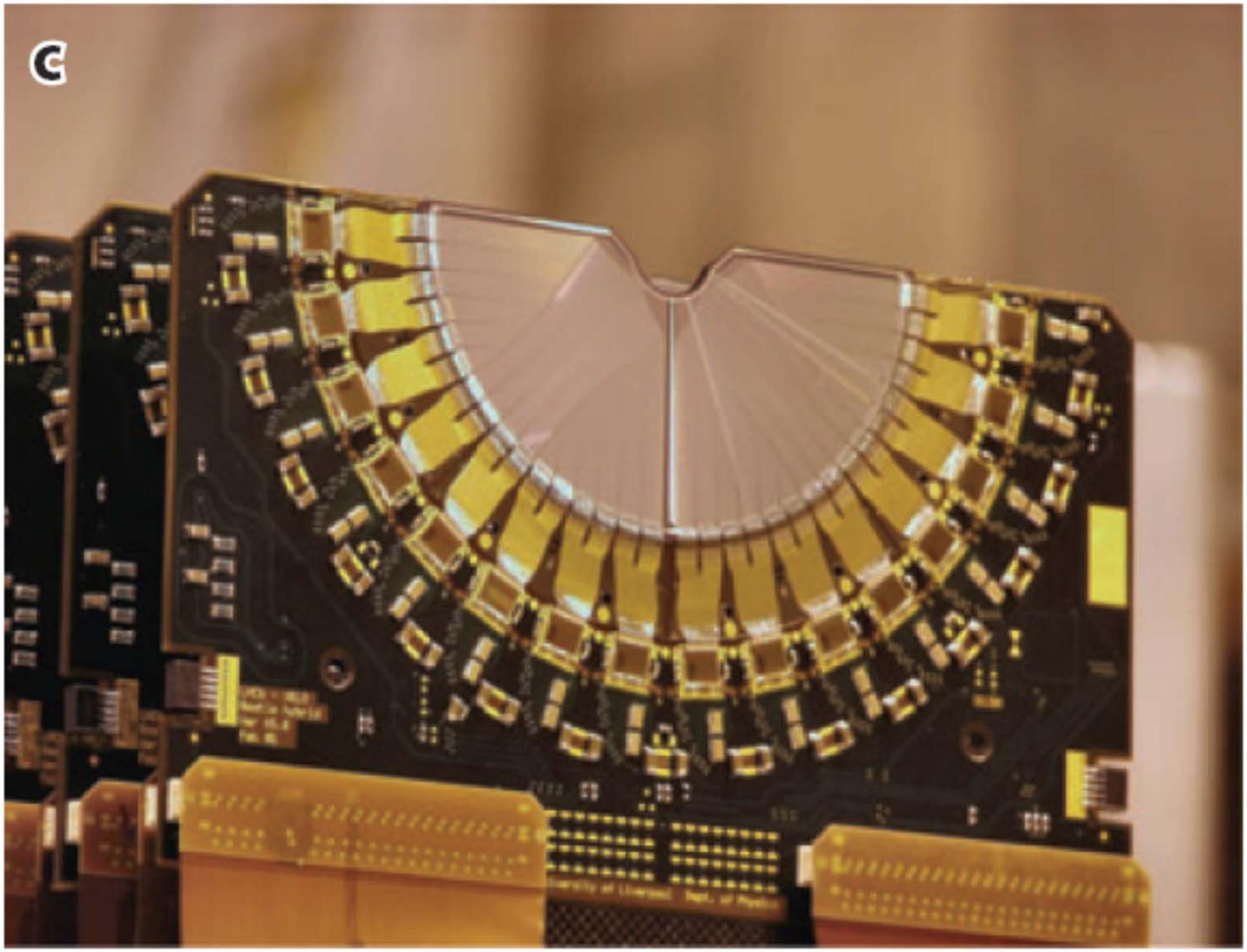
c

The ATLAS Inner Detector

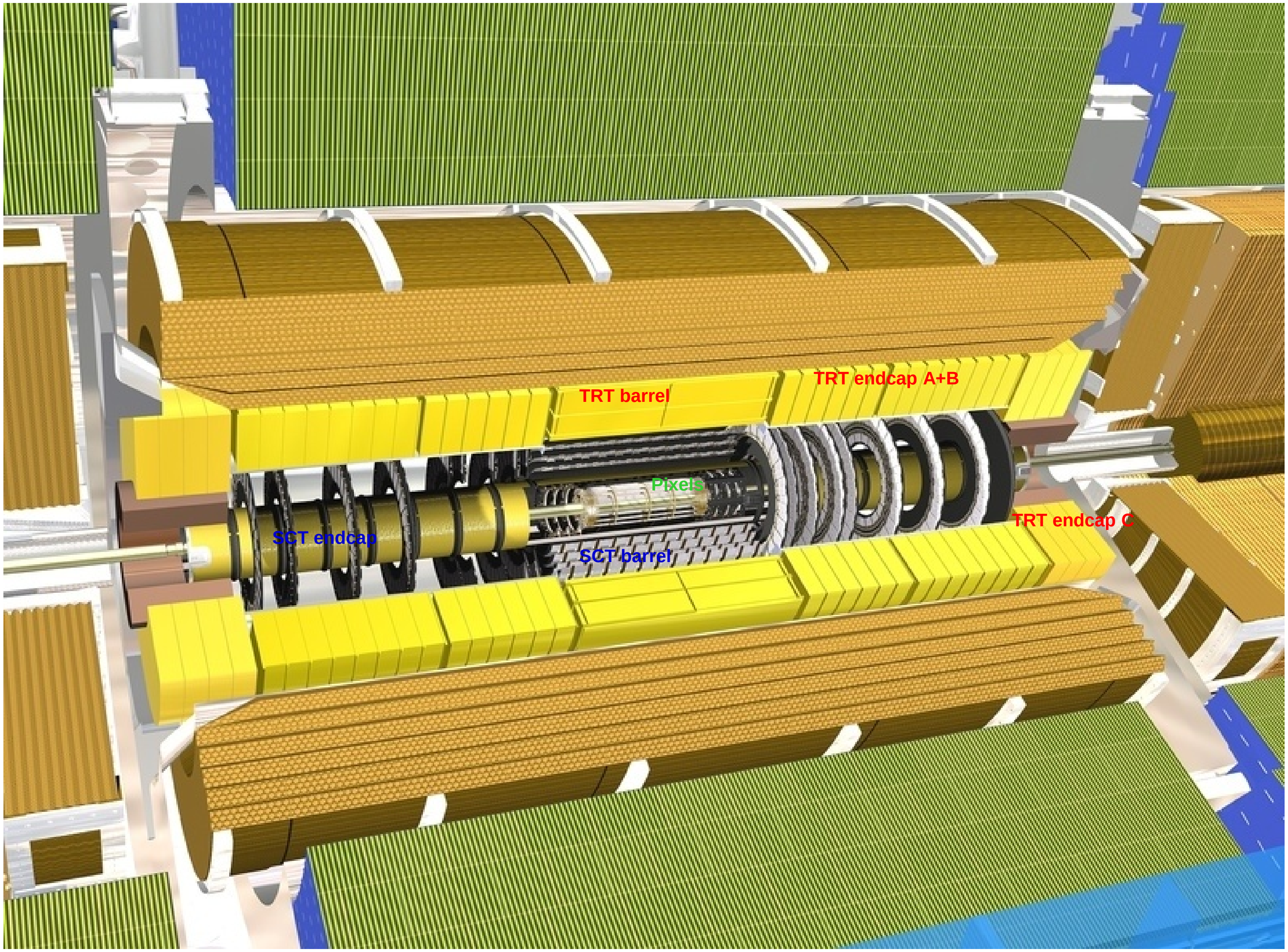

Inner Detector (ID)

The Inner Detector (ID) comprises four sub-systems:

- Pixels (0.8 10^8 channels)
- Silicon Tracker (SCT) (6 10^6 channels)
- Transition Radiation Tracker (TRT (4 10^5 channels)

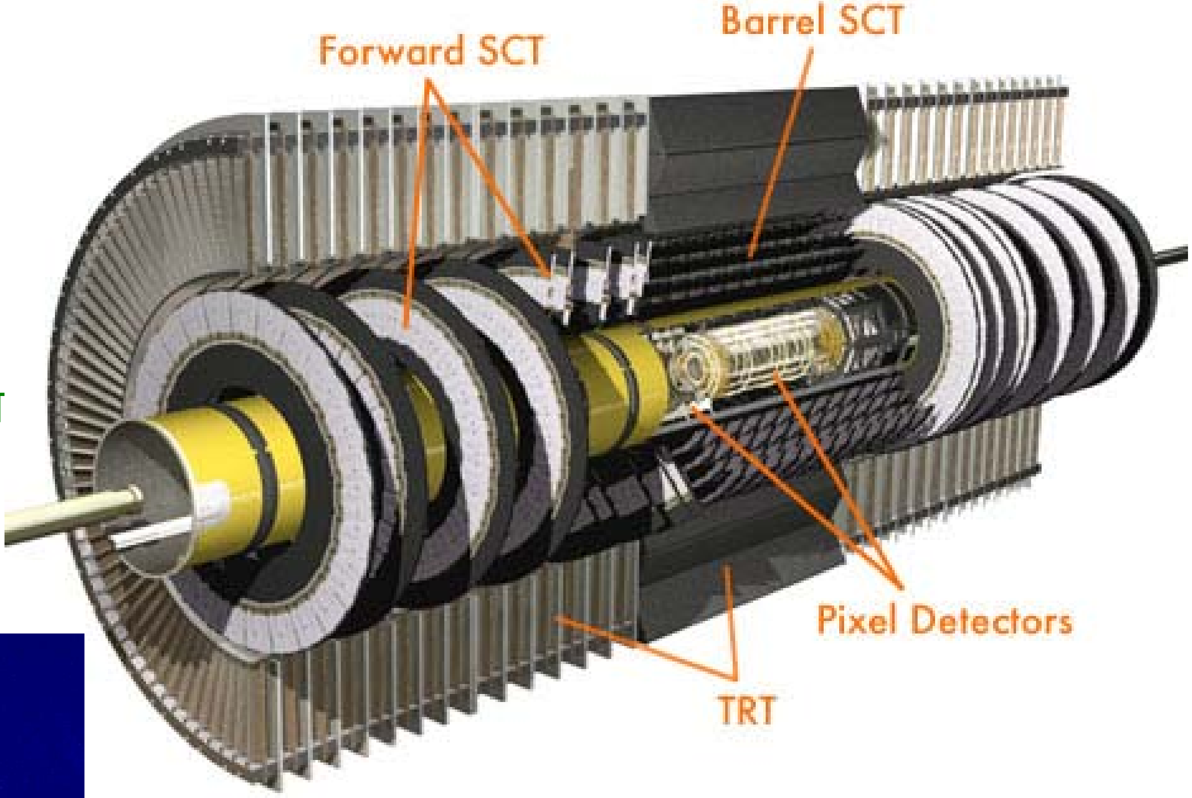

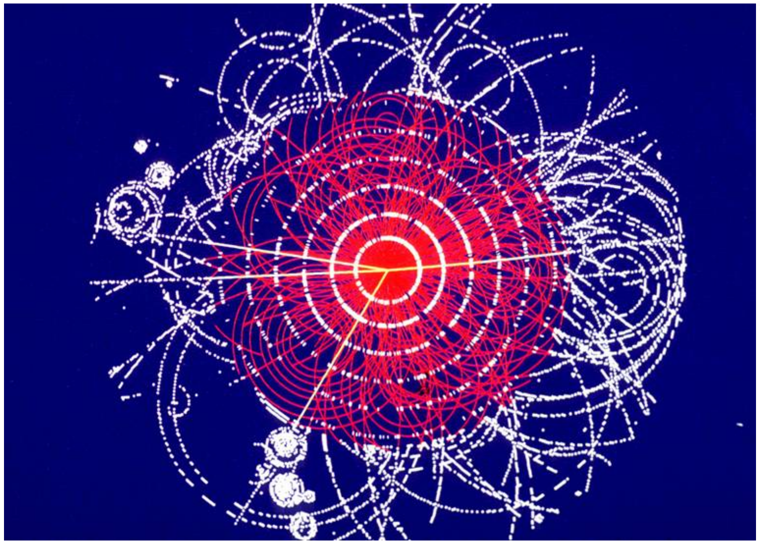

SCT barrel

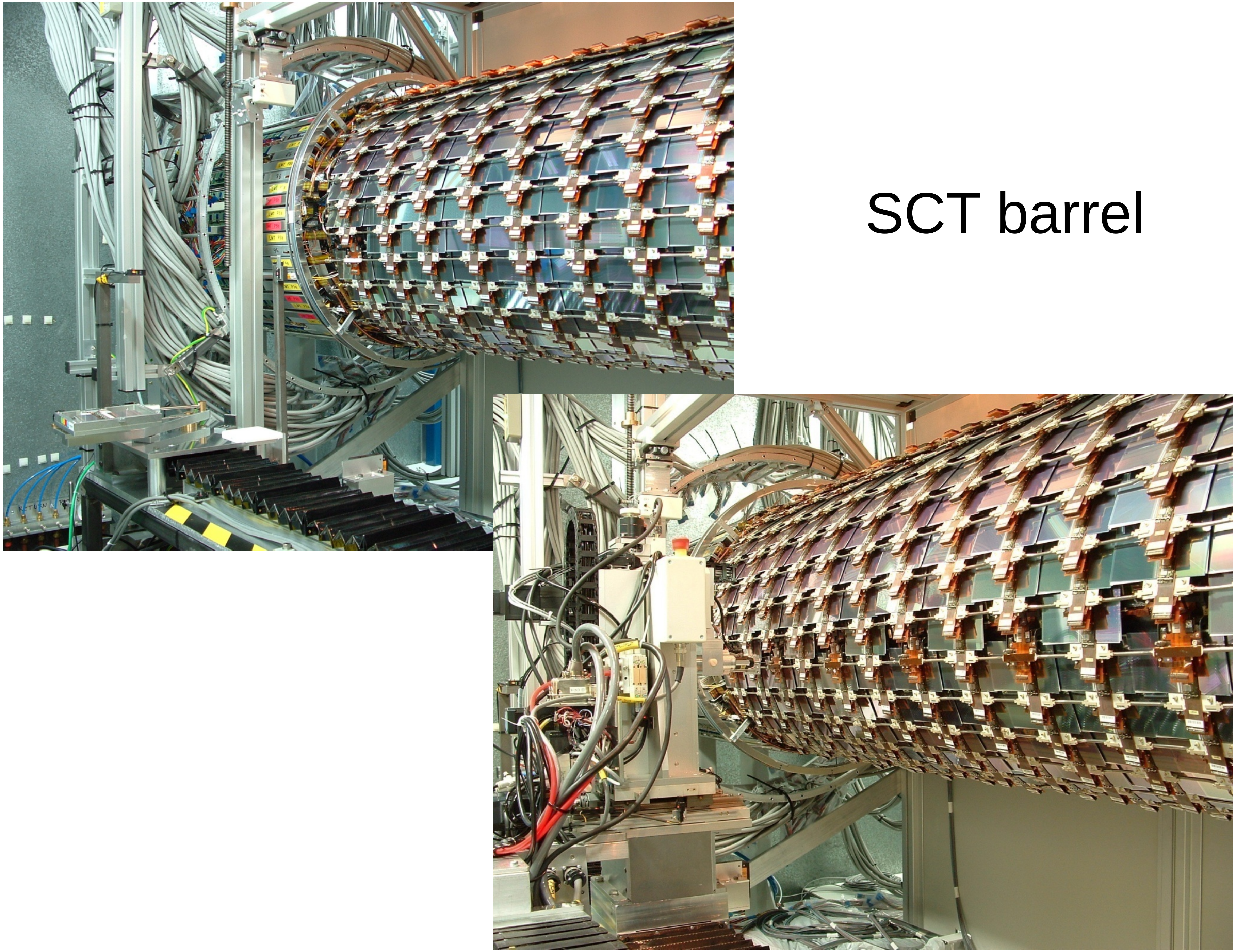

SCT EndCap

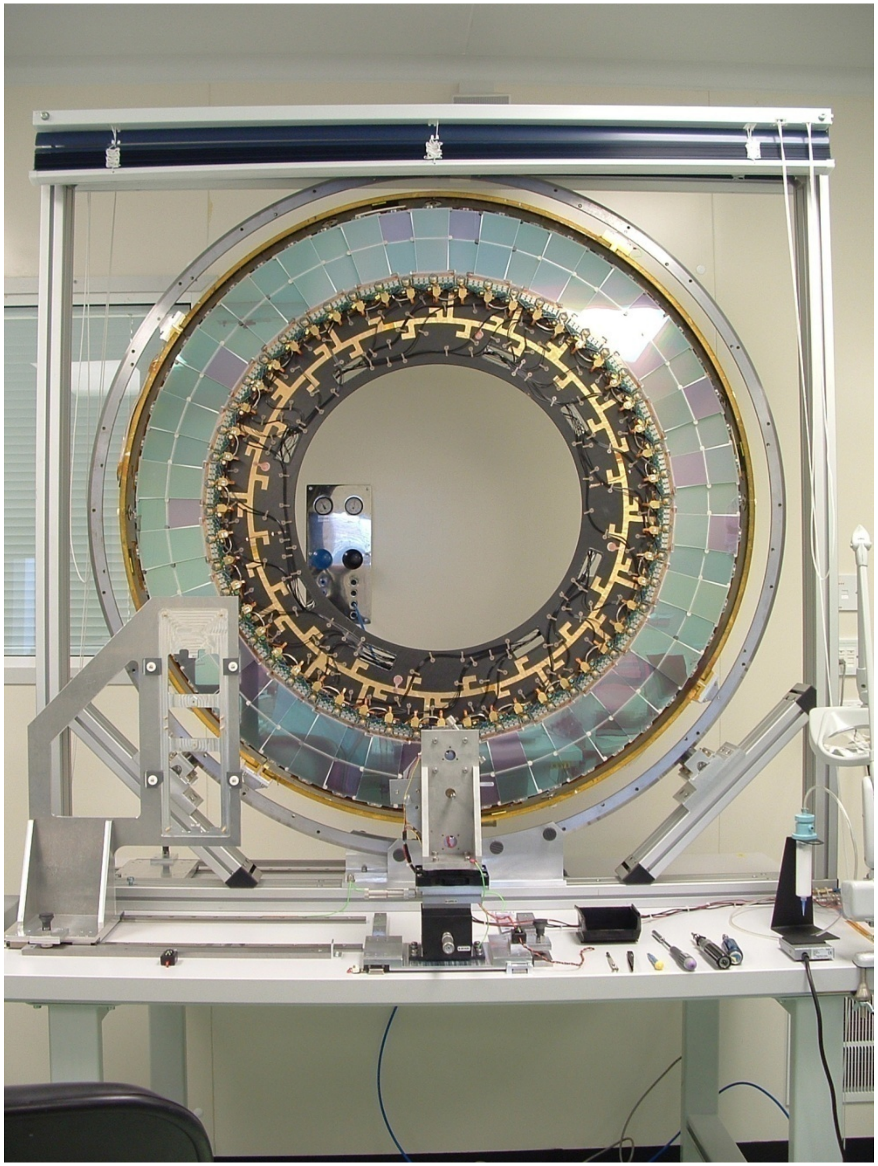

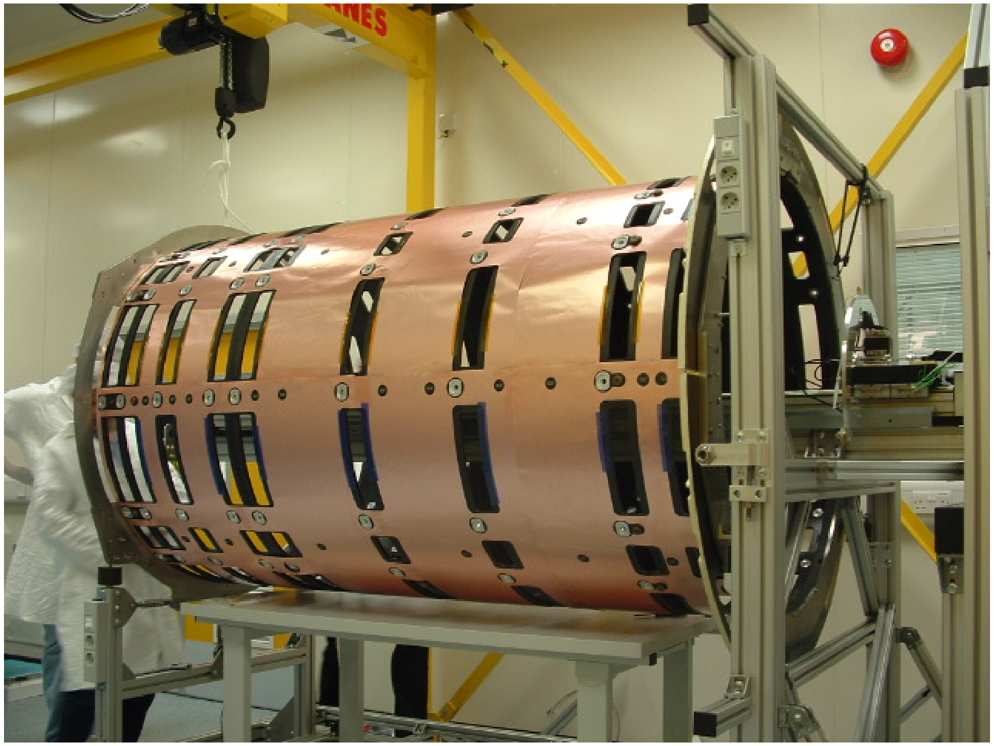

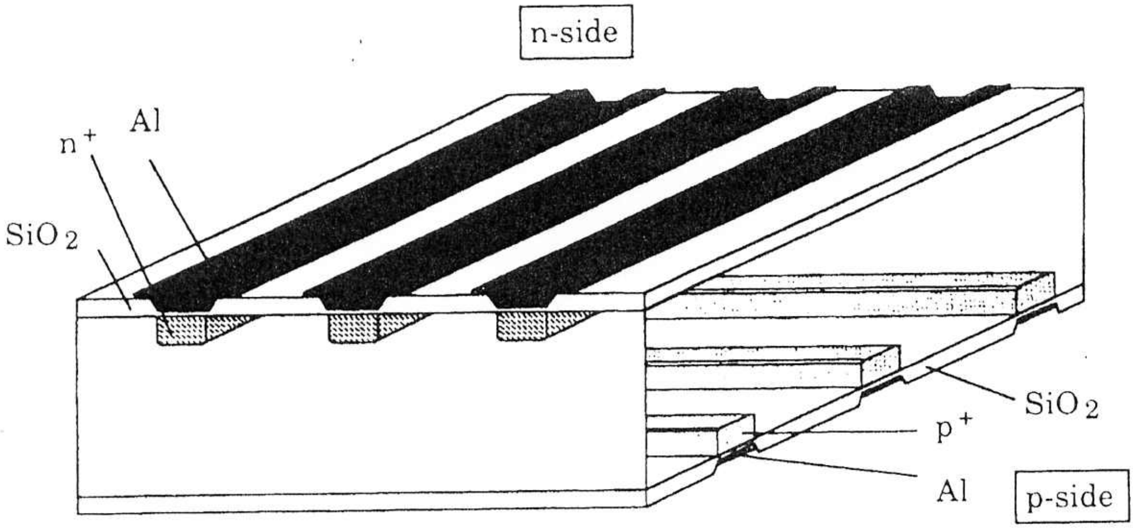

Double-sided silicon strip detector. (From Hubbeling et al.

Space Point

- Harder to fabricate (more expensive)
- Less material – less MCS

Pixel Detector

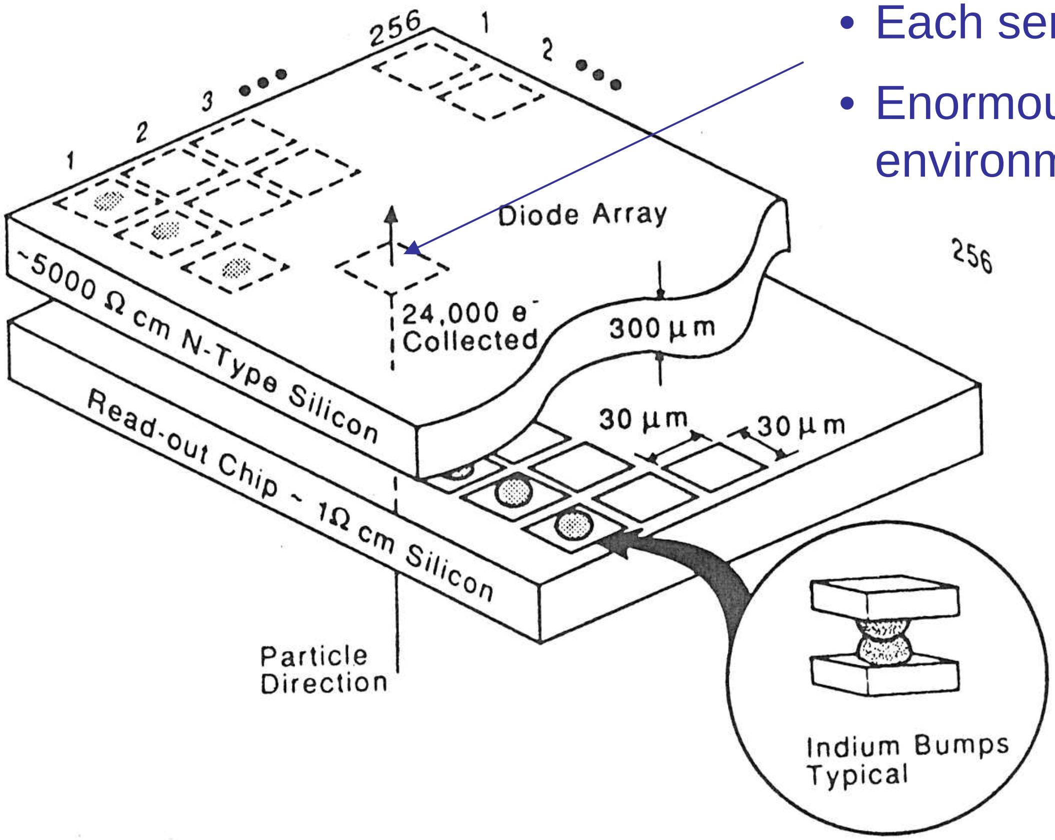

- Each sensor gives a space point
- Enormous advantage in high occupancy environment

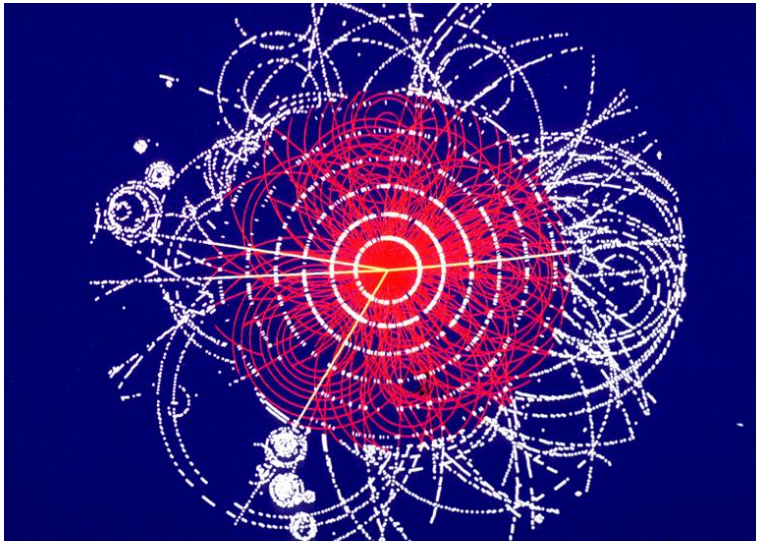

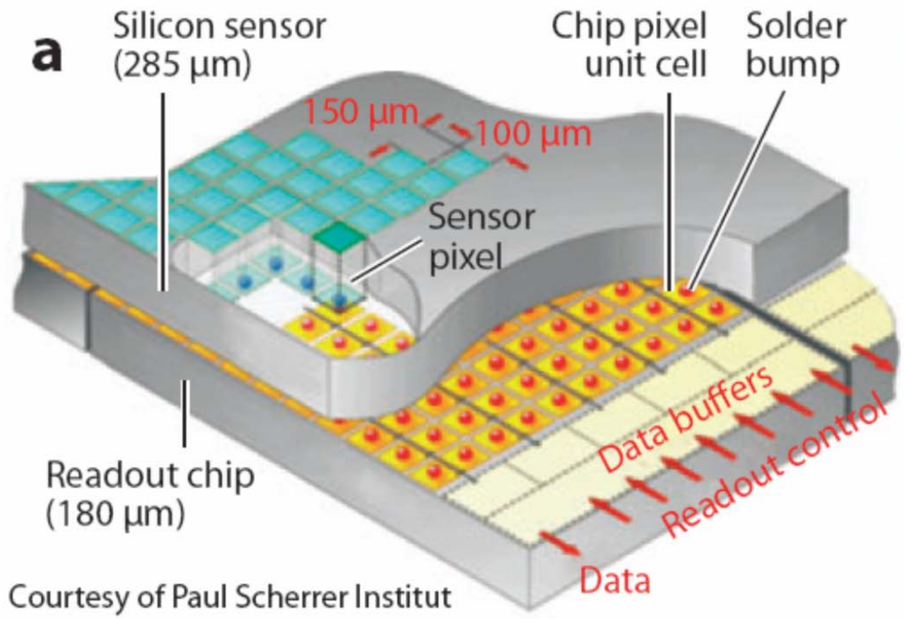

Courtesy of Paul Scherrer Institut

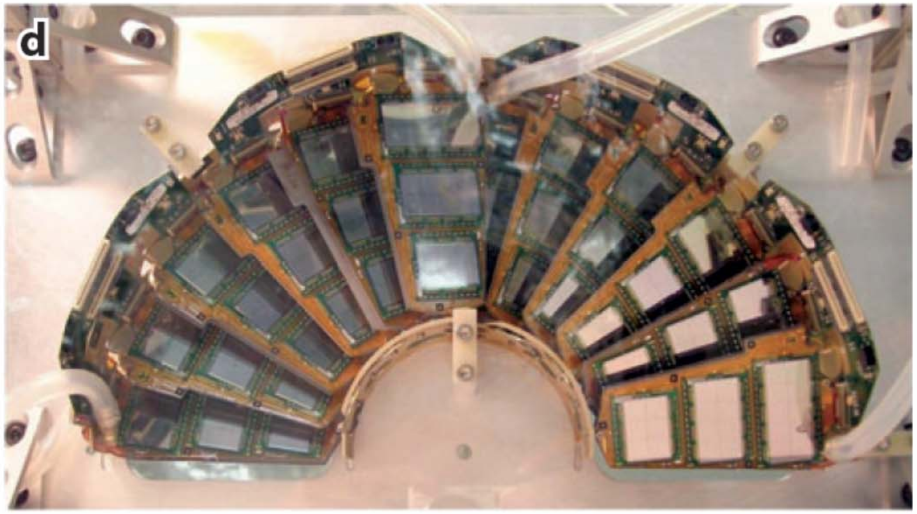

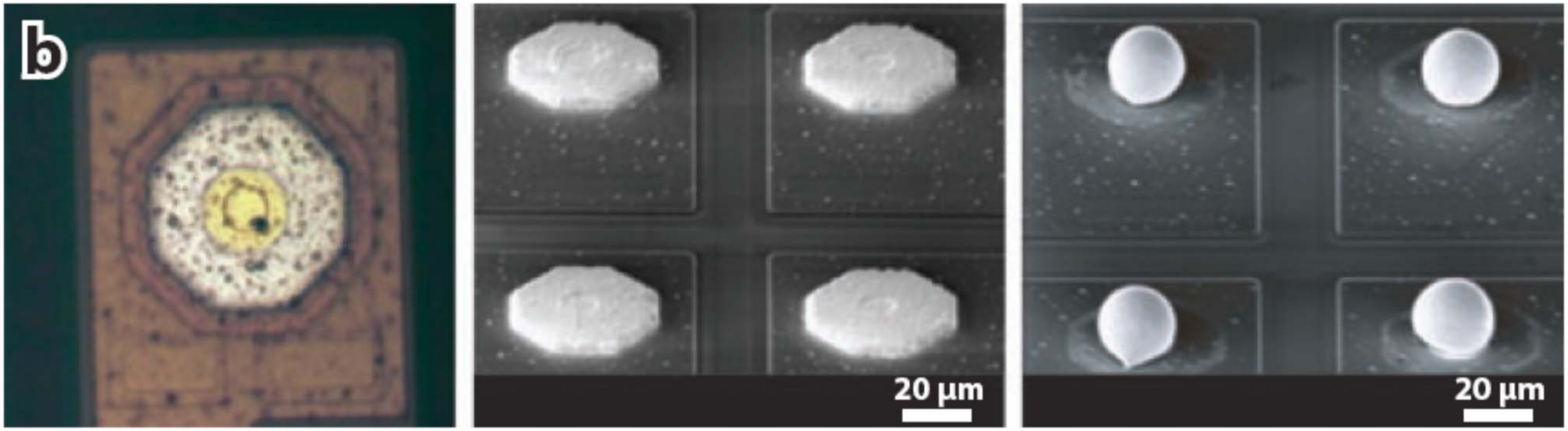

Pixel System

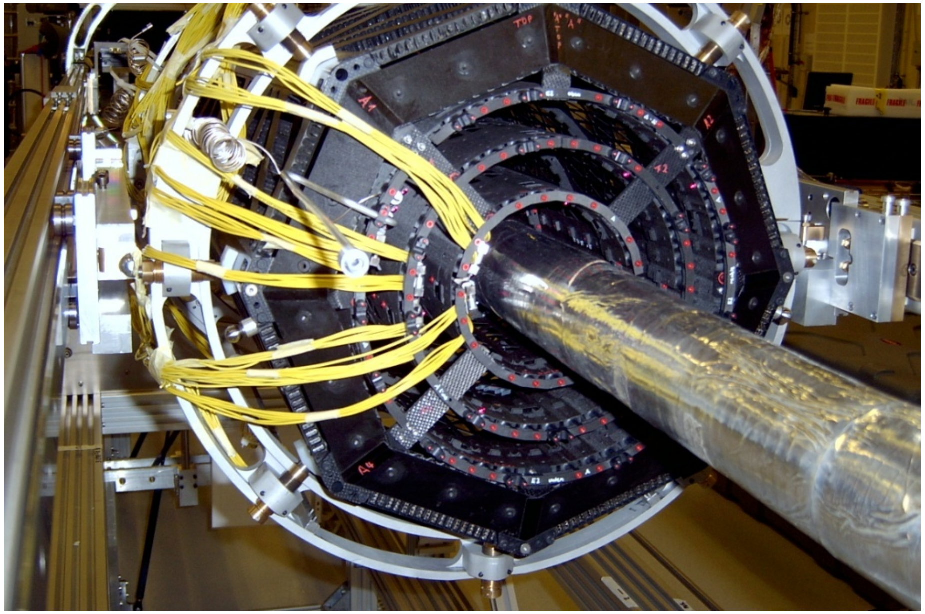

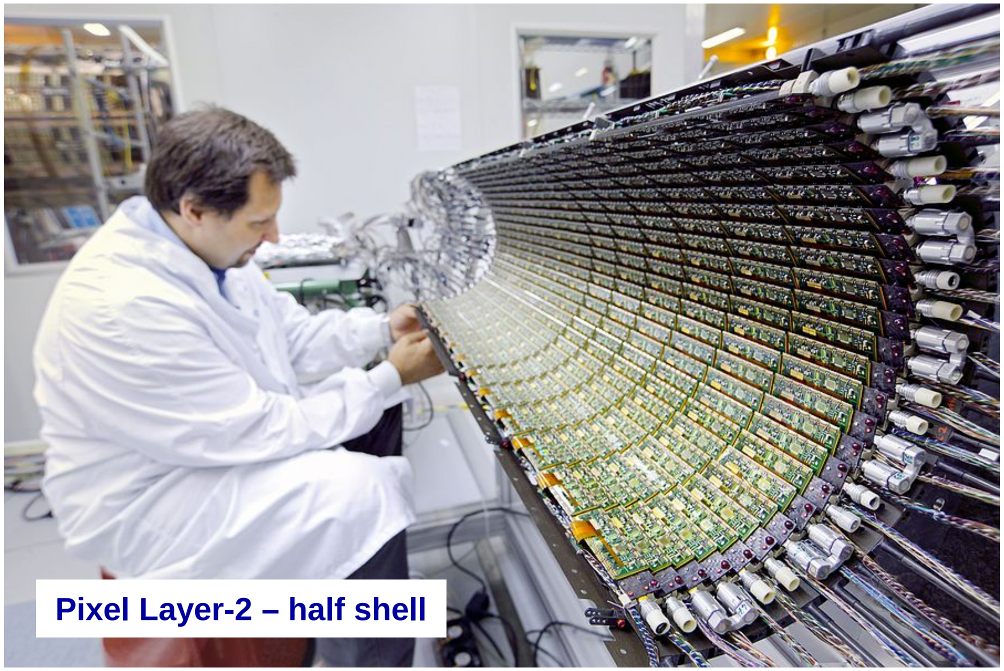

Pixel Layer-2 – half shell

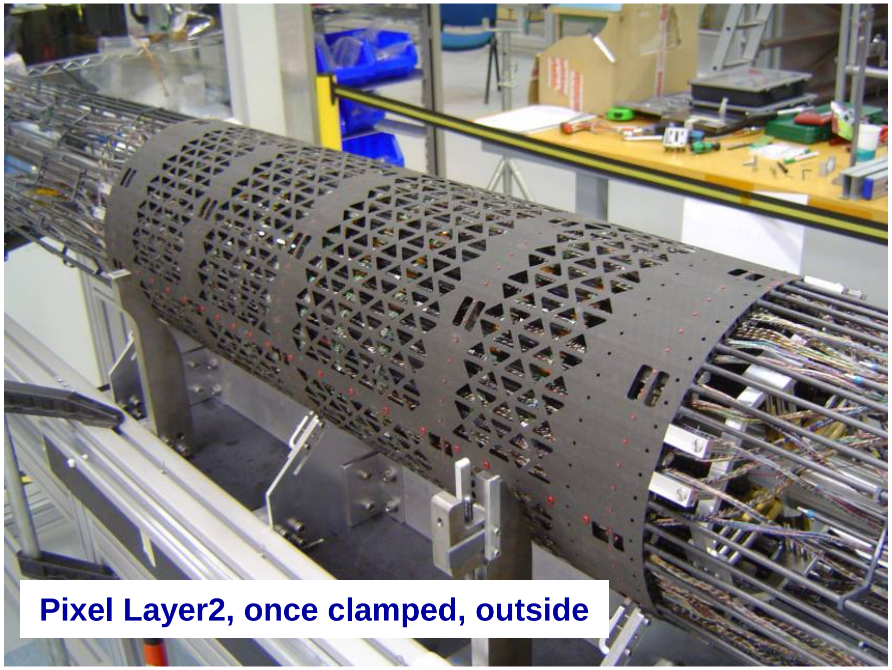

Pixel Layer2, once clamped, outside

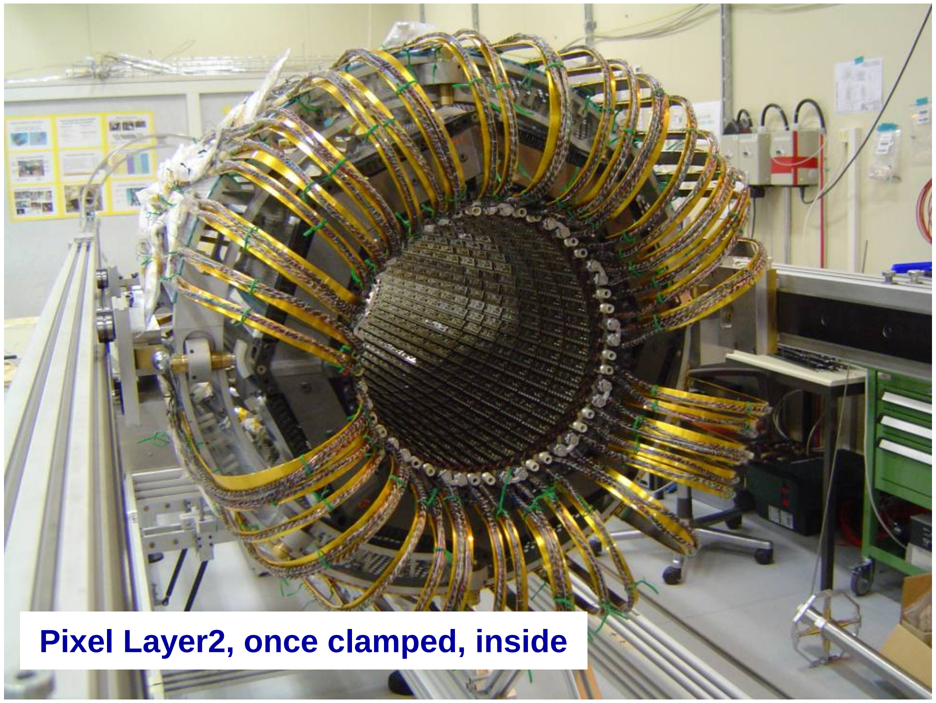

Pixel Layer2, once clamped, inside

“Ready for installation” date is 1st April 2007

CCD USE MOS STRUCTURE

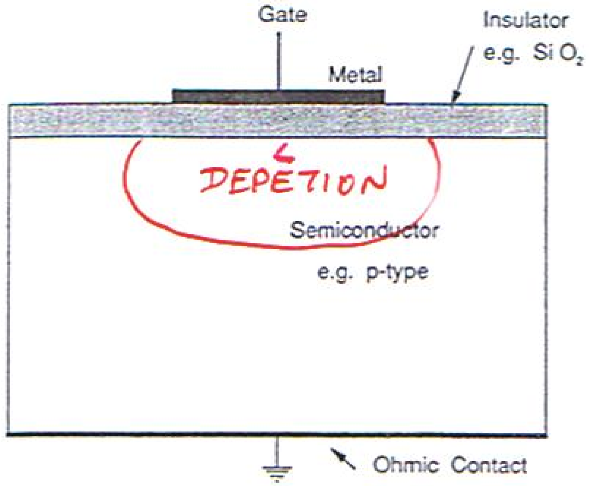

Figure 8: Cross section of a Metal-Oxide-Semiconductor (MOS) structure.

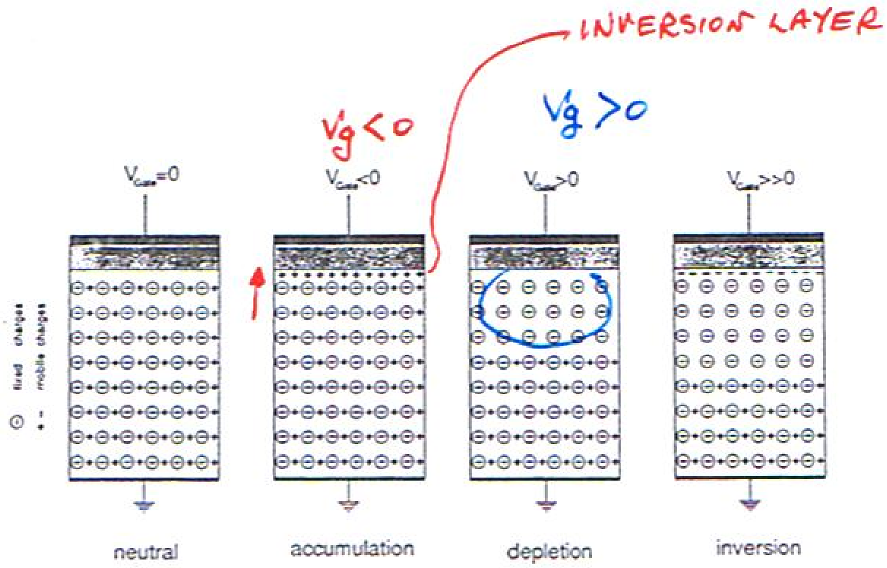

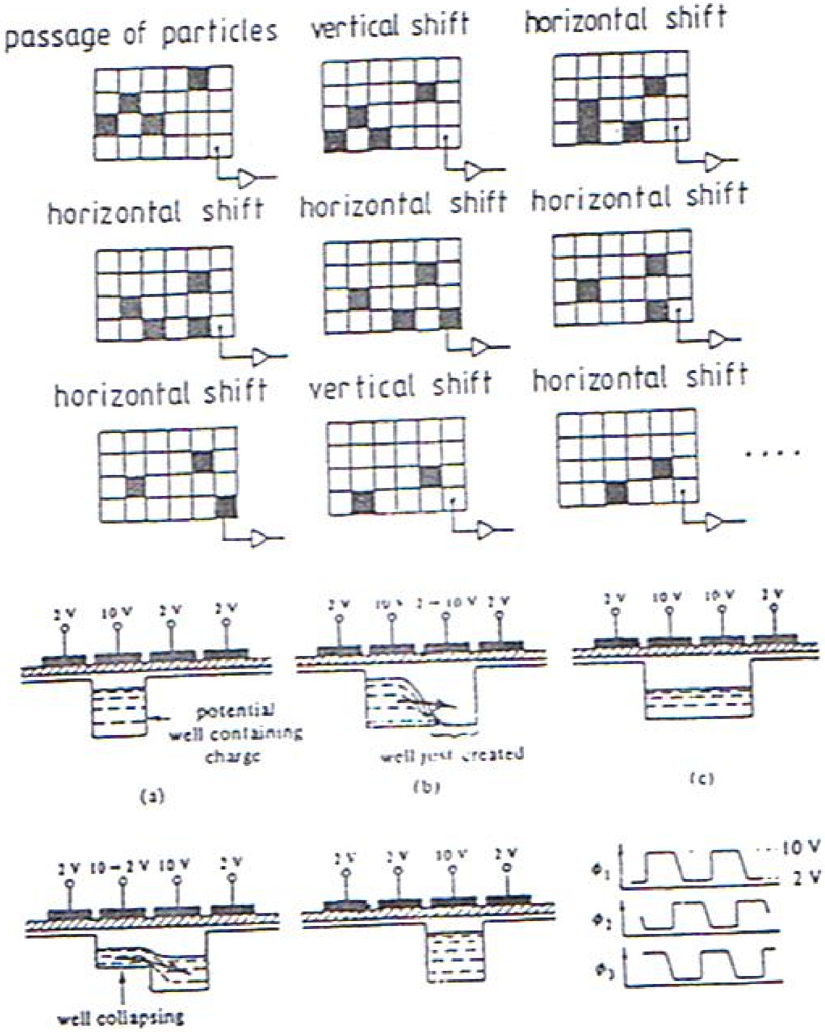

Fig. 3.5 Principle of a CCD.

PIXEL Chip

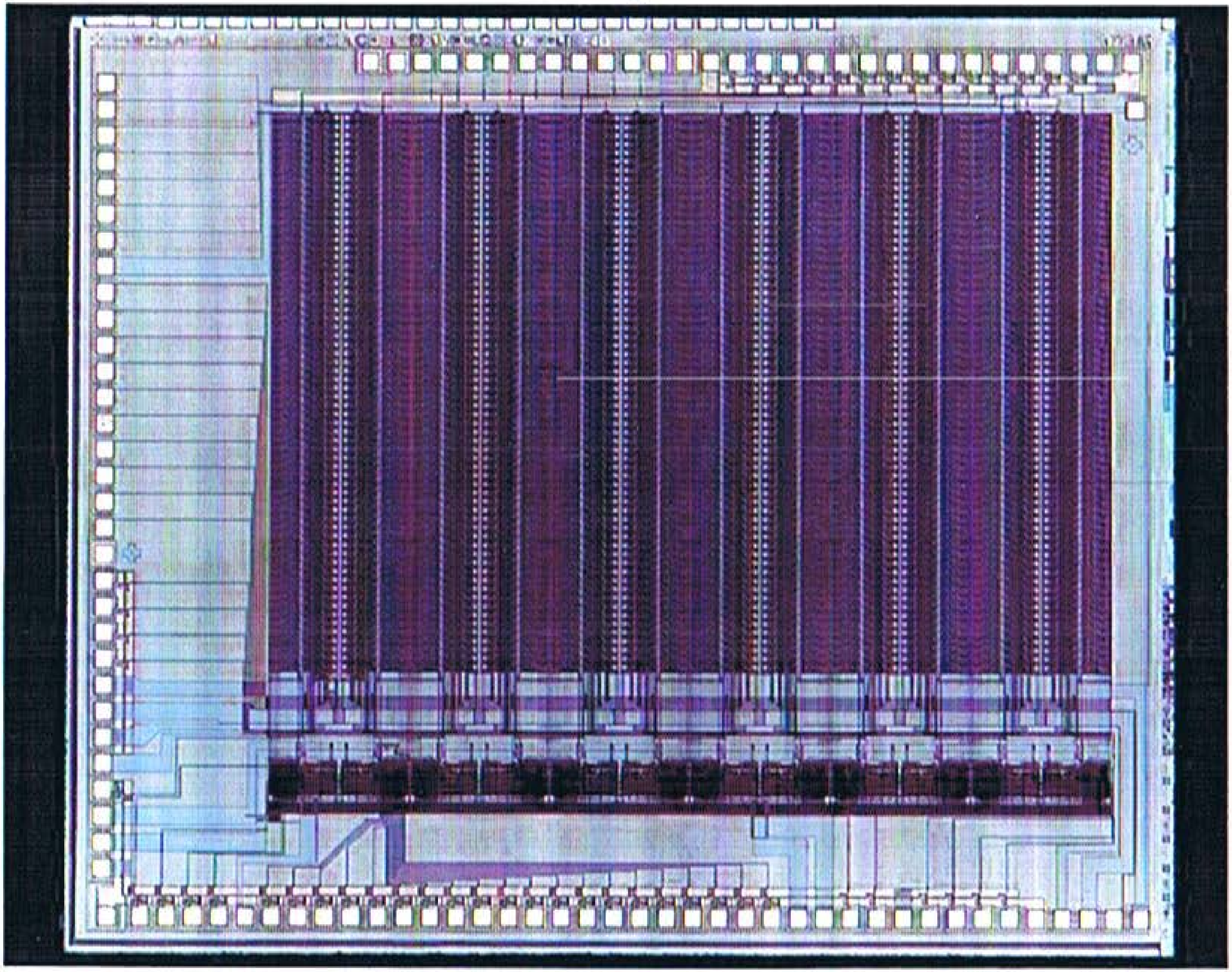

RADIATION DAMAGE TO SILICON

IMPORTANT ISSUE @ HIGH LUMINOSITY

PARTICLES TRAVERSING SENSOR

- DISPLACE ATOMS
- DEFORM LATTICE
- CREATE COMPLEX STRUCTURES

ALL THESE LATTICE DEFECTS POPULATE NEW ENERGY LEVELS IN THE BAND GAP

- INCREASE LEAKAGE CURRENT
- CHANGE DEPLETION VOLTAGE
  - NEW ACCEPTOR LEVELS
- DECREASE CHARGE COLLECTION DUE TO TRAPPING

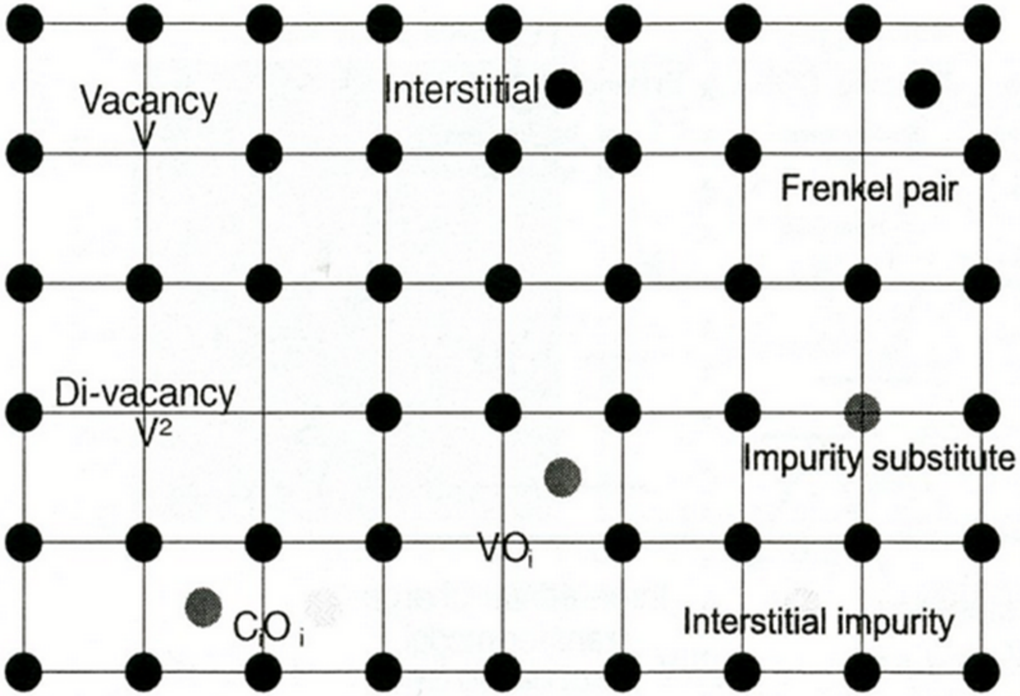

Fig. 1.50 The figure shows an exemplary selection of atomic displacements in the lattice after collision with traversing particles. These vacancies, interstitials and complex clusters are creating new levels in the energy scheme of the semiconductor and therefore change the elementary properties. As abbreviation, vacancies are labeled V, interstitials I, di-vacancies V_2. Impurities are labeled with their atomic sign, their index defines their position as substitute or interstitial, e.g. C_s or C_i

ANNEALING

INTERSTITIALS AND VACANCIES MOBILE $T > 150K$

AFTER RADIATION DAMAGE PROPERTIES CHANGE WITH TIME

FAST
- FRENKEL PAIR RECOMBINATION
- VACANCY + INTERSTITIAL RECOMBINATION

SLOW
- RECOMBINATION OF COMPLEX STRUCTURES

INITIAL BENEFICAL ANNEALING FOLLOWED BY LONG TERM DEGRADATION

ANNEAL AT 60°C FOR 80 MIN

↳ THEN FREEZE ANNEALING AT < 20°C

with $\alpha_I \sim 1.25 \cdot 10^{-17}\,\mathrm{A/cm}$, $\beta \sim 3 \cdot 10^{-18}\,\mathrm{A/cm}$ and $t_0 = 1\,\mathrm{min}$. τ_I takes the annealing temperature T_α dependence into account, where

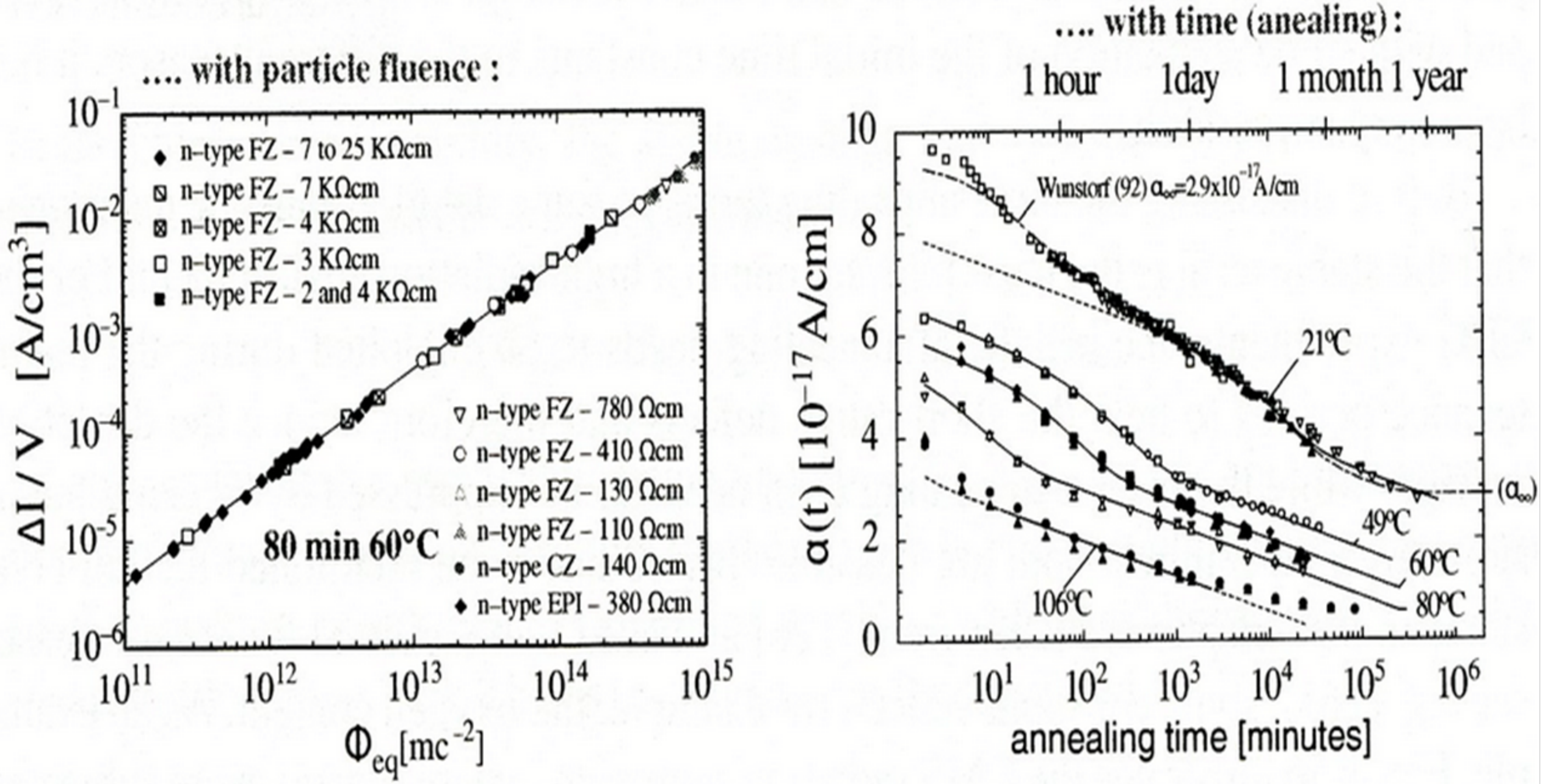

Fig. 1.54 Leakage current vs. fluence and annealing time [126, 166]

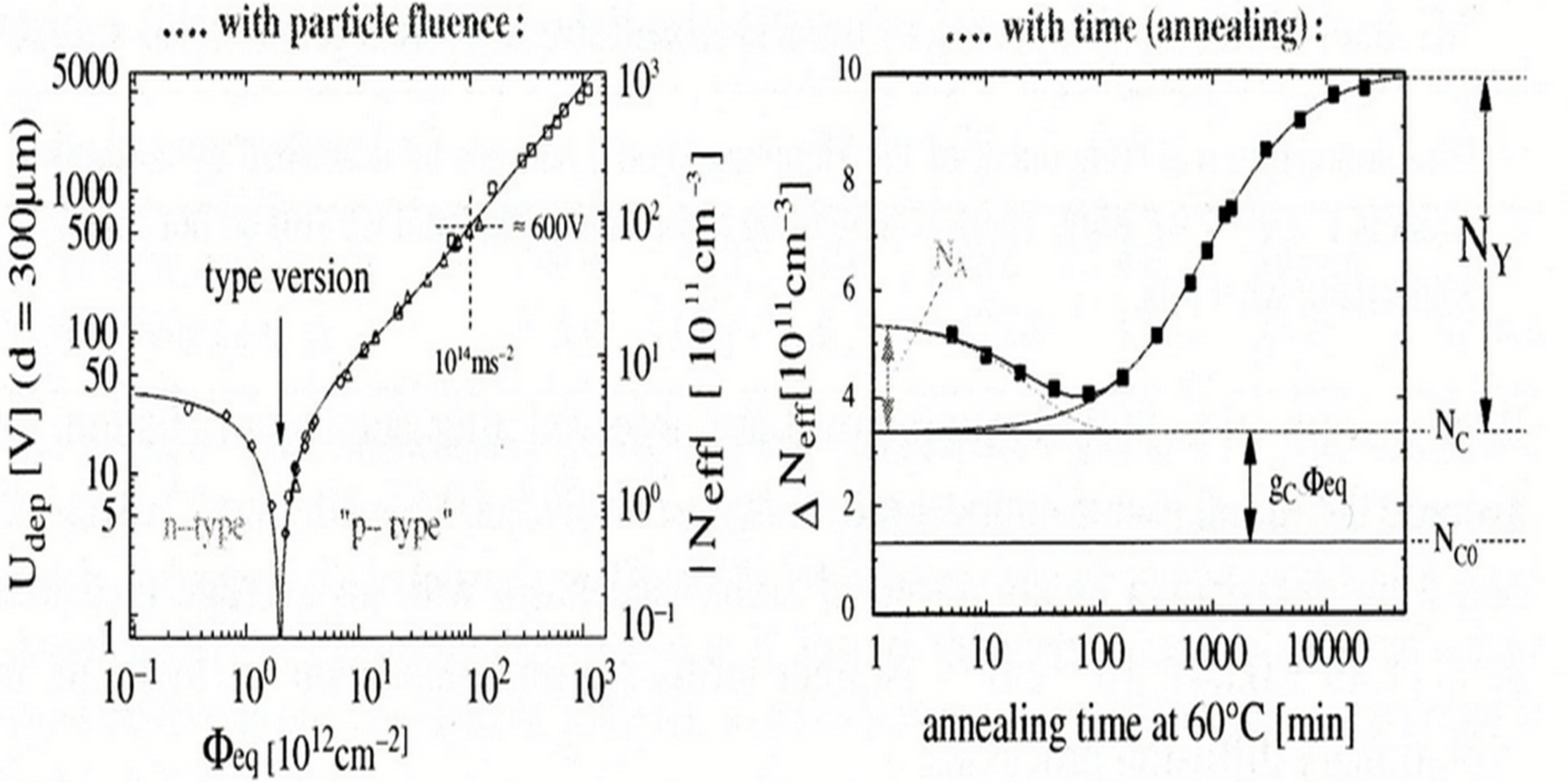

Fig. 1.55 Depletion voltage current vs. fluence and annealing time [126]

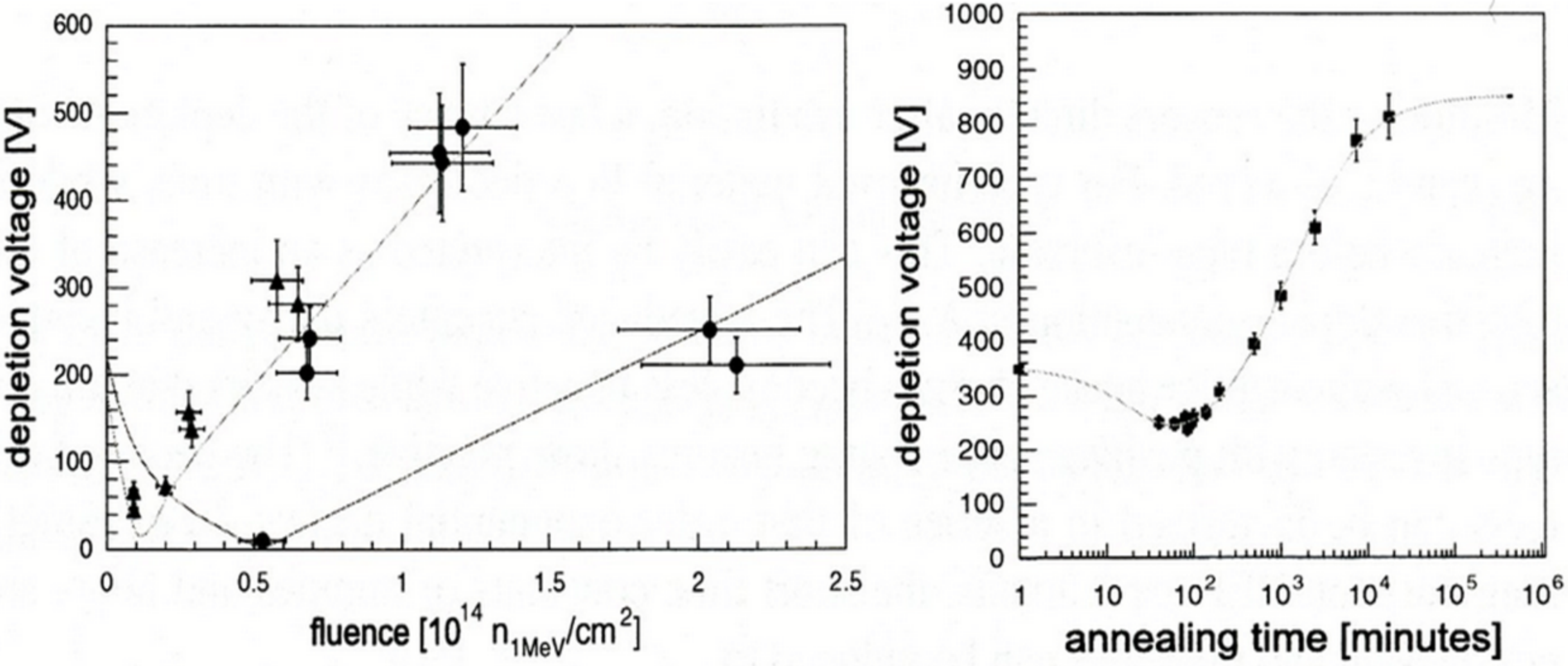

Fig. 1.56 Evolution of V_{FD} for different fluences and annealing durations. To have a basis for radiation evaluation, CMS irradiated several sensors and modules to get actual adapted fit parameters to the Hamburg model for the specific procured sensors. In this case, the beneficial constants g_a were found to be $1.11 \pm 0.16 \cdot 10^{-2} \mathrm{cm}^{-1}$ and $t_a(60°\mathrm{C}) = 21 \pm 8$ min; the reverse constants are $\mathrm{G}_y = 4.91 \pm 0.27 \cdot 10^{-2}\,\mathrm{cm}^{-1}$ and $\mathrm{t_y}\,(60°\mathrm{C}) = 1290 \pm 262$ min.
The different V_{FD} curve behaviours in the *left plot* can be explained by the different sensor thicknesses of 500 μm (upper curve) and 320 μm (lower curve) – mind $V_{FD} \sim N_{eff} \cdot D^2$. At fluences of 10^{14}, V_{FD} of the thick sensor would have increased above 1000 V. The initial compatible V_{FD} values are due to the different sensor resistivities. Data are compared to calculations for an annealing time of 80 min and an annealing temperature of 60°C at each fluence step. More about this study is described in Sect. 5.1.2 and [162]

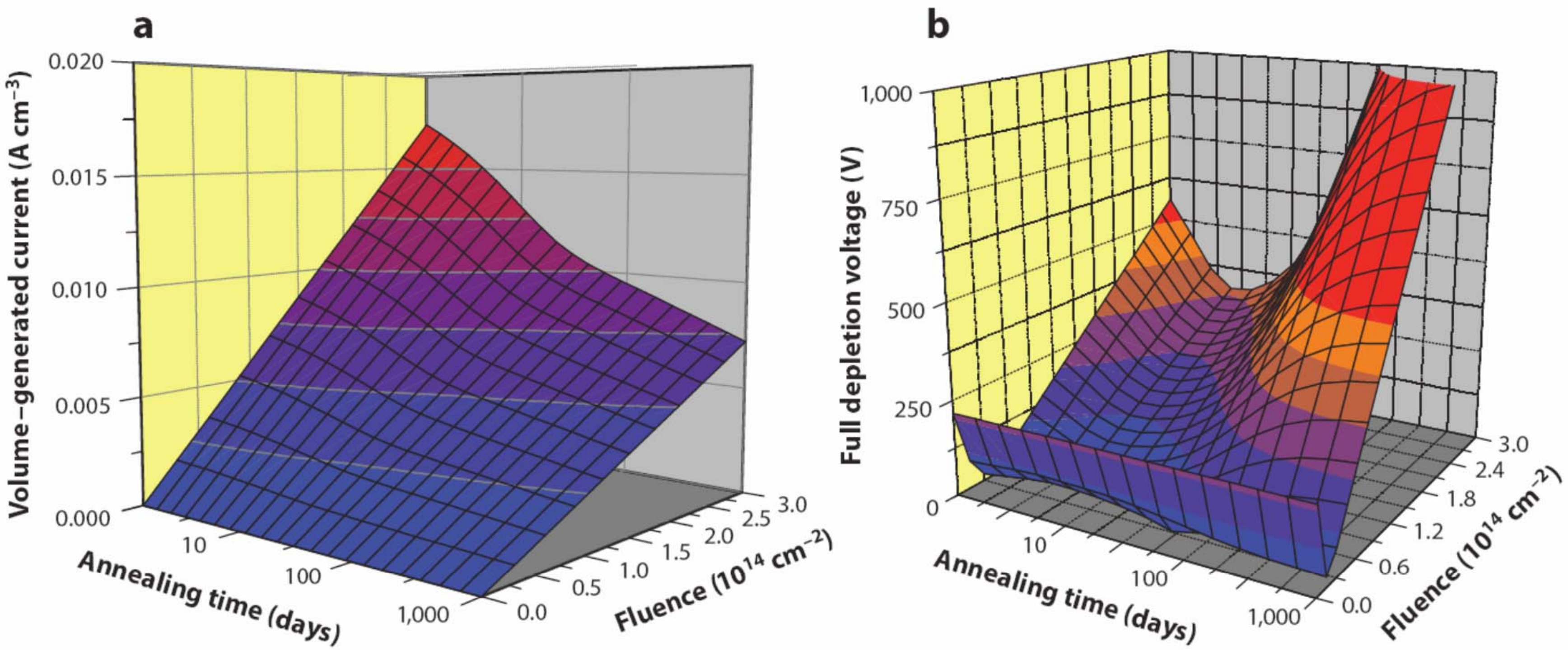

Figure 6

The evolution of current and full depletion voltage ($\sim|N_{\text{eff}}|$) versus fluence and further annealing at room temperature (22). In panel *b*, the dip around 0.5×10^{14} in the fluence axis reveals the space charge sign inversion point; the minimum in the time axis illustrates when the reverse annealing becomes relevant.

TYPE INVERSION ONLY HAPPENS FOR n-BULK

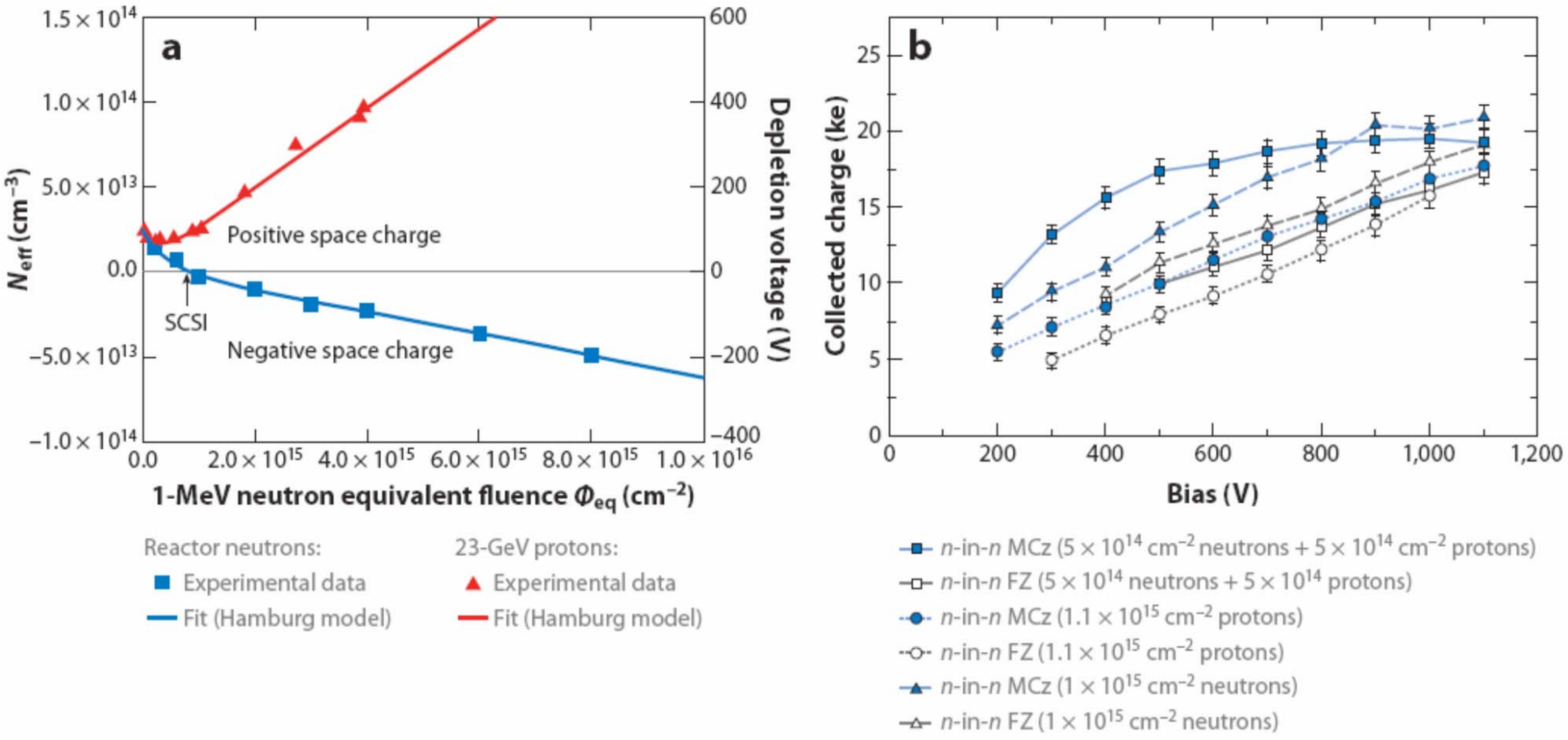

PROTON + NEUTRON ADD UP FOR FLOAT ZONE

CANCEL FOR CZOCHRALSKI

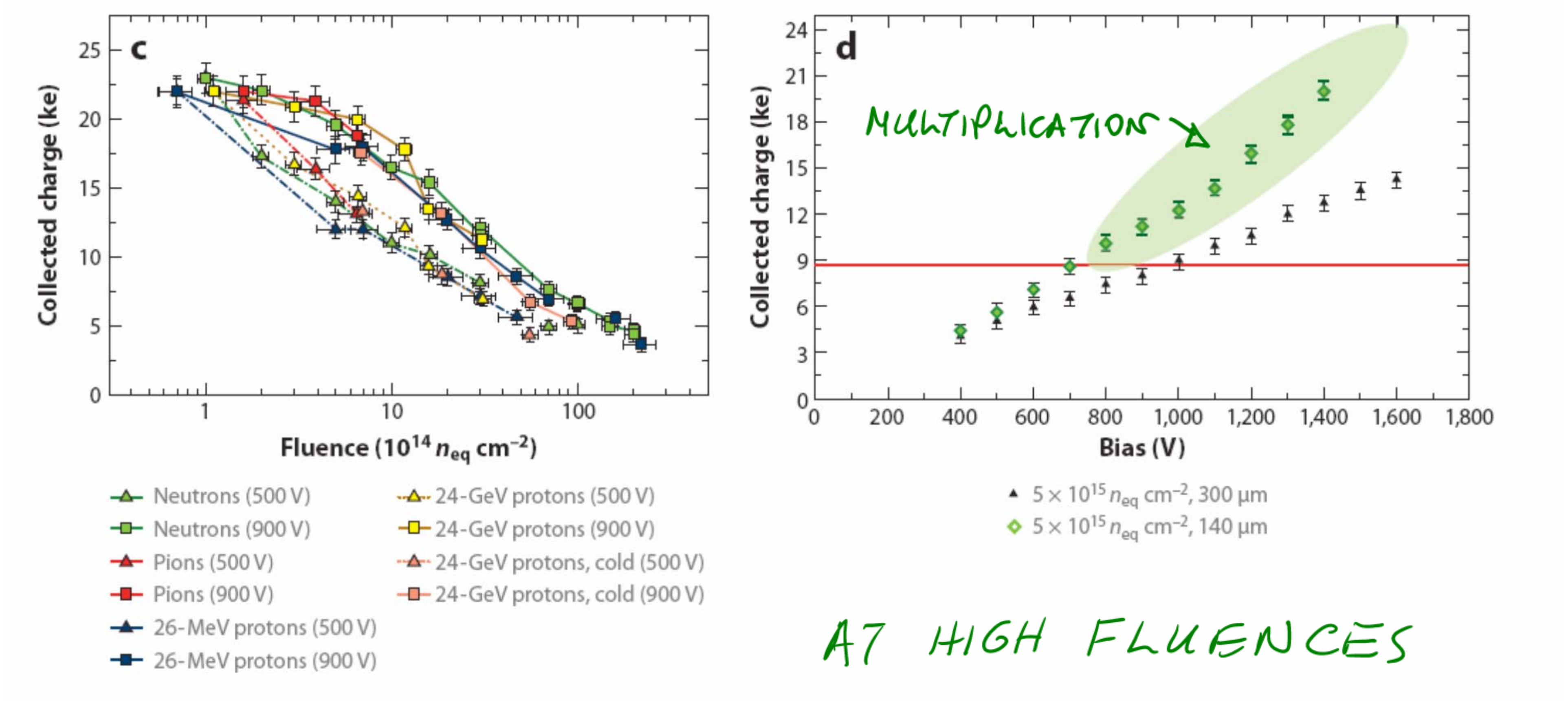

AT HIGH FLUENCES
CHARGE COLLECTION
EFFICIENCY BECOMES
PARTICLE INDEPENDENT
N-IN-P

AT HIGH FLUENCES
SEE ELECTRON MULTIPLICATION

Experimental Study and Empirical Modeling of Long Term Annealing of the ATLAS18 Sensors

Robert S. Orr

On behalf of the ATLAS ITk Collaboration

Motivation

- The ATLAS ITk – or for that matter any silicon detector - will suffer radiation damage and temperature dependent annealing
  - Increase of leakage current - operational consideration
  - Increase of Full Depletion Voltage – operational consideration
  - Reduction of Charge Collection Efficiency
    - At some level of degradation this will adversely affect the efficiency for track finding
  - Annealing is reduced at low temperature
  - Not possible to just keep detector at very low temperature permanently
    - For the ITK this period would be 14 years
    - Detector maintenance
    - Cooling system maintenance
    - Other possible warm ups
  - While the phenomenon of annealing after radiation damage is interesting in its own right, we have taken a more empirical approach

Parametrisation of Long Term Annealing

- Rather than trying to develop a deep theoretical understanding, I wanted to come up with some "physically motivated" parametrisation.
- The Hamburg Model seems to be the standard way of understanding annealing effects – so this is a starting point
- Initially looked at some ATLAS12 data
  - ATLAS*yy* are a series of strip sensor prototypes produced by Hamamatsu Photonics from designs by ATLAS ITk – ATLAS18 is the production series
  - The ATLAS12 data has been published in NIM A 924 (2019) 128-132 L. Wiik-Fuchs et al
  - That publication is a subset of data from Leena Diehl – Freiburg Ph.D. Thesis 2018
  - Leena Diehl kindly provided me with the numerical data, and also some additional measurements from her thesis

W649_C-P9 2e14 neq/cm^2

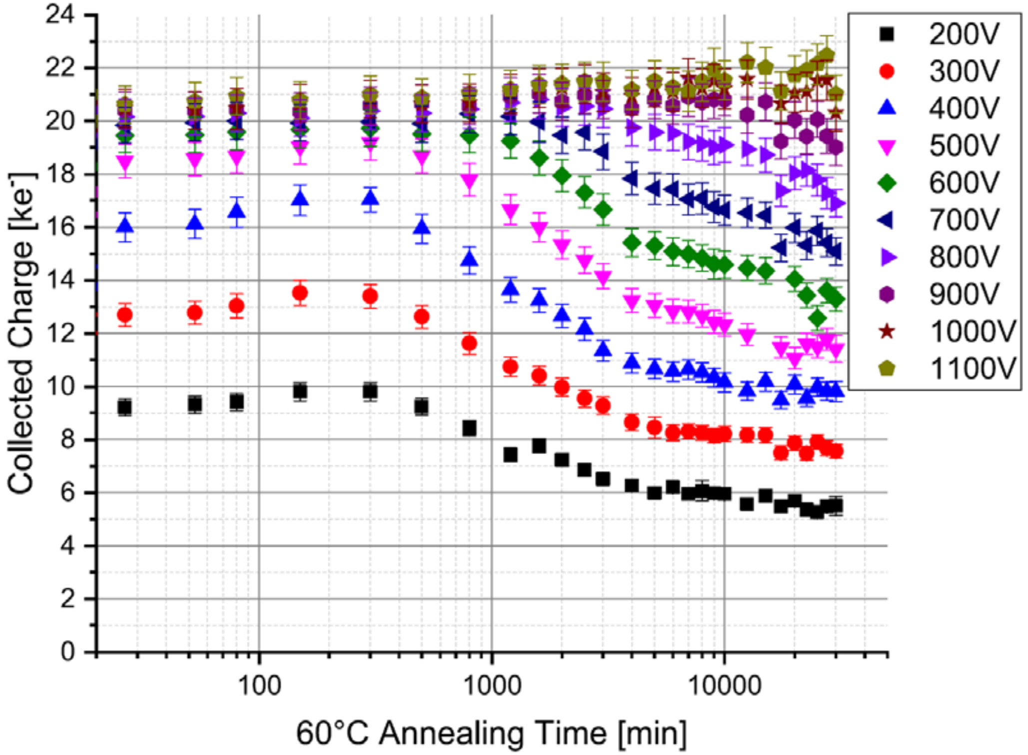

NIM A 924 (2019) 128-132 L. Wiik-Fuchs et al

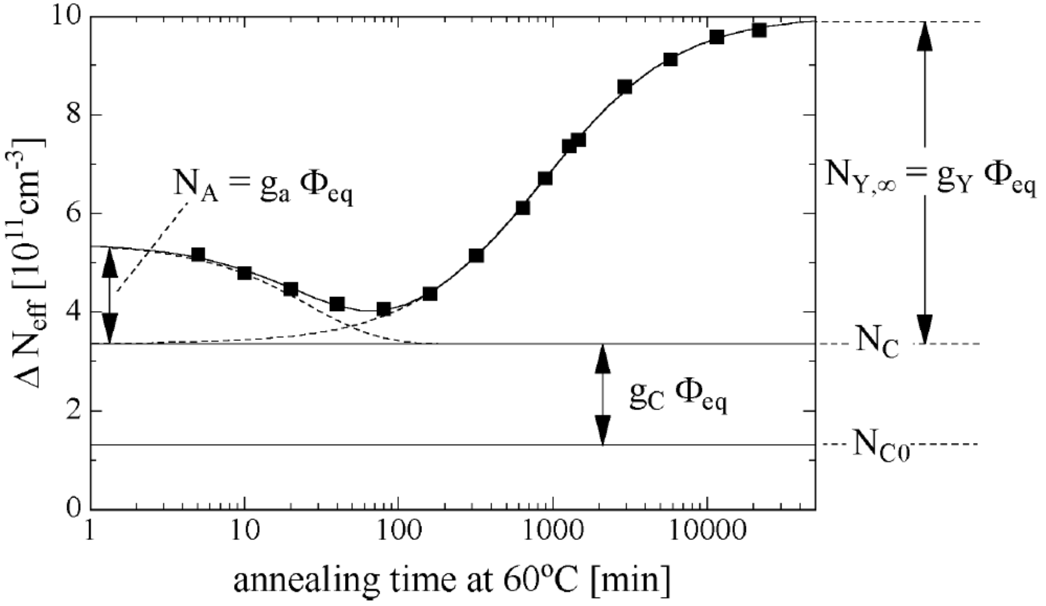

Figure 5.9: Annealing behavior of the radiation induced change in the effective doping concentration ΔN_{eff} at 60°C. The shown example is a sample of type WE-25kΩcm irradiated with a fluence of $1.4 \times 10^{13}\,\mathrm{cm}^{-2}$.

Michael Moll – DESY Thesis 99-040

Hamburg Model

- Effective doping concentration N_{eff} depends on Φ_{eq} - fluence of irradiation and time.
- The model hypothesises that there are three phases of annealing in time.
  - Short Term beneficial annealing

$$N_A(\Phi_{eq},t) = \Phi_{eq} g_a \exp(-t/\tau_a)$$

  - Constant

$$N_C(\Phi_{eq}) = N_{C,0}\Phi_{eq} g_a \left(1-\exp(C\Phi_{eq})\right) + g_C \Phi_{eq}$$

  - Long term degradation

$$N_Y(\Phi_{eq},t) = \Phi_{eq} g_Y \left(1-\exp(-t/\tau_Y)\right)$$

  - Ansatz = Guess $CCE \propto (1/N_{eff})$

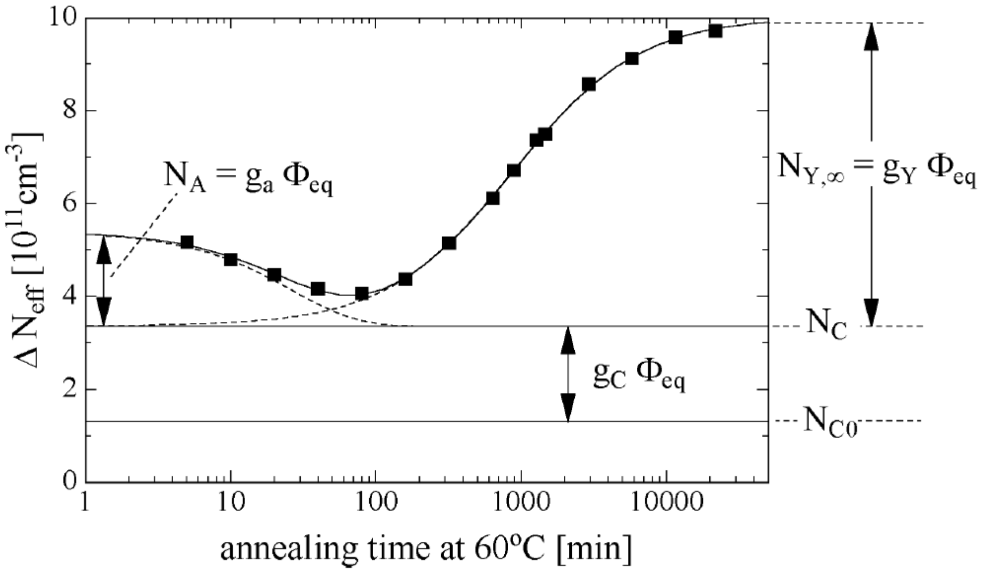

Figure 5.9: Annealing behavior of the radiation induced change in the effective doping concentration ΔN_{eff} at 60°C. The shown example is a sample of type WE-25kΩcm irradiated with a fluence of 1.4×10^{13} cm^{-2}.

We parametrize the collected charge as a function of irradiation fluence as :

$$1 \Big/ \left(g_a \exp\left(-t/\tau_a\right) + g_C + g_Y \left(1 - \exp\left(-t/\tau_Y\right)\right) \right)$$

g_a - Coefficient for short term annealing

τ_a - Diffusion time for short term annealing

g_C - Constant term

g_Y - Coefficient for long term annealing

τ_Y - Diffusion time for long term annealing

The dependence of the collected charge on fluence is incorporated in the g-coefficients

Miniature Sensors

- Each wafer produced by Hamamatsu contains full size sensors which are rectangular or trapezoidal in shape.
- This leaves space for other structures around the periphery of the wafer.
- ATLAS populates this area with test structures and miniature sensors.
- The miniature sensors are “identical” to full size sensors – same strip and bias/guard ring structures, and several sizes. The miniature sensors in this study are 1cm x 1cm with 104 strips of 8 mm length.
- In this study the miniature sensors were irradiated with 24 MeV protons (ATLAS12 at Karlsruhe) and reactor neutrons (ATLAS12 and ATLAS18 at Ljubljana)

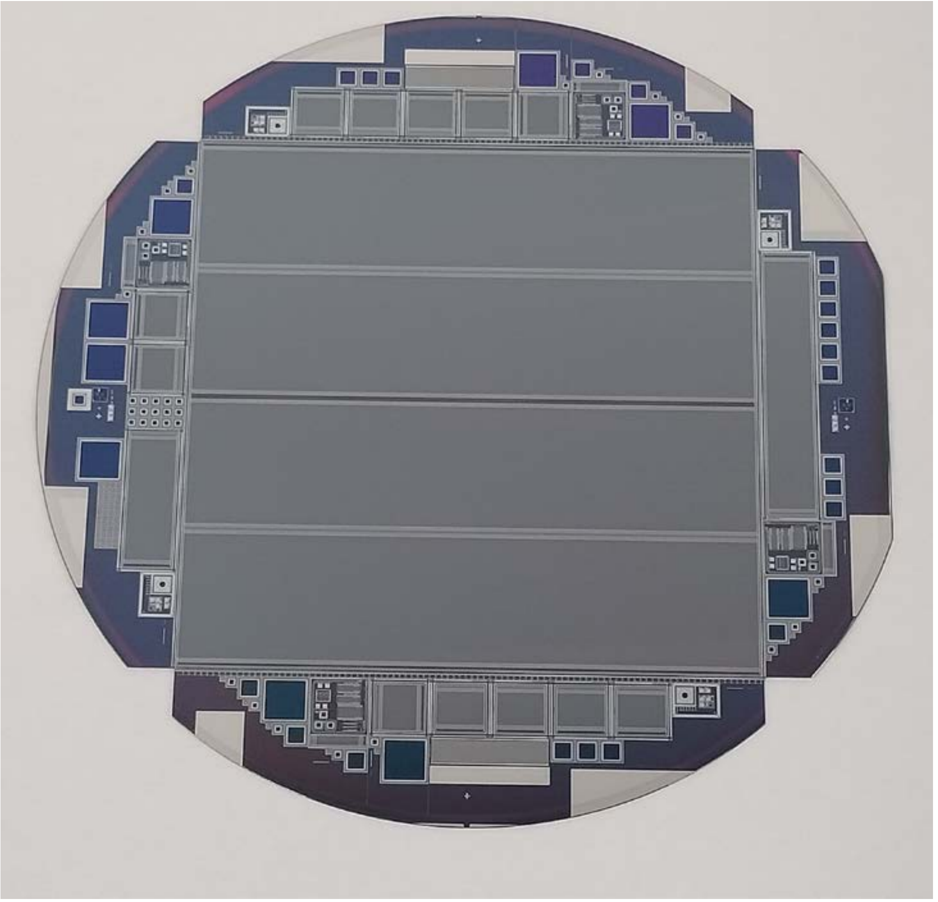

ATLAS18 Wafer

Fitting Procedure

- Initially fit distribution at each fluence with all parameters free
- To have some predictive power need to reduce number of parameters
- While the g-coefficients are functions of the irradiated fluence, it seems reasonable that the diffusion times are not.
- Refit the distributions at each fluence, with the diffusion times fixed.
  - We used the diffusion times from the fit at 2e14 neq/cm^2
- This extracts a set of g-parameters at each fluence
- We then fit an empirical function to the g-parameters as a function of fluence
- Then use fixed diffusion times and fitted function of g-parameters to give a “prediction” or closure test.
- We have data at many bias voltages
- Unirradiated full depletion voltage is 300V, and the ITk is limited to 500V – so we have only studied 400V and 500V in detail

Fit model to 24 MeV Proton Data

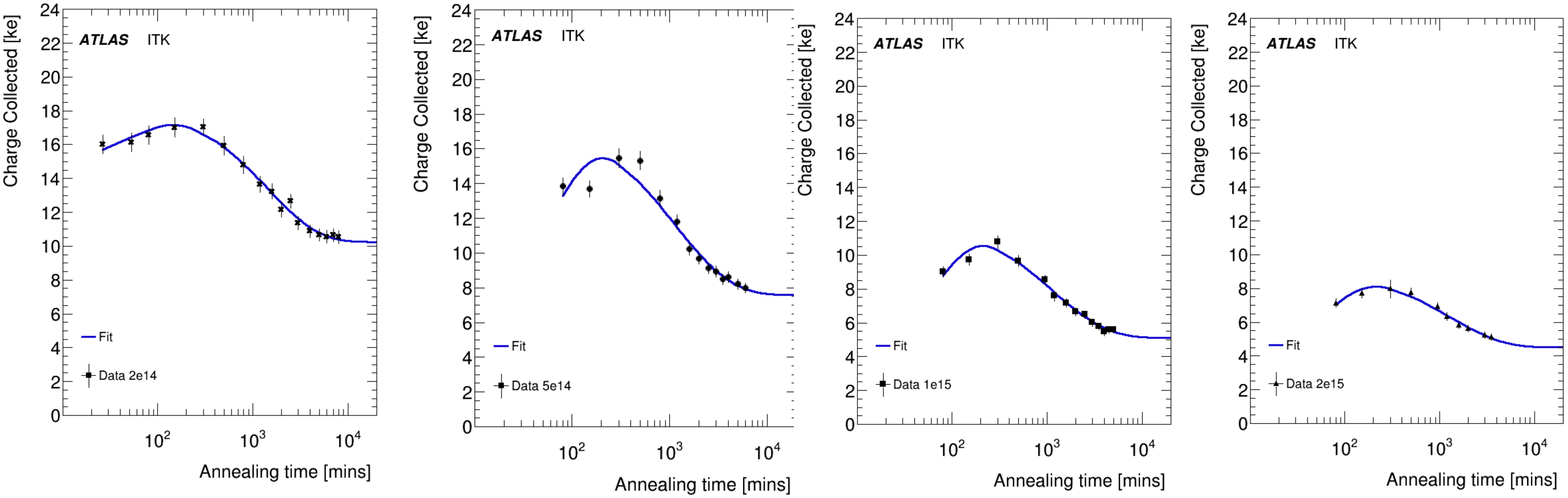

- Measured at Freiburg
- Annealing at 60 C
- ATLAS12
- 400 V Bias

- g- coefficients free at each fluence
- Diffusion times fixed to same value at each fluence $\tau_a = 53s, \tau_Y = 2296s$

Functional Model for Dependence of Coefficients on Fluence

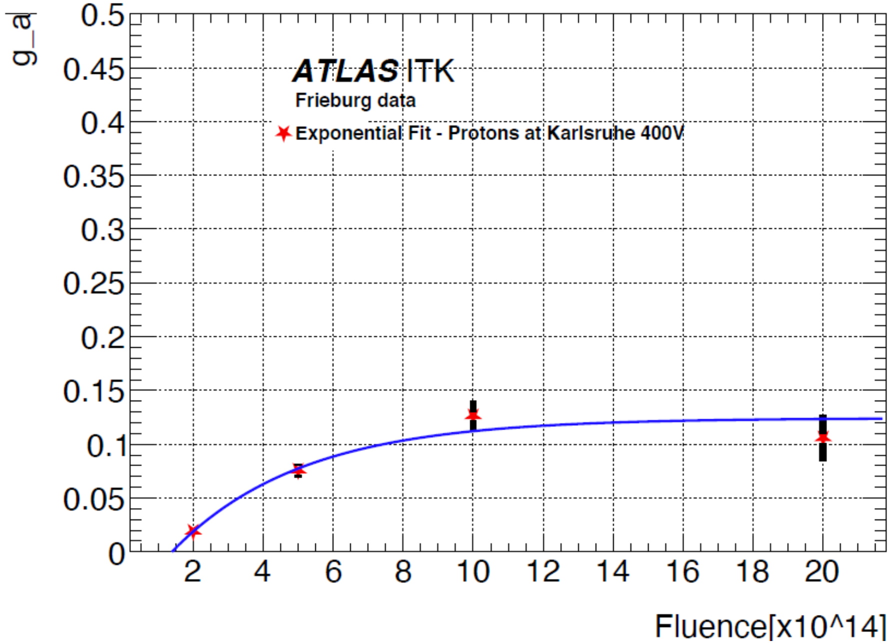

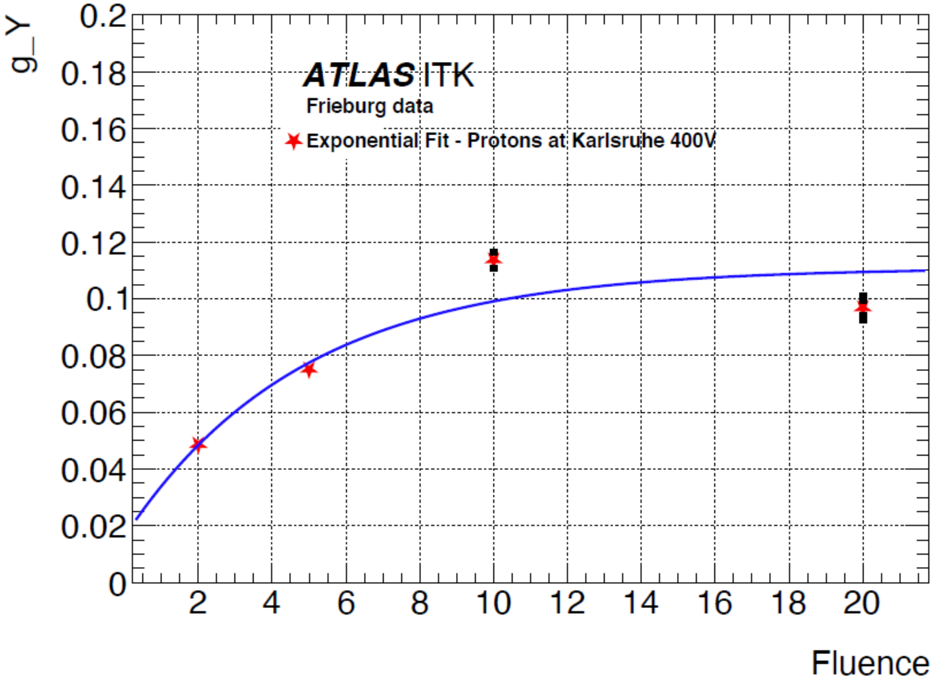

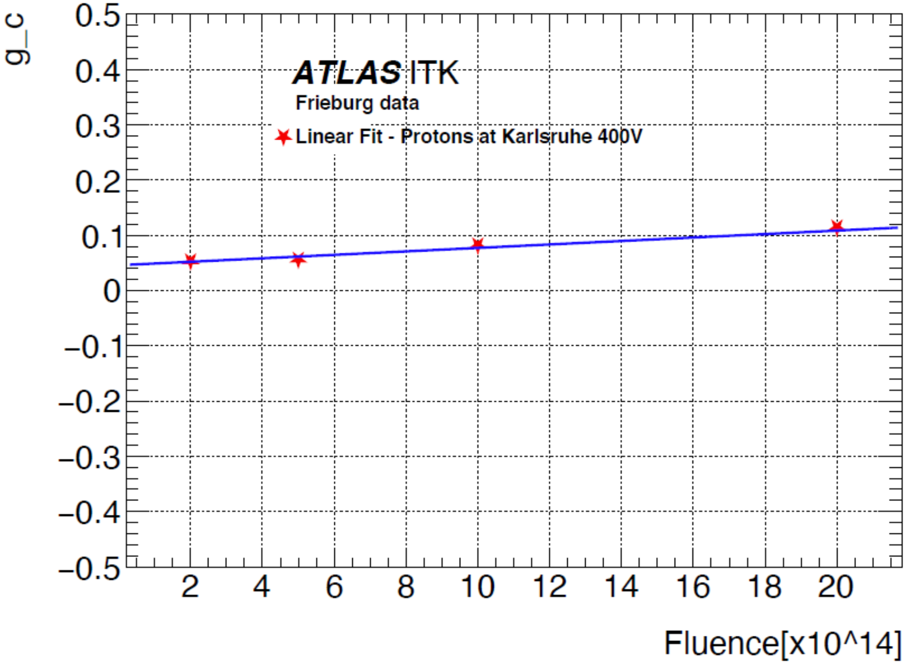

fitted g_a and g_Y to the form $a+b\left(1-\exp\left(-c\times fluence\right)\right)$ and g_C was taken as linear.

24 MeV protons at Karlsruhe – Closure Test

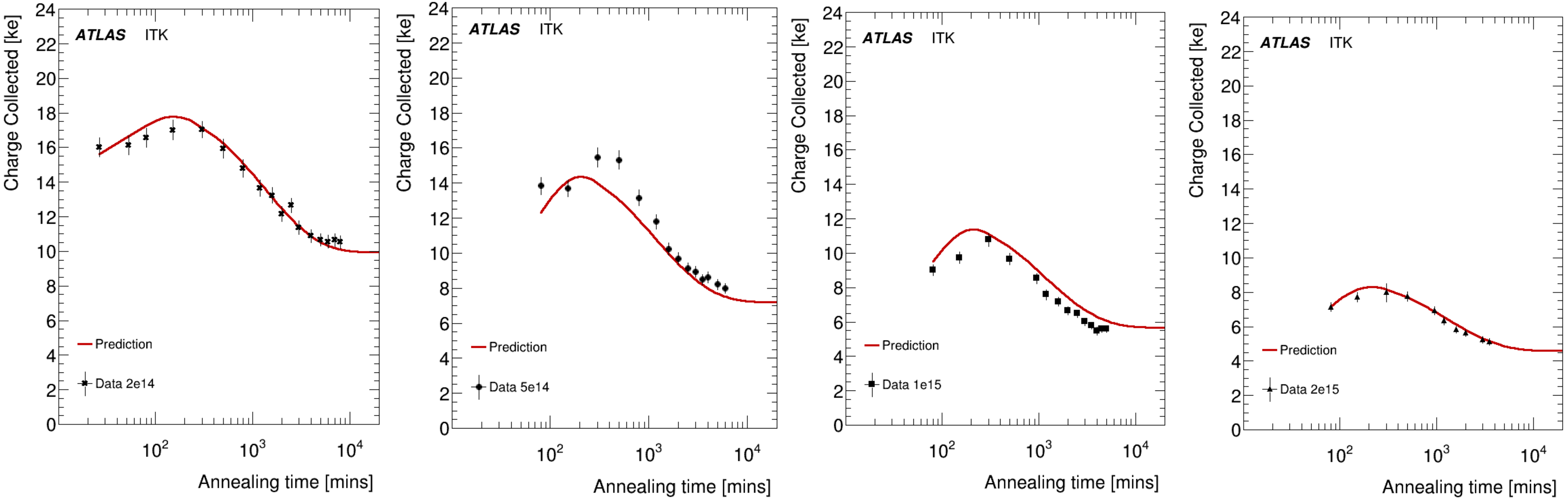

The fitted functional form of the g-parameters is used to predict the Collected Charge

24 MeV protons at Karlsruhe – Closure Test

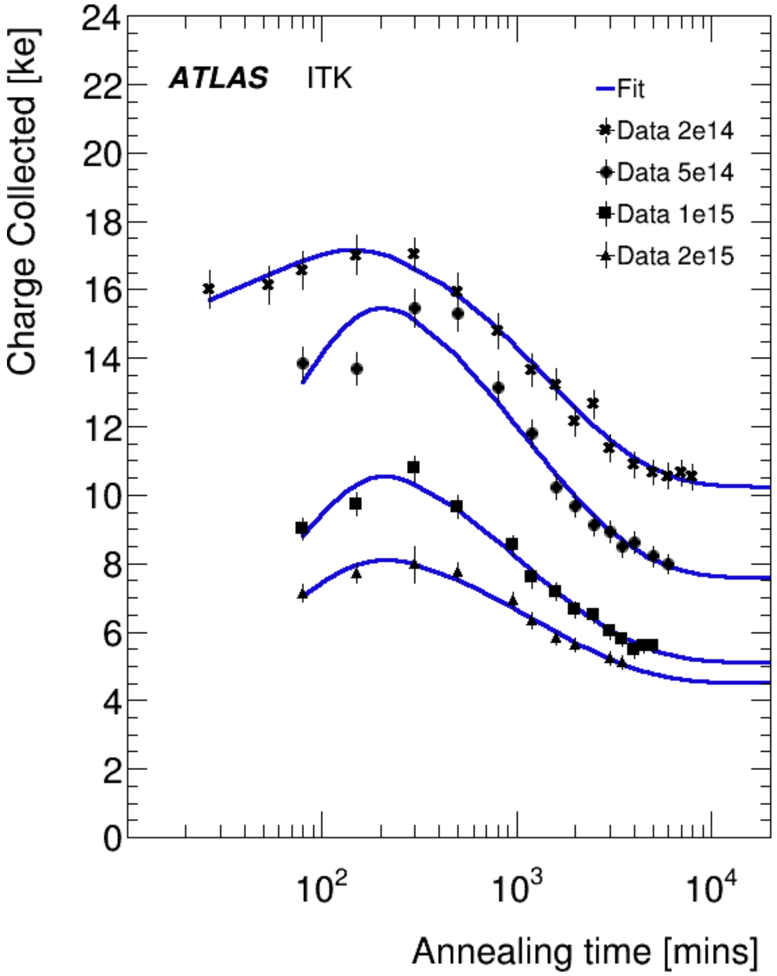

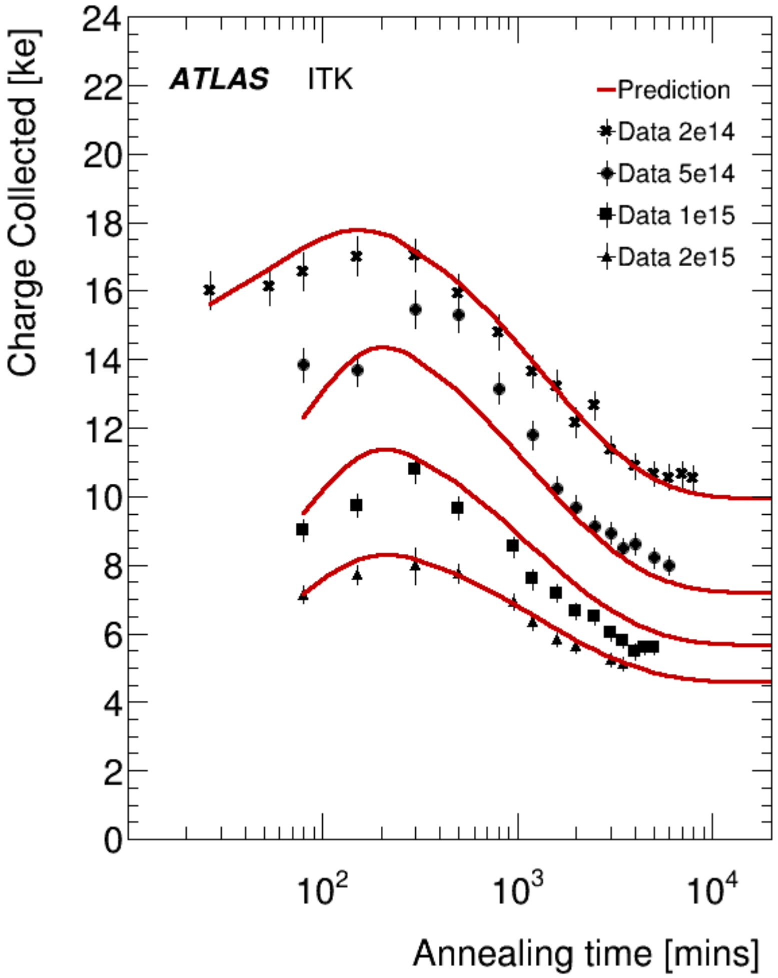

- ATLAS12
- 400 V Bias Voltage
- Measured at Freiburg
- Annealing at 60 C
- "Fit" is the independent fit to each fluence
- "Prediction" is the prediction of the model using the fitted coefficients as a function of fluence

This is a condensation of last three slides

24 MeV protons at Karlsruhe – Closure Test

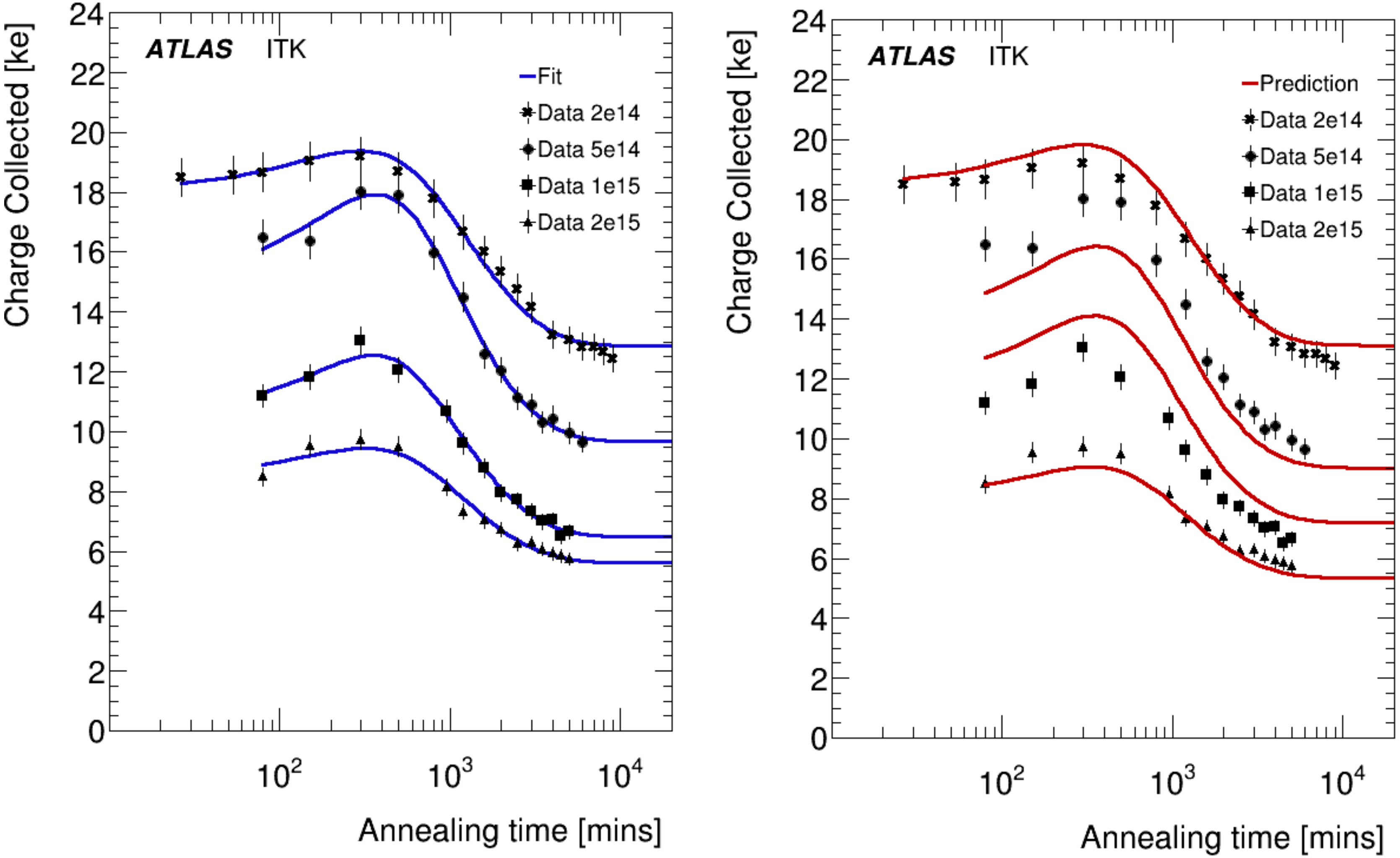

- ATLAS12
- 500 V Bias Voltage
- Measured at Freiburg
- Annealing at 60 C
- Fits to the coefficients are done independently at 400V and 500V

Reactor Neutrons – Closure Test

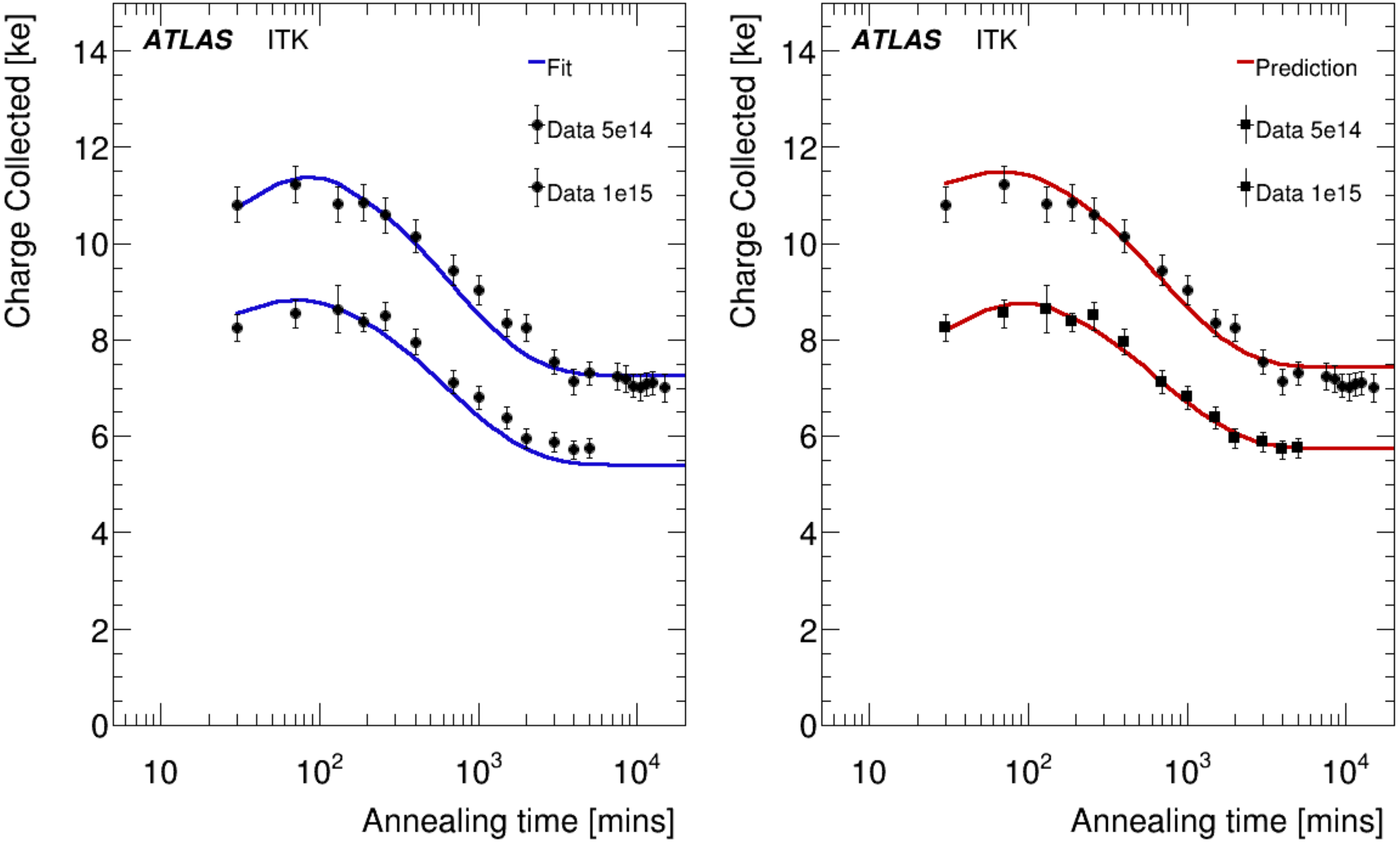

- ATLAS12
- 500 V Bias Voltage
- Annealing at 60 C
- Measured at Freiburg
- All neutron data irradiated at Ljubljana

Toronto Measurement of CCE of Miniature Sensors

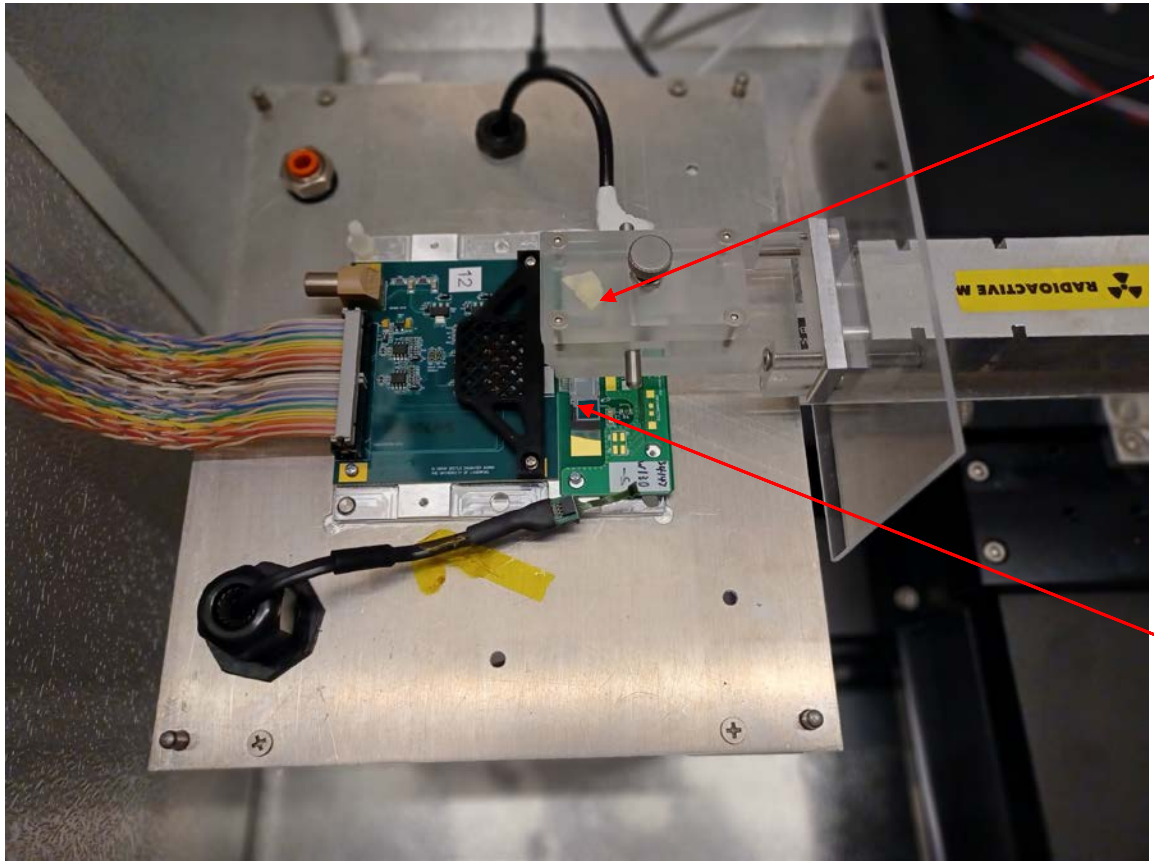

^{90}Sr

Mini-sensor

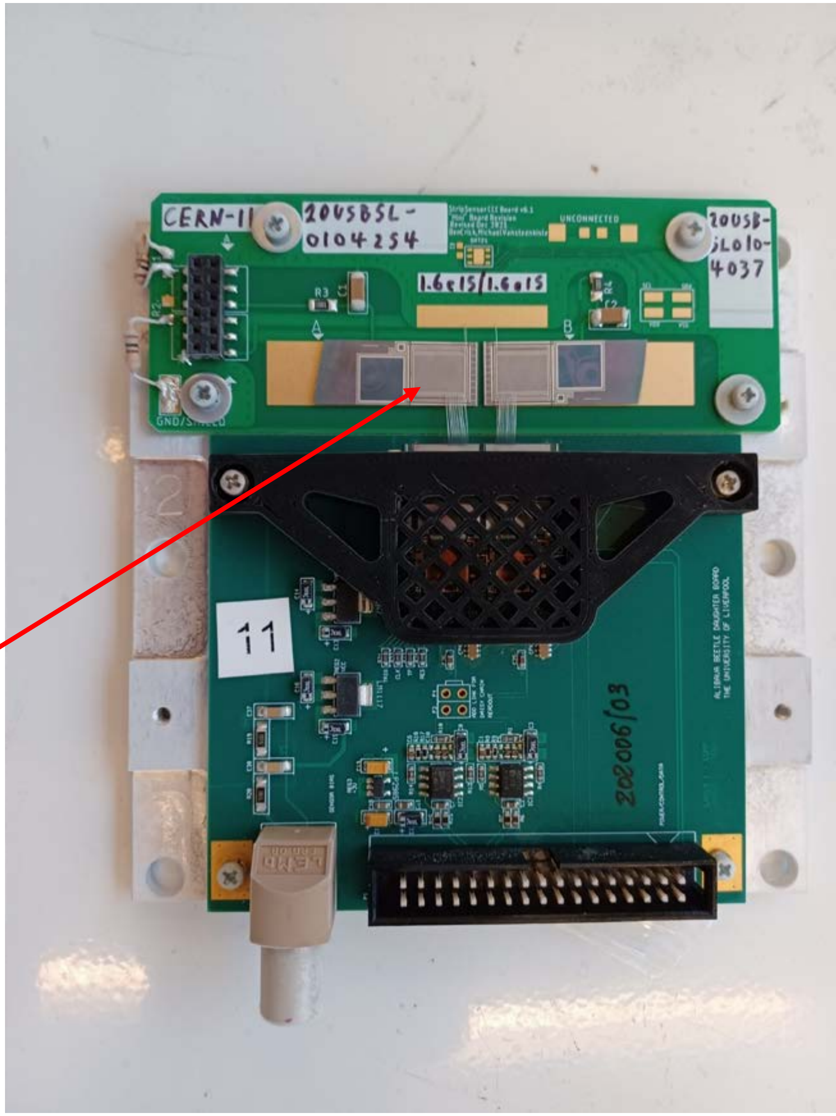

Uses Alibava readout system to measure pulse height spectrum
Measurements done in freezer at -27 C

Measurement Procedure at Toronto

- Gain of all Alibava daughter boards calibrated as a function of temperature
- Used sensor mounting board with improved HV filtering
- Took data for Bias Voltage 50V to 1100V
- Pulse height spectra fitted to Landau + Gaussian
- Most probable value of Laudau plotted

150 Mins Annealing at 60 deg

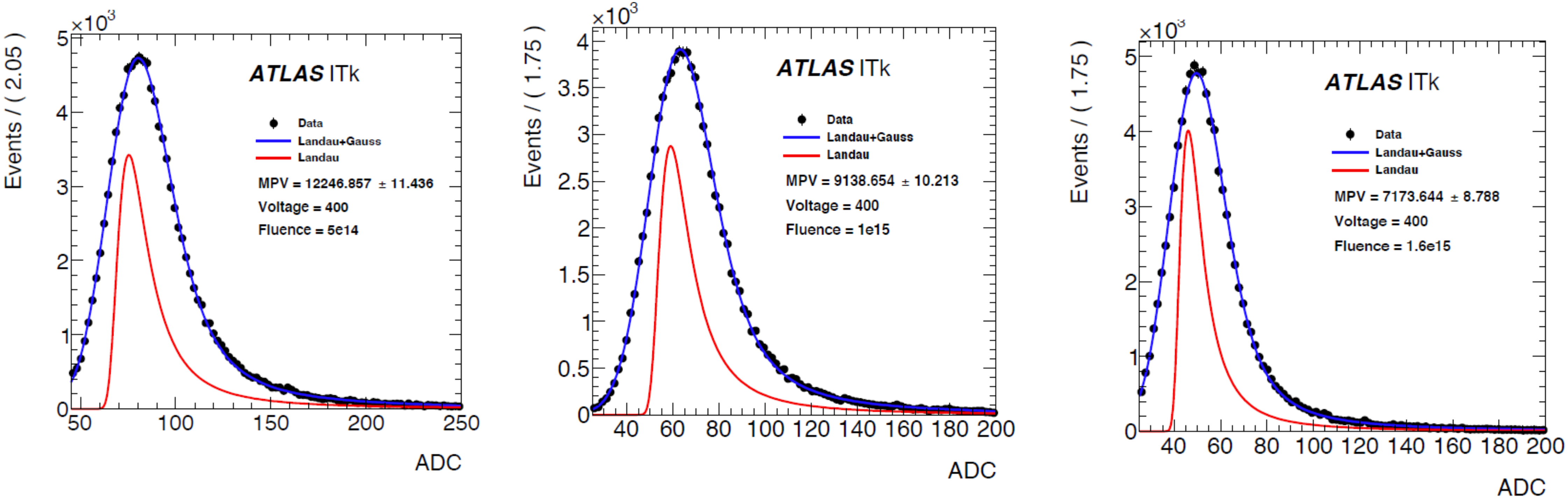

Fits and Closure of ATLAS18 - Neutrons

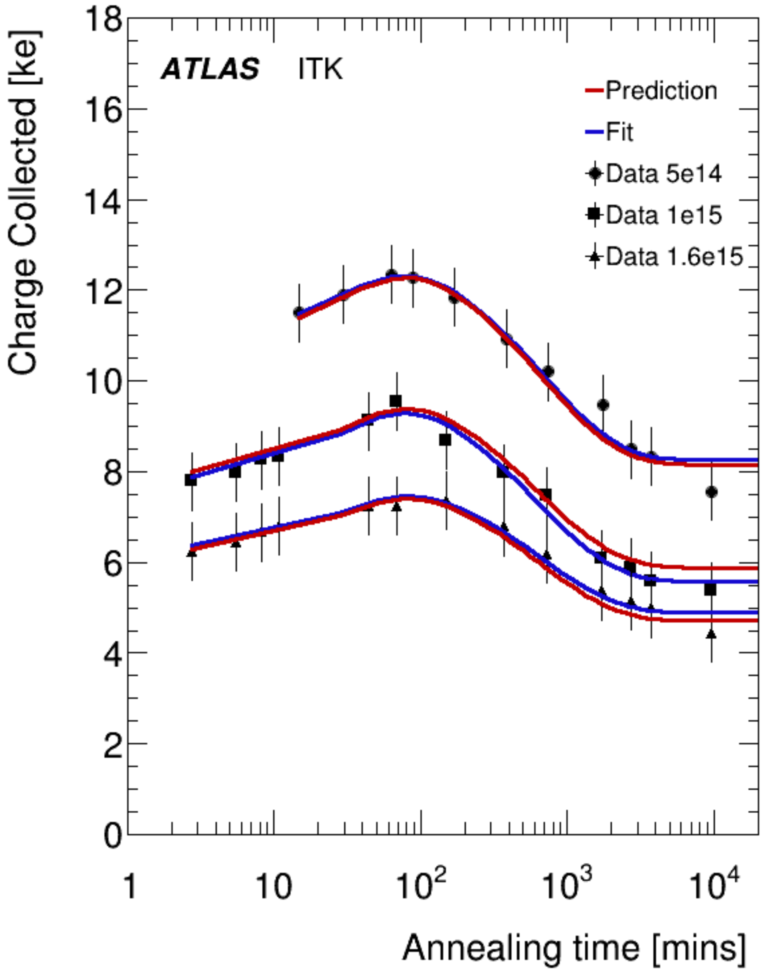

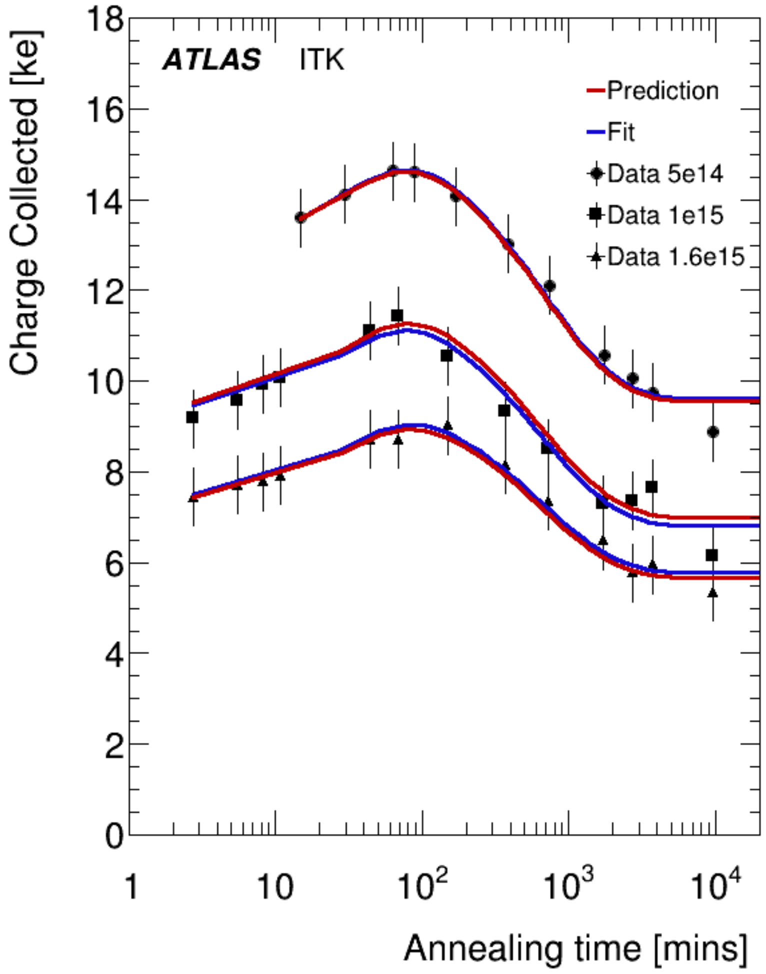

- Measured in Toronto
- 400V Bias Voltage
- Annealing at 60 C

- Measured in Toronto
- 500V Bias Voltage
- Annealing at 60 C

g-coefficients for ATLAS18 Neutrons

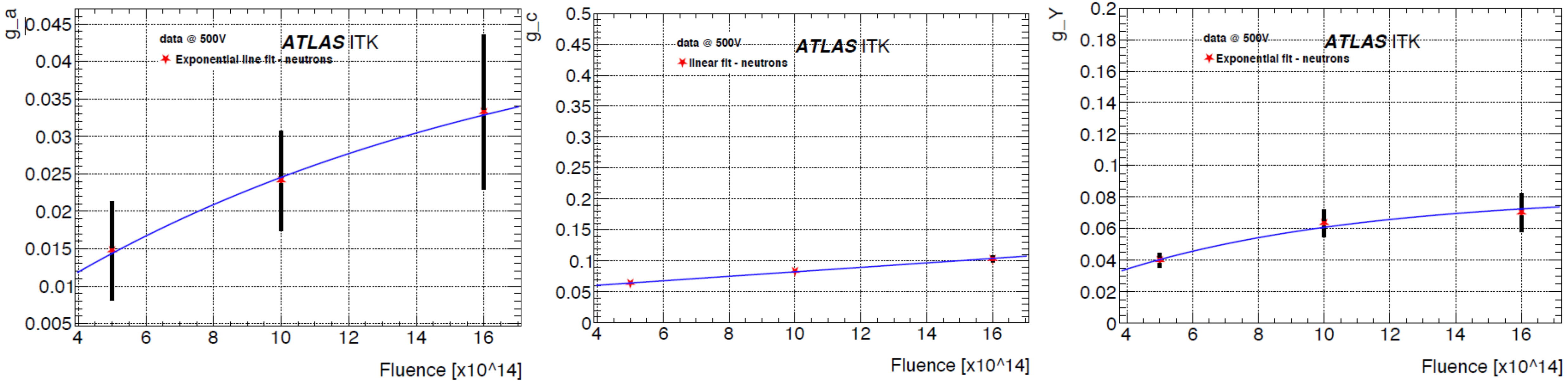

- Measured in Toronto
- 500V Bias Voltage

Use of Model in Assessing Long Term Running Scenarios

We have used model to investigate the end of life CCE in several possible situations

1) Alternative temperature Profiles during running
   - Starting cold -25C, and running cold except for
     - Long warmups
     - Short warms ups
   - Starting at room temp and progressively reducing temperature
- Allows data/model comparison

2) A staging scenario where the pixel installation was delayed until Long Shutdown#5 (LS5), but the Strips were installed in LS4, run cold, and then warmed up for 100 days in LS5

3) A scheduled maintenance of the CO_2 cooling system, during which the ITk is warmed up for 10 days each year and 40 days in LS4 and LS5

CCE measured using Ljubjana Alibava setup

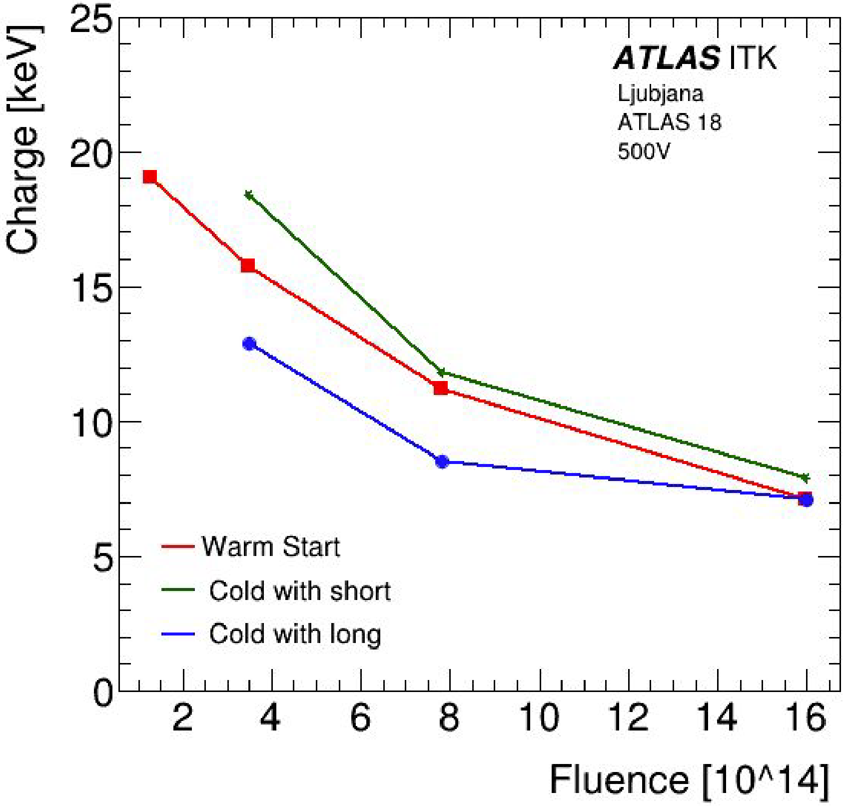

- In all three scenarios the collected charge remained greater than 6350 electron equiv
- This corresponds to Signal/Noise = 10 , and corresponds to the worst case *viz* detector end-of-life

Comparison of model with experiment

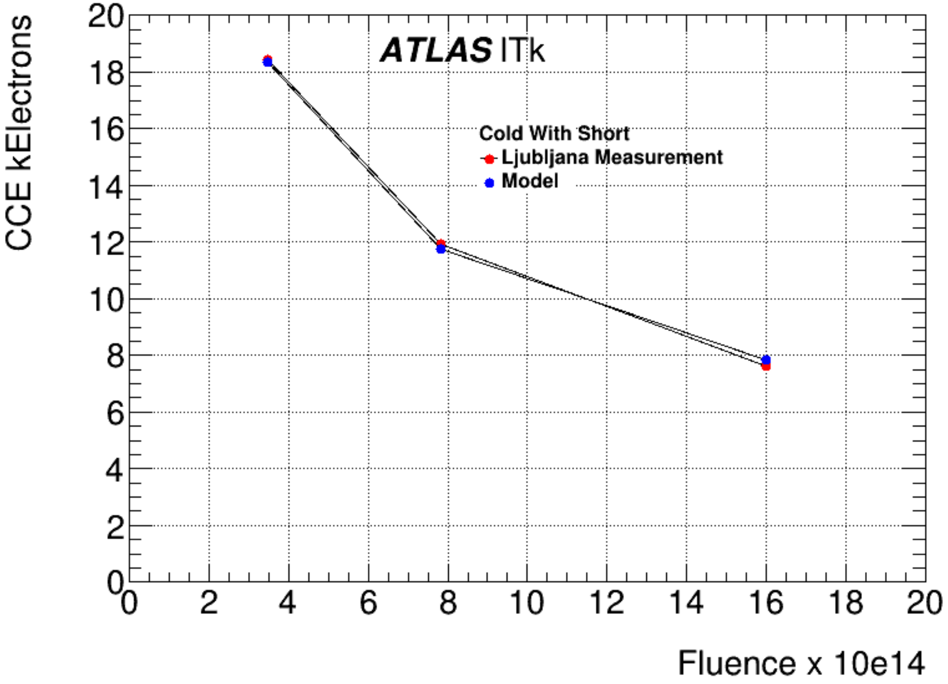

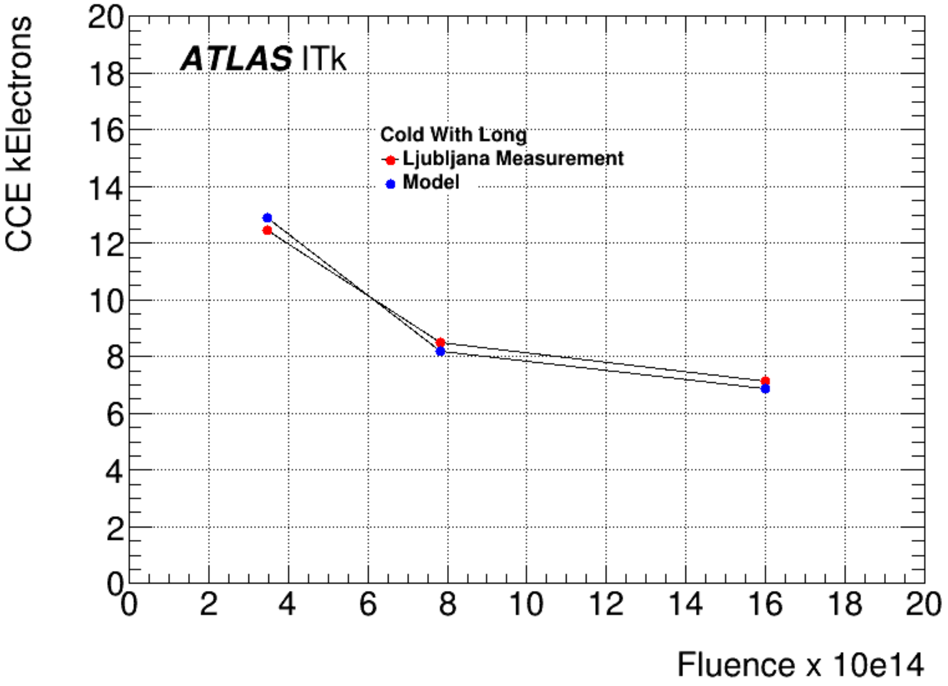

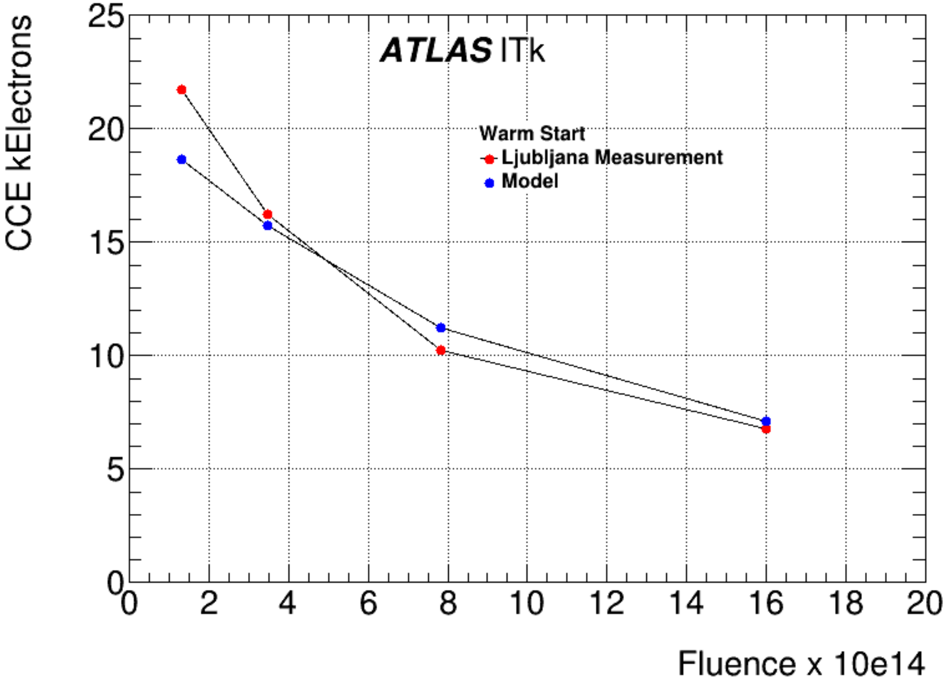

Conclusions

- We have constructed a simple, data driven, model of the dependence of collected charge on annealing time / temperature for the ATLAS18 strip sensors
- It reproduces annealing measurements at end-of-life to better than 5%
- We have used the model in temperature/schedule planning extending over the foreseen lifetime of the ITk
- The model does have shortcomings, viz:

    - Present approximation:
        - Apply fluence as a delta function
        - Run model for time@temp
        - Apply fluence as a delta function
        - Run model for time@temp
        - Force continuity
        - Iterate

  - Empirically this is a good approximation for long cold periods interspersed with short warm ups - See three running scenarios
  - In real running irradiation occurs concurrently with annealing
  - Try to build differential equation with phenomenological parameters

Additional

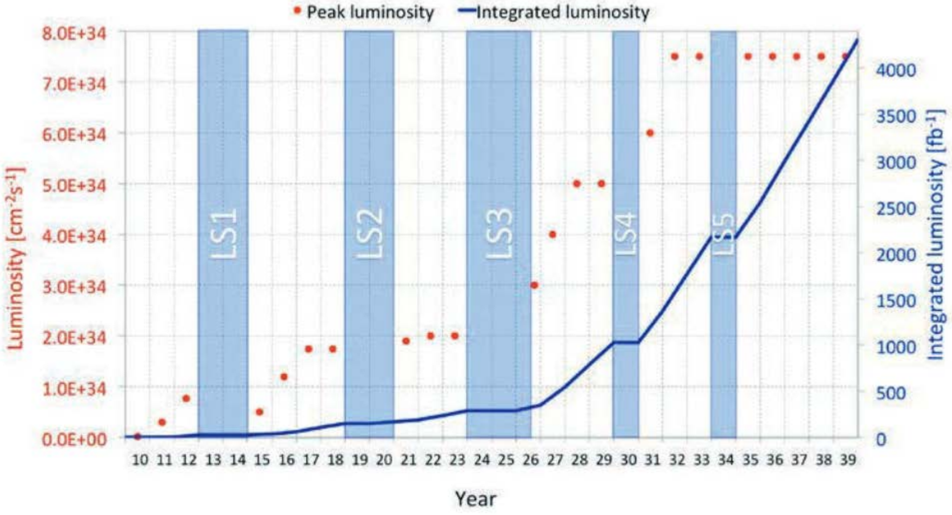

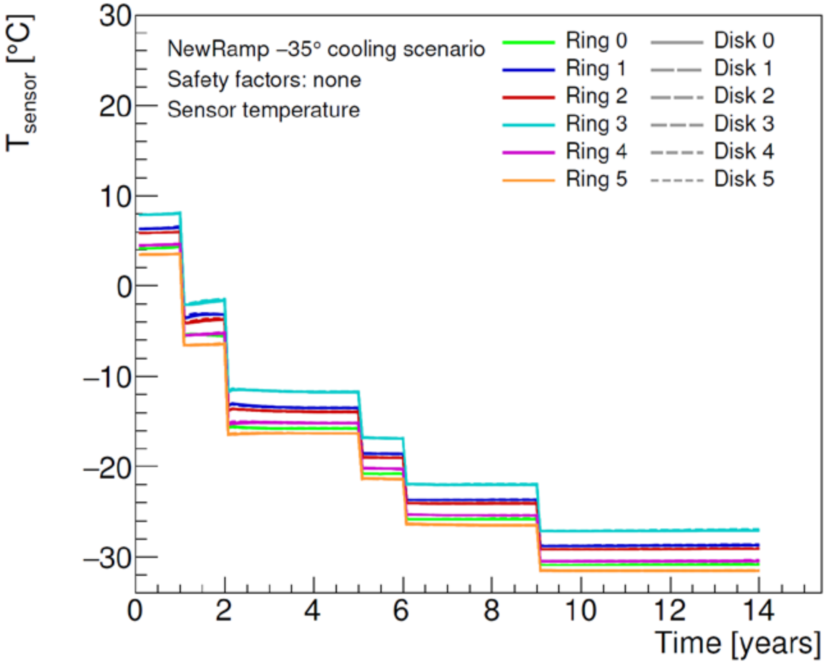

NIM A 969 (2020) 164023

- Studies are based on luminosities and shutdown periods of the “ultimate HL-LHC parameters” described in CERN-2017-007-M

- Possible running scenarios have included the “warm start” to exploit the TID bump. Start above 0º. As fluence increases run at progressively lower temp, to reduce leakage current.
- Studies have shown that pre-irradiation of ASICs reduced the TID bump by an order of magnitude.
- Pre-irradiation has been included in the ASIC production procedure.
- It could be that the warm start scenario is no longer necessary.

Alternative Temperature Variation during Running Scenarios

- Irradiated ATLAS 18 miniature R0 sensors at Ljubljana reactor
- Final irradiation corresponds to final integrated luminosity of 4000 fb^{-1} with a safety factor of 1.5
- Annealing is done at 60^{o}, corrected to simulated temperature using activation energy of 1.07 eV

$$T_{eff}(\theta_{eff}) = T_{ann}(\theta_{ann})\exp\left(\frac{E_{act}}{k_B}\left(\frac{1}{\theta_{eff}} - \frac{1}{\theta_{ann}}\right)\right)$$

- Cycled repeatedly through- irradiate, anneal, measure CCE for three operation scenarios:
  - Warm start
    - 2 year fluence, anneal 1 year (equiv) 7^{o} then 1 year at -3^{o}.
    - 3 year fluence, then anneal 4 years at -13^{o} .
    - 4 year fluence, then anneal 3 years at -20^{o} .
    - 5 year fluence, then anneal 5 years at -25^{o} .

  - Cold start – short warm ups
    - Operation at -25^{o} , 10 days at room temp during LS4 and LS5
  - Cold start – long warm ups
    - Operation at -25^{o} , 100 days at room temp during LS4 and LS5

Proposed Staging of Pixels

- Assumed 13 month warmup in LS4, addditonal 100 days warm in LS5
- Ran Model for two fluence scenarios
  - Used tool https://atlas-service-radsim.web.cern.ch/radsim_noerrs
  - Radius = 40 cm, z =150. This is inner edge of strip endcap closest to interaction point
  - Phase 2 ITk Step3.1Q6 geometry model
  - Si 1 MeV neutron equivalent (NIEL)
  - GEANT4
  - Twice this fluence – More or less strip "nominal safe"
- In reality neutrons only contribute 50% of fluence
  - Other 50% is protons – which are less damaging – further "safety" factor

Total Fluence	LS4	LS4->LS5	LS5	End of Life
8e14	14.8	14.9	12.9	10.
16e14	11.5	11.6	10.2	6.6

cf. 6.350

Use in Scheduling Studies II – Proposed CO2 Cooling line WarmUp

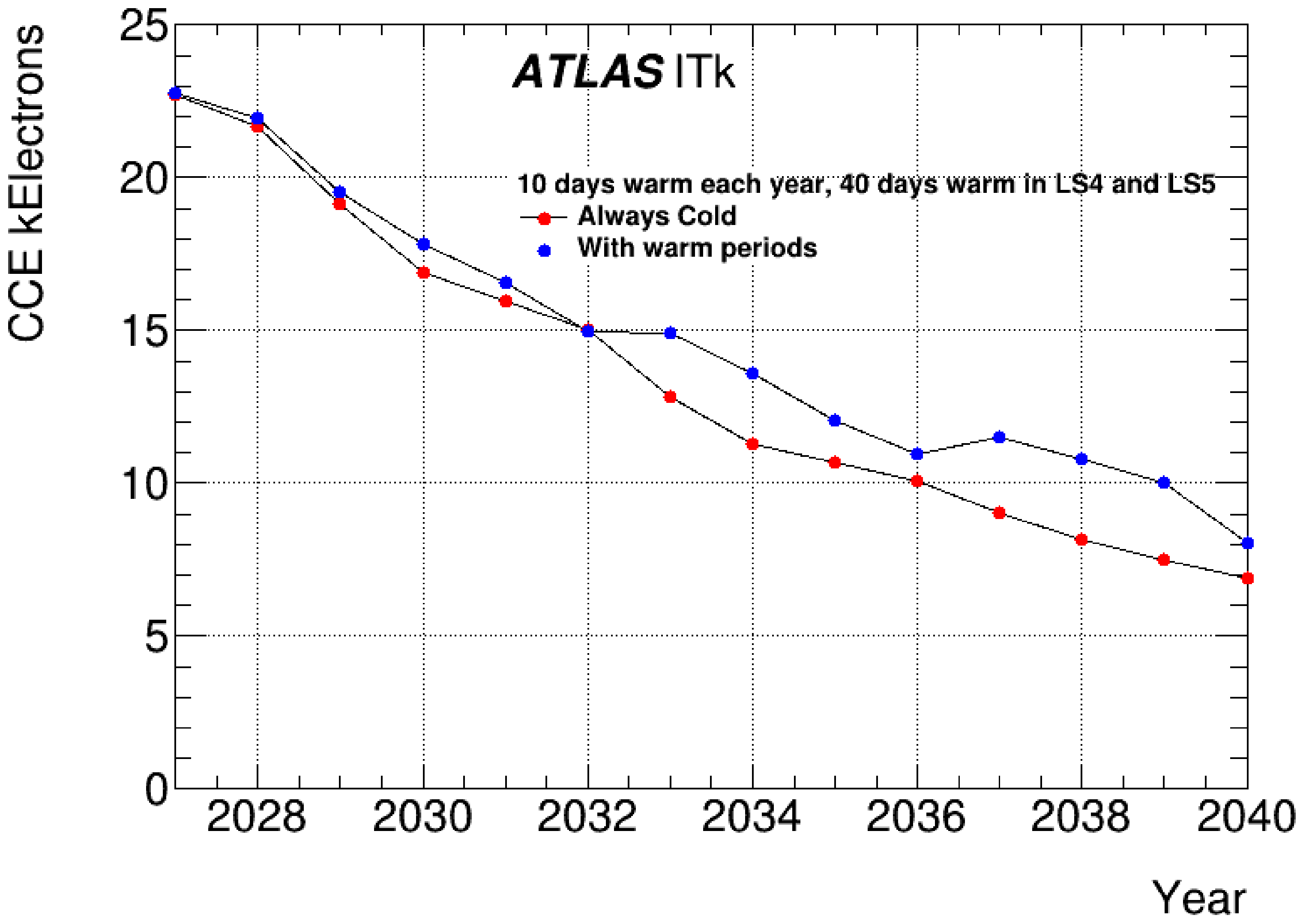

Lines are just root joining the dots

cf. 6.350

Inner Detector Replacement

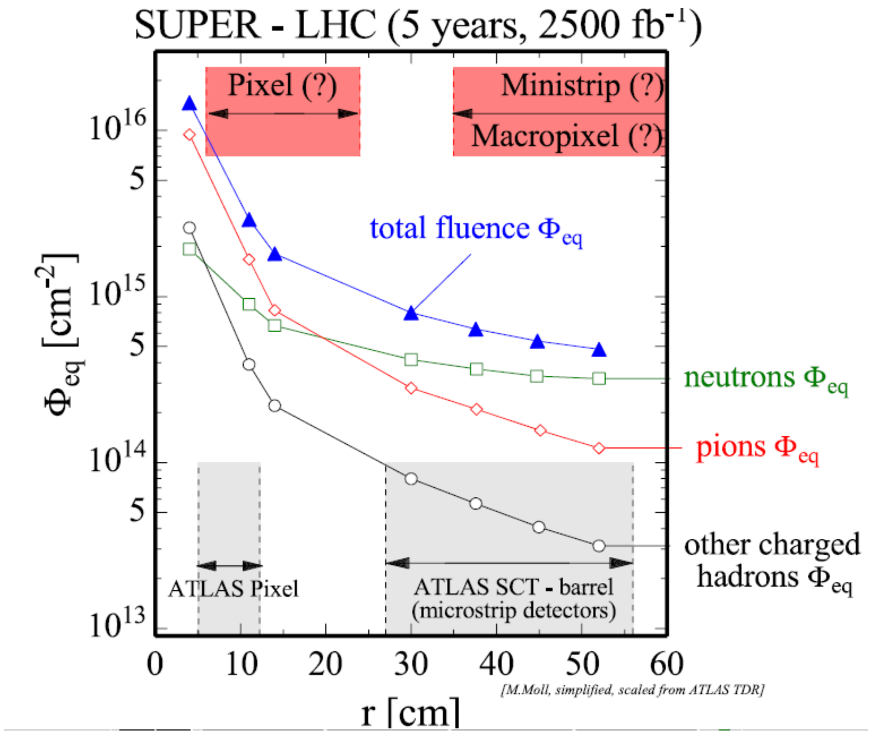

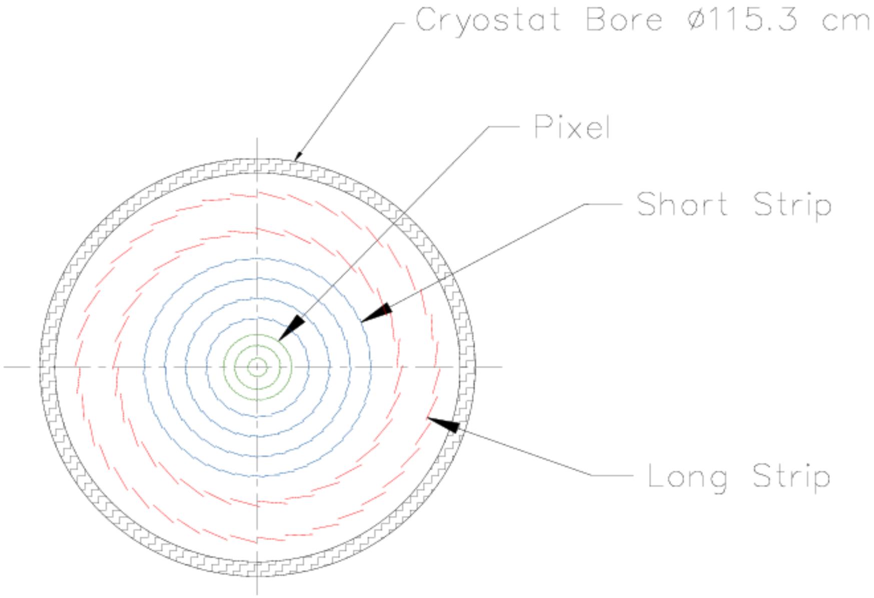

- Order of magnitude increase in Data rates, Occupancy, Irradiation
- No TRT – Si strips
- Pixels moved to larger radius
- New technology for inner layers
- R&D required on sensors, readout, and mechanical engineering

3-d SILICON → SHORTER DRIFT DISTANCE
— LESS TRAPPING

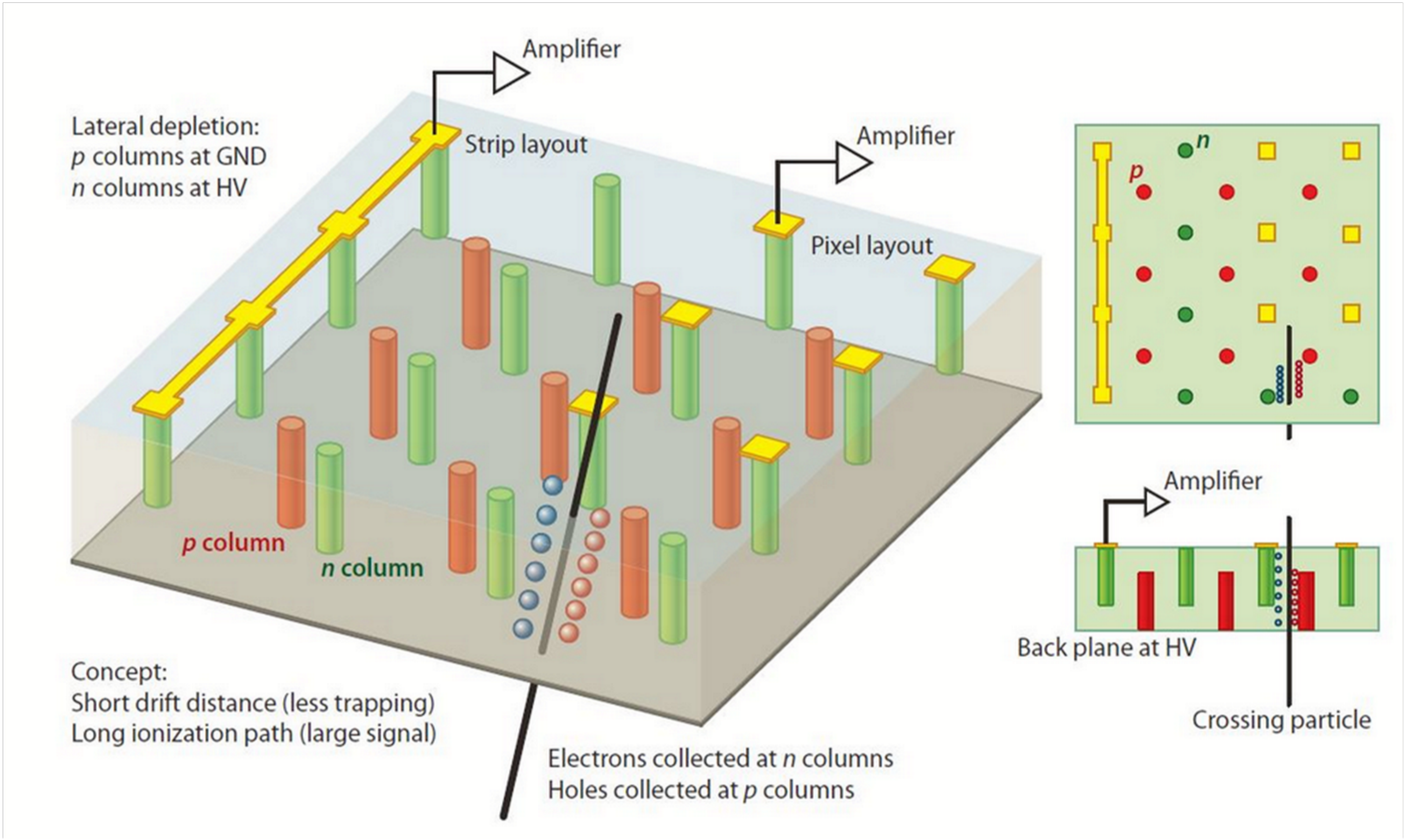

Pixel-layer Technologies

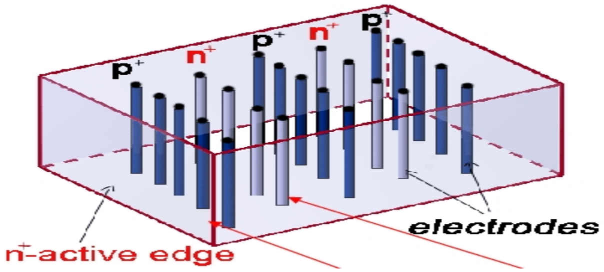

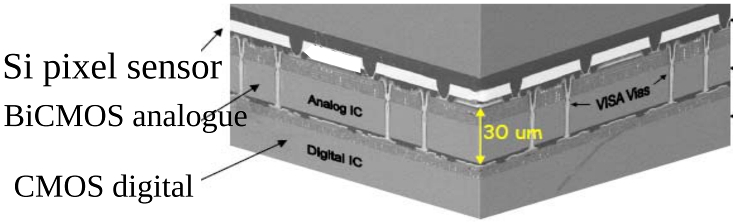

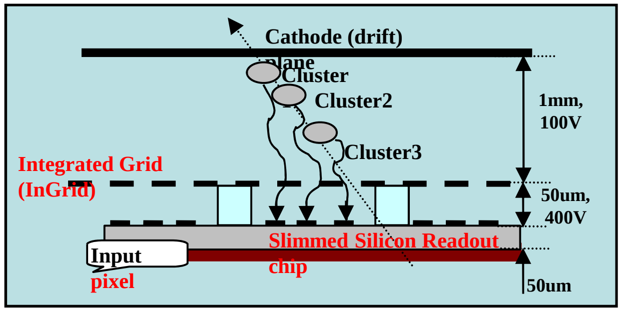

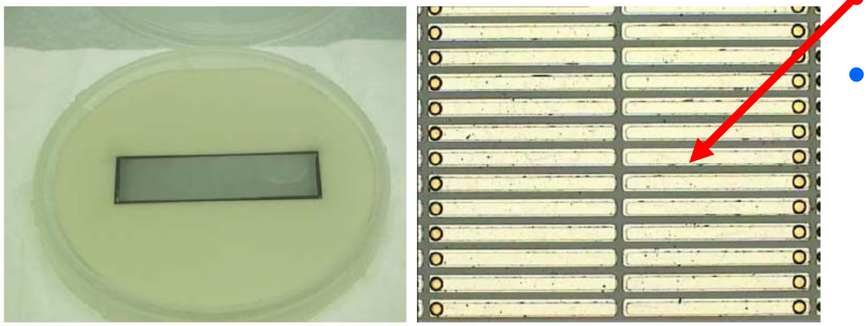

Figure 5: (a) Photograph of the ATLAS pixel diamond mounted in the carrier ready for bump bonding. (b) Zoom view of the pixel pattern after the under-bump metal is deposited.

- Harshest radiation environment (R~4cm)
  - – investigate new technologies
- 3D Si
- Thin silicon + 3D interconnects
- Gas over thin pixel (GOSSIP)
- *Diamond pixels*
- May test in pre-SLHC b-layer replacement (~2012)

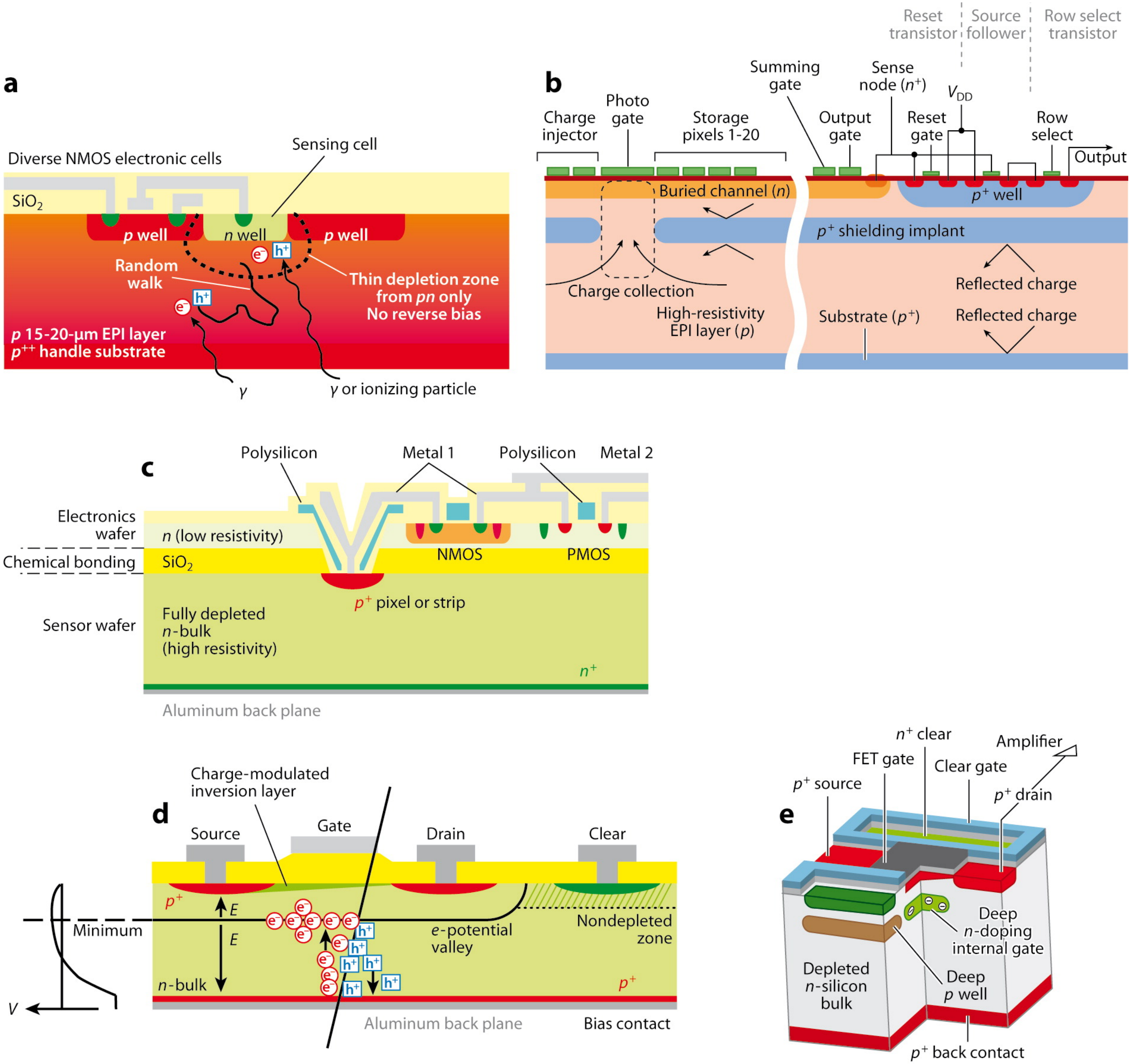

Hartmann F, Kaminski J. 2011